POLITECNICO DI MILANO

SCUOLA DI INGEGNERIA CIVILE, AMBIENTALE E TERRITORIALE

Tensile behavior of Fabric Reinforced Cementitious Matrix (FRCM) composites

Relatore: Prof. Carlo Poggi

Correlatore: Prof. Antonio Nanni

Elaborato di:

Giacomo Mesaglio, Matr. 801535

Anno accademico 2013/2014

ACKNOWLEDGEMENTS

I am extremely and sincerely thankful to Dr. Poggi, for allowing me to undertake this amazing experience, for his constant support and help to solve every problem I faced in these months.

My gratitude goes also to Dr. Antonio Nanni, for his great patience and support, for his incredible ability to give me the right hint to make a better job and for all the time he spent with me. He made me feel proud of working in his team.

Many thanks go also to Dr. Arboleda, for helping me every time I needed, with a smile on her face. She was able to be a great advisor but at the same time a friend for me and also the hard work was awesome and exciting with her in the lab.

I would like to say thank you also to Giulia Carozzi, her patience with me was limitless and she was always available for me.

TABLE OF CONTENTS

ABSTRACT ..... **XI**

SOMMARIO ..... **XII**

1 GENERAL **1**

1.1 INTRODUCTION 1
1.2 COMPOSITE MATERIALS 3
1.3 FRCM COMPOSITE MATERIAL: DESCRIPTION AND APPLICATION 8
1.4 FRCM SYSTEMS: TECHNICAL SPECIFICS 12
1.4.1 Unidirectional system *12*
1.4.2 Bidirectional carbon system *12*
1.5 EXAMPLES OF FRCM APPLICATION 13
1.5.1 Unreinforced concrete vault strengthening *13*
1.5.2 Trestle bridge base confinement *14*
1.5.3 Strengthening of unreinforced masonry chimney *15*
1.5.4 Strengthening of reinforced concrete bridge pier *16*
1.6 OBJECTIVES 17

2 MECHANICAL PROPERTIES OF FRCM COMPOSITE **19**

2.1 MECHANICAL BEHAVIOR OF THE FRCM SYSTEM 19
2.2 TENSILE PROPERTIES 23
2.2.1 Different gripping mechanisms *23*
2.3 BOND ADHESION PROPERTIES 28
2.3.1 Single and double push-pull shear test *28*
2.3.2 Pull-Off *33*
2.4 INTERLAMINAR PROPERTIES 36
2.5 BENDING & SHEAR REINFORCEMENT 38

3 TENSILE CHARACTERIZATION **43**

3.1 FRCM CONSTITUTIVE LAW: TWO IDEALIZED MODEL 43
3.2 TEST SETUP 48
3.2.1 Machine *48*
3.2.2 Extensometer *48*
3.2.3 Gripping mechanism *49*
3.3 MATERIAL DESCRIPTION 50
3.3.1 Fabric *50*
3.3.2 Mortar *52*
3.4 SPECIMEN PREPARATION AND GEOMETRY 57
3.5 TAB APPLICATION 59
3.6 MATRIX OF THE SPECIMENS TESTED 60
3.7 PARAMETER CALCULATION 61
3.8 PROBLEMS RELATED WITH THE DATA ANALYSIS 63
3.9 EXPERIMENTAL RESULTS 66
3.9.1 Unidirectional system *66*
3.9.2 Bi-directional system *76*
3.10 FAILURE MODE 78

4 ANALYSIS OF THE RESULTS **81**

4.1 UNCRACKED ELASTIC MODULUS E1 81
4.2 TRANSITION POINT AND POINT OF THE FIRST CRACK 83
4.3 LAP SPLICES 84
4.4 SINGLE PLY VS. TWO PLIES SPECIMENS 86
4.5 COMPARISON OF BI-DIRECTIONAL AND UNIDIRECTIONAL SYSTEMS 88

4.6 TAB LENGTH COMPARISON 90

5 DURABILITY 95

5.1 DURABILITY ON FRCM SYSTEM: INTRODUCTION 95
5.2 ENVIRONMENT DESCRIPTION 96
5.3 EXPERIMENTAL RESULTS 97
5.3.1 Alkaline resistance 97
5.3.2 Sea water resistance 99
5.3.3 Water vapor resistance 100
5.3.4 Freezing and thawing resistance 102
5.4 ANALYSIS OF THE RESULTS 103
5.4.1 Comparison of the results 103
5.5 CONCLUSION 106

6 FINAL CONCLUSIONS 109

LIST OF FIGURES

Figure 1. 1 - Different technologies to reinforce the concrete, Hagger et al. (2004) . 1
Figure 1. 2 - Simplified composite material model 4
Figure 1. 3 - Mechanical behavior of organic polymer matrix composite..... 5
Figure 1. 4 - Upper and lower bound for the elastic modulus 6
Figure 1. 5 - Elastic modulus for different direction of the load..... 6
Figure 1. 6 - Example of composite material applications..... 7
Figure 1. 7 - Examples of composite material applications in civil engineering..... 8
Figure 1. 8 - FRCM Application, Leardini et al. (2013) 9
Figure 1. 9 - Flexural reinforcement with FRCM, Arboleda et al. (2014)..... 10
Figure 1. 10 - Shear reinforcement with FRCM, Arboleda et al. (2014) 10
Figure 1. 11 - Column reinforcement with FRCM, Arboleda et al. (2014)..... 11
Figure 1. 12 - Reinforcement of a masonry wall with FRCM, Arboleda et al. (2014) 11
Figure 1. 13-Unreinforced concrete vault strengthening..... 14
Figure 1. 14- Trestle bridge base 15
Figure 1. 15 - Trestle confinement..... 15
Figure 1. 16 - Strengthening of unreinforced masonry chimney..... 16
Figure 1. 17 - Strengthening of reinforced concrete bridge pier 17

Figure 2. 1 - External reinforcement failure modes, D'ambrisi et al. (2011) 20
Figure 2. 2 - Slippage failure of a FRCM system, Loreto et al. (2013)..... 20
Figure 2. 3 - Delamination failure of a FRCM system , Loreto et al. (2013)..... 21
Figure 2. 4 - Telescopic failure 21
Figure 2. 5 - Debonding failure occurred in a four-plies strengthened beam, Leardini et al. (2013)..... 22
Figure 2. 6 - Gripping mechanism group one: clamping of the fabric, De Santis and De Felice (2014) 25
Figure 2. 7 - Gripping mechanism group two: constrain on the mortar, De Santis and De Felice (2014) 26
Figure 2. 8 - Different specimen shapes and gripping mechanisms, Contamine et al.(2011)..... 27
Figure 2. 9 - Single lap shear test set-up, Sneed et al. (2014)..... 29
Figure 2. 10 - Double-lap shear test set-up, Carozzi et al. (2015)..... 29
Figure 2. 11 - Push-Pull double shear test, D'Ambrisi et al. (2012)..... 30
Figure 2. 12 - Peak load vs. bond length, D'Ambrisi et al. (2012) left, peak stress vs. bond length, Sneed et al. (2014) right 31
Figure 2. 13 - Force at debonding vs. bond length, Pascucci et al. (2013) 31
Figure 2. 14 - Possible failure modes for a Push-Pull shear test, Pascucci et al. (2013)..... 32
Figure 2. 15 - Load-displacement curves for G-FRCM with different bond lengths, Carozzi et al.(2015) 33

Figure 2. 16 - Pull-Off machine, Bianchi et al. (2013) *34*
Figure 2. 17 - Core drill to cut the specimens, Bianchi et al. (2013) *34*
Figure 2. 18 - Possible failure mode for the Pull-Off test according to AC434, Bianchi et al. (2013) *35*
Figure 2. 19 - Short beam shear test configuration (ASTM D2344) *36*
Figure 2. 20 - Possible failure modes in Short Beam Test for FRP composites *37*
Figure 2. 21 - Different strengthening configurations, D'ambrisi and Focacci (2011) *40*
Figure 2. 22 - Shear strengthening, D'Ambrisi and Focacci (2011) *40*

Figure 3. 1 - Tri-linear stress-strain curve, Arboleda et al. (2014) *44*
Figure 3. 2 - Bi-linear stress-strain curve, Arboleda et al. (2014) *45*
Figure 3. 3-Clevis and clamped grip *46*
Figure 3. 4 - Different load transfer mechanisms, Arboleda et al. (2014) *46*
Figure 3. 5-Comparison of the results with different grips, Bianchi et al. (2013) *47*
Figure 3. 6 - Extensometer application: on the specimen and on the tabs *49*
Figure 3. 7 - Clevis-type gripping mechanism according to AC434 ..... *50*
Figure 3. 8 - Unidirectional carbon-mesh (left) and bidirectional carbon mesh (right) *50*
Figure 3. 9 - Unidirectional fabric *51*
Figure 3. 10 - Bidirectional fabric *51*
Figure 3. 11 - Uniaxial compressive test on the mortar *55*
Figure 3. 12 - Specimens preparation *58*
Figure 3. 13 - Tabs application *59*
Figure 3. 14 - Interpolation of the AC434, Bianchi et al. (2013) *62*
Figure 3. 15 - Dissymmetry of the reinforcement in the thickness of the specimen, Carozzi et al. (2015) *63*
Figure 3. 16 - Dissymmetry of the reinforcement in the width of the specimen *64*
Figure 3. 17 – Effect of the warping of the specimen, Carozzi et al. (2015) *64*
Figure 3. 18 - Anchorage length *65*
Figure 3. 19 - Control specimens one-ply with 100mm tab length *66*
Figure 3. 20 - One-ply with 150mm tab length *68*
Figure 3. 21 - Tab debonding and solution *69*
Figure 3. 22 - Control condition tests for two plies with 150mm tab length *70*
Figure 3. 23 - One-ply with 200mm tab length *71*
Figure 3. 24 - Two-ply with 200mm tab length *73*
Figure 3. 25 - Control condition tests for lap with 150mm tab length *75*
Figure 3. 26 - Control condition one ply 150 mm tab length *76*
Figure 3. 27 - Specimen failure *79*

Figure 4. 1 - AC434 idealized curve *83*
Figure 4. 2 - Lateral view of a tested lap specimen *85*
Figure 4. 3 - One ply and two plies systems tested with 150 mm tab length *87*
Figure 4. 4 - Cracking pattern behavior: unidirectional and bi-directional systems *88*
Figure 4. 5 - Unidirectional and Bi-directional comparison : stiffness *89*
Figure 4. 6 - Representative graphs for the three different tab lengths *92*
Figure 4. 7 - Ultimate strength with error band for different tab length *93*

Figure 5. 1 - Alkaline resistance *97*
Figure 5. 2 - sea water resistance *99*
Figure 5. 3 - Water vapor resistance *100*
Figure 5. 4 - Freezing and thawing resistance *102*
Figure 5. 5 - Ultimate strength after exposure to different environments *106*
Figure 5. 6 - Cracked elastic modulus after exposure to different environments ... *106*

LIST OF TABLES

Table 1. 1- Technical specifics of the unidirectional system *12*
Table 1. 2 - Technical specifics of the bidirectional system *13*

Table 3. 1 - Void content *54*
Table 3. 2 - Strength after 7 days *56*
Table 3. 3 - Strength after 28 days *56*
Table 3. 4 - Matrix of the specimens tested *60*
Table 3. 5 - Ultimate strength for one-ply specimens with 100 mm tab length *67*
Table 3. 6 - Parameters for one-ply with 150 mm tab length *68*
Table 3. 7 - Parameters for control tests for two plies with 150mm tab length *70*
Table 3. 8 - Parameters for control tests for one ply with 200mm tab length *72*
Table 3. 9 - Parameters for control tests for two plies with 200mm tab length *73*
Table 3. 10 - Parameters for control tests for lap specimens with 150mm tab length 75
Table 3. 11 - Parameters for control tests for bidirectional specimens *77*

Table 4. 1 - -Cross section of the specimens with one ply and the tab length of 150mm *82*
Table 4. 2 - Uncracked modulus with respect to the cross section of the specimen *82*
Table 4. 3 - Comparison between transition point and point of the first crack *83*
Table 4. 4 - Comparison between one ply and two plies system *86*
Table 4. 5 - Tab length comparison: ultimate stress *90*
Table 4. 6 - Parameters comparison for different tab length *91*

Table 5. 1 - Parameters for Alkaline resistance tests *98*
Table 5. 2 - Parameters for Sea Water resistance tests *99*
Table 5. 3 - Parameters for Water Vapor resistance tests *101*
Table 5. 4- Parameters for Freezing and thawing tests *102*
Table 5. 5 - Parameters comparison *104*
Table 5. 6- Result from t-test analysis: ultimate stress *105*
Table 5. 7 - Result from t-test analysis: cracked elastic modulus *105*

ABSTRACT

The rehabilitation of existing buildings that may have deteriorated as a result of aging or that need to meet new requirements, has long been a challenge in the construction industry. Composite materials are widely used in repair of structural elements such as beams, columns, slabs, or walls that require strengthening. The objective of this research is to study the tensile behavior of Fabric Reinforced Cementitious Matrix (FRCM) composite, developed as an alternative to Fiber Reinforced Polymer (FRP) materials. FRCM is different from FRP in that dry fabrics are used with a cementitious matrix instead of fibers impregnated with an organic matrix. While this composite material has a brittle behavior, the cementitious mortar allows for a better bond with the concrete substrate and offers potential fire protection.

To obtain a better understanding of material parameters for design, laboratory tests are fundamental in the determination of tensile behavior, which is not yet standardized. Two of the important variables that influence FRCM tensile performance are specimen geometry and gripping configuration. Clevis-type (pin-action) grips are used with metal tabs bonded to the specimen to apply the longitudinal load by surface shear in the contact area, with the contact length being a variable. This choice of grip represents the boundary condition in the field application of FRCM, where the fabric is not anchored at its ends and the failure mode of the FRCM in tension is by slippage of the fibers.

The main target of this work is to understand how the tab length affects the strain-stress behavior and to confirm if increasing the tab length can approach the full strength of the fabric, as it happens with the clamped grips, or if there is a limit and an ideal tab length required to be used for characterization. Moreover, studies of the durability behavior of the FRCM composite material and tests on multiple plies systems were conducted, to enlarge the knowledge of this innovative strengthening system.

SOMMARIO

La riabilitazione di edifici esistenti i quali hanno subito deterioramenti a causa di invecchiamento o che necessitano di garantire nuovi requisiti, è da tempo una sfida per l'industria delle costruzioni. I materiali compositi sono largamente utilizzati per riparare elementi strutturali quali travi, colonne, piastre o pareti che necessitano di essere rinforzati. L'obiettivo di questa ricerca è quello di studiare il comportamento a tensione dell'FRCM (Fabric Reinforced Cementitious Matrix), sviluppato in alternativa all'FRP (Fiber Reinforced Polymer). L'FRCM si distingue dall'FRP per avere un tessuto secco con matrice cementizia invece che avere delle fibre impregnate da una matrice organica. Mentre l'FRP ha un comportamento fragile, la matrice cementizia permette un miglior legame con il substrato di calcestruzzo o muratura e offre un'ottima resistenza al fuoco.

Per comprendere meglio i parametri del materiale necessari per la progettazione, test di laboratorio sono fondamentali per determinare il comportamento a trazione, test che al giorno d'oggi non è ancora standardizzato. Due delle più importanti variabili che condizionano il comportamento a trazione dell'FRCM sono la geometria del provino e il sistema di ancoraggio. Per questo studio sono stati utilizzati degli ancoraggi di tipo clevis, vincolati a delle piastre metalliche incollate sul provino e il carico viene applicato tramite taglio sull'area di contatto, la lunghezza della quale è variabile. Questo tipo di ancoraggio è stato scelto poiché più rappresentativo delle condizioni in sito dell'FRCM, dove il tessuto non risulta essere ancorato e il meccanismo di rottura dell'FRCM in tensione è per scorrimento delle fibre all'interno della matrice.

Il principale obiettivo di questo lavoro è quello di capire come la lunghezza di contatto tra le piastre metalliche ed il provino influenzi la relazione sforzo-deformazione, e comprendere se all'aumentare ti tale lunghezza è possibile arrivare alla rottura delle fibre, come accade per l'ancoraggio tradizionale ad incastro, o se esiste un limite e una lunghezza ideale da usare per la caratterizzazione del materiale.

In aggiunta sono stati svolti degli studi sulla durabilità dell'FRCM e sul comportamento di provini con più strati di tessuto.

1.

GENERAL

1.1 Introduction

In the last years, many researches on new composite materials for civil engineering have been undertaken. An interesting alternative to the steel reinforced concrete, the most famous and used composite material in civil engineering, is the textile reinforced concrete (TRC). This innovative composite material is made from a concrete matrix and a textile reinforcement, which may be made by polymer, synthetic (carbon, aramid), metallic (steel) or mineral (glass) materials. Differently from fiber reinforced concrete (FRC), which is made by short disperse fibers, the reinforcement is made by continuous fibers in the form of a mesh or fabric, with filaments aligned in the direction of the tensile stresses, like steel reinforced concrete (Figure 1.1).

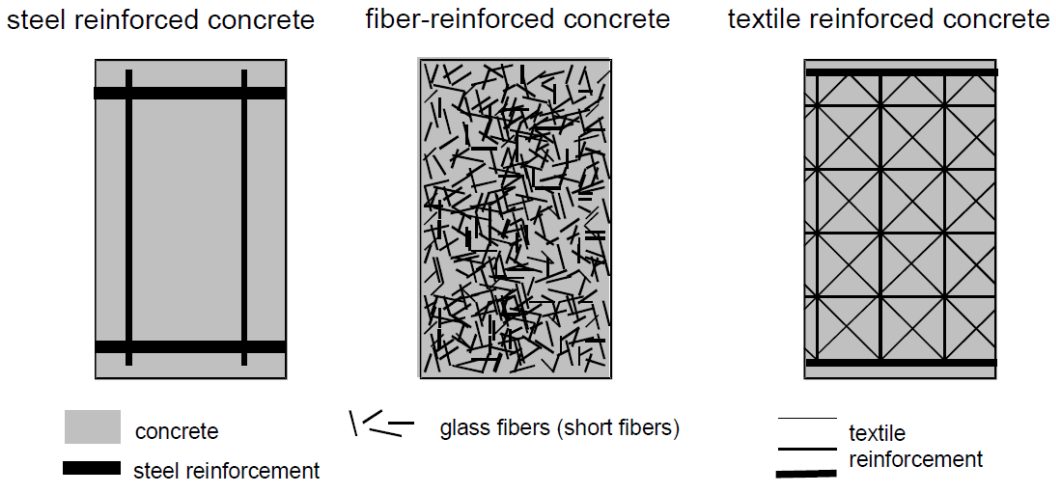

Figure 1. 1 - Different technologies to reinforce the concrete, Hagger et al. (2004)

In this way the load-carrying capacity results much higher with respect to FRC, and this new technology allows to create very thin an light concrete elements with high strength in tension and compression. TRC can be used in new construction or as external repair and strengthening of existing structures that need rehabilitation.

The issue of structural rehabilitation of existing buildings has an important role in Italy, particularly due to the high number and variety of structures that have deteriorated as a result of aging or that need to meet new requirements. This aspect is very critical in our country because many constructions were built according to old seismic codes, but recently the whole national territory was declared under seismic risk. For this reason, there is a need of seismic upgrade in order to be in compliance with the new seismic design. Many rehabilitation techniques have been used in the past, such as steel plate bonding, external post-tensioning and ferrocement, but in the 90's fiber reinforced polymer (FRP) composites started to be used for this purpose because of the advantages related to these composite systems. These types of composite materials are very light and easy to apply, as well as having improved mechanical performances and high corrosion resistance. However, there are some drawbacks related to the organic polymer resin that impregnates the fibers, which are:

- Incompatibility with some substrate materials;
- Poor behavior at elevated temperatures;
- Low ductility at failure;
- Low vapor permeability that can cause moisture accumulation resulting in damage of the substrate;
- Toxicity of the epoxy that can be unhealthy for the installer.

For these reasons, an alternative composite material was developed replacing the organic polymer matrix that characterize the FRP materials, with a cement based matrix. This material is known as Fabric Reinforced Cementitious Matrix (FRCM). The most important difference between organic and inorganic binders is that in the latter case the fabric remains dry, because the cement based matrix cannot fully penetrate and impregnate the fibers. This type of matrix gives the composite material a higher compatibility with the substrate and also allows for reversibility. Unlike FRP, this material provides a good vapor permeability that allows for the preventions of moisture accumulation. The drawbacks associated with this composite are the high coefficient of variance and difficulty related to material characterization.

1.2 Composite materials

A composite material is a heterogeneous material made from two or more different phases with different physical properties, that work together in order to obtain a new material with better mechanical properties.

The matrix is the weaker part and may be considered, at least in the first approximation and for usual composite materials, a continuous homogeneous and isotropic material. As a result, it can be characterized from a mechanical viewpoint, knowing the two independent properties (for example E and G). The other part is dispersed in the matrix and it is the stronger phase, which is a continuous homogeneous anisotropic material called the reinforcement. This dispersed phase is also characterized by its:

- Geometry: shape, size and size distribution;
- Orientation: orientation of the fibers with respect to the geometrical axis of the body;
- Concentration: volume fraction and concentration distribution.

The composite system that arises from this combination is always a non-homogeneous and often anisotropic material.

The most common reinforcing fibers are:

- Glass: has the advantages of low cost and high resistance but on the other hand has a low elastic modulus, high density, is sensitive to humid environments and has a low fatigue resistance;
- Carbon: is a material with high elastic modulus, high strength and low density, but the cost is higher and has a low deformation at fracture;
- Aramid: are polymeric synthetic fibers with high toughness, high strength and low cost, but the limitations of low compression strength and low UV resistance.

In order to design for a composite material, it is fundamental to know the various properties related to its mechanical behavior, for example the elastic modulus E and ultimate tensile strength. One way to obtain a theoretical upper and lower bound of the elastic modulus of the composite is by using the general rule of mixtures, that is a weighted mean between the elastic moduli of the matrix (E_m) and of the fiber (E_f), knowing their respective volume fraction.

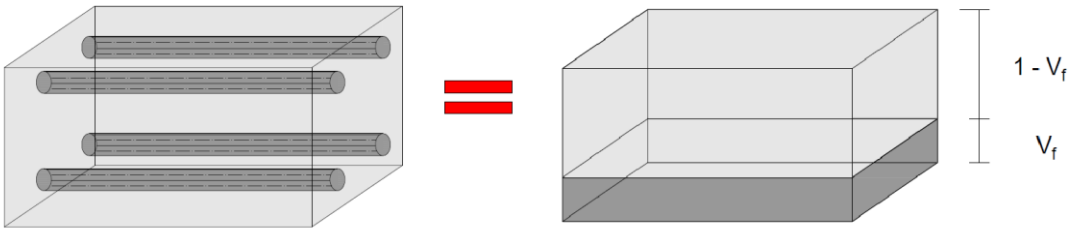

Figure 1. 2 - Simplified composite material model

In Figure 1.2 is shown a very simple model in which both the fiber and the matrix are represented by a solid block with the volume proportional to their relative abundance in the composite. The volume fraction of the fibers is:

$$v_f = \frac{V_f}{V_f + V_m}$$

Where:

- V_f is the volume of the fibers:
- V_m is the volume of the matrix.

It is thus possible to derive the longitudinal elastic modulus of the composite E_{11} (with the fibers parallel to the direction of the load) and the transverse's modulus E_{22} (with the fibers perpendicular to the load). In the first case the matrix and the fibers undergo the same deformation, behaving as parallel springs, while in the second case the two phases have the same stress state, like two springs in series. Considering this the results are:

$$E_{11} = E_f v_f + E_m v_m = E_f v_f + E_m(1 - v_f)$$

$$E_{22} = \frac{E_f E_m}{E_f v_m + E_m v_f}$$

Where:

- E_f is the elastic modulus of the fibers;
- E_m is the elastic modulus of the matrix;
- v_f is the volume fraction of the fibers;
- v_m is the volume fraction of the matrix.

In the first mixture rule, if there is a property of a material that is much higher than other material it is possible to neglect the contribution given by the second material. For example, it is possible to neglect the contribution of the matrix in the equation for E_{11}, being $E_m \ll E_f$ in most cases. On the other hand, in the second mixture rule the lower property will be predominant as in the case of the equation to compute E_{22}, where the contribution of the matrix prevails. Figure 1.3 represents the mechanical behavior of a composite material where the ultimate strain of the matrix is higher than that of the fiber.

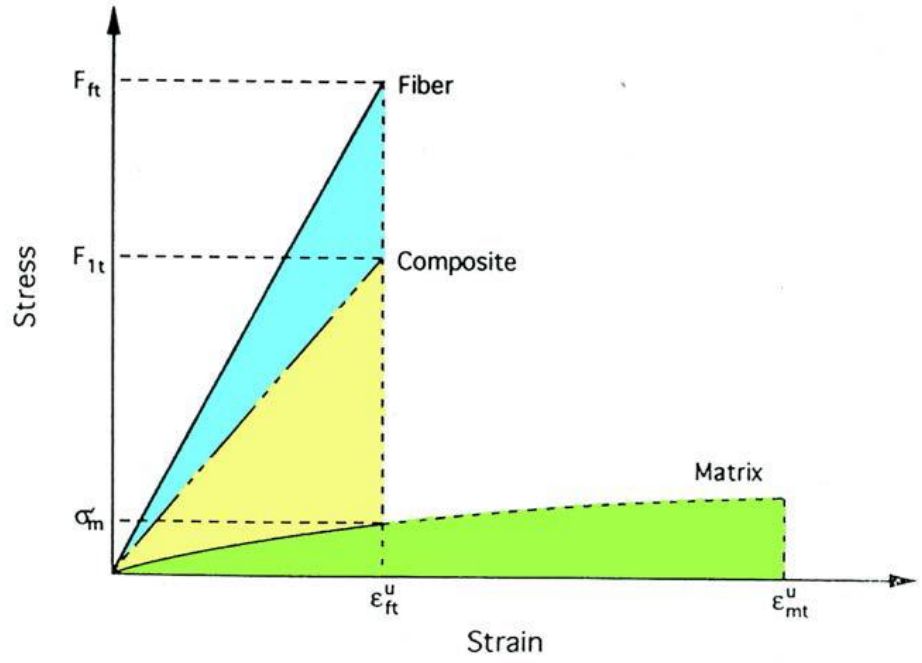

Figure 1. 3 - Mechanical behavior of organic polymer matrix composite

These very simplified models give very good results, compared to the experimental outcomes, for the longitudinal characteristics of the composite, but not very precise results in the transversal direction.

The graph shown in Figure 1.4 indicates the upper (E_{11}) and the lower (E_{22}) bound for the elastic modulus of the composite with varying fiver volume. Below the value of $v_f = 0.15$ the material is no longer a composite, and above $v_f = 0.70$ is not possible to go (0.90 theoretically speaking and 0.5 for most of the application).

A composite material is considered a non-isotropic material, so its properties change on the basis of the direction in which the load is applied. For a given value of the fibers volume fraction $\bar{v}_f$, the elastic modulus of the composite is in between the

lower bound $E_{22}(\bar{v}_f)$, obtained with an angle θ between the fibers and the applied load equal to 90°, and the upper bound $E_{11}(\bar{v}_f)$, for which the angle θ is equal to 45° (Figure 1.5).

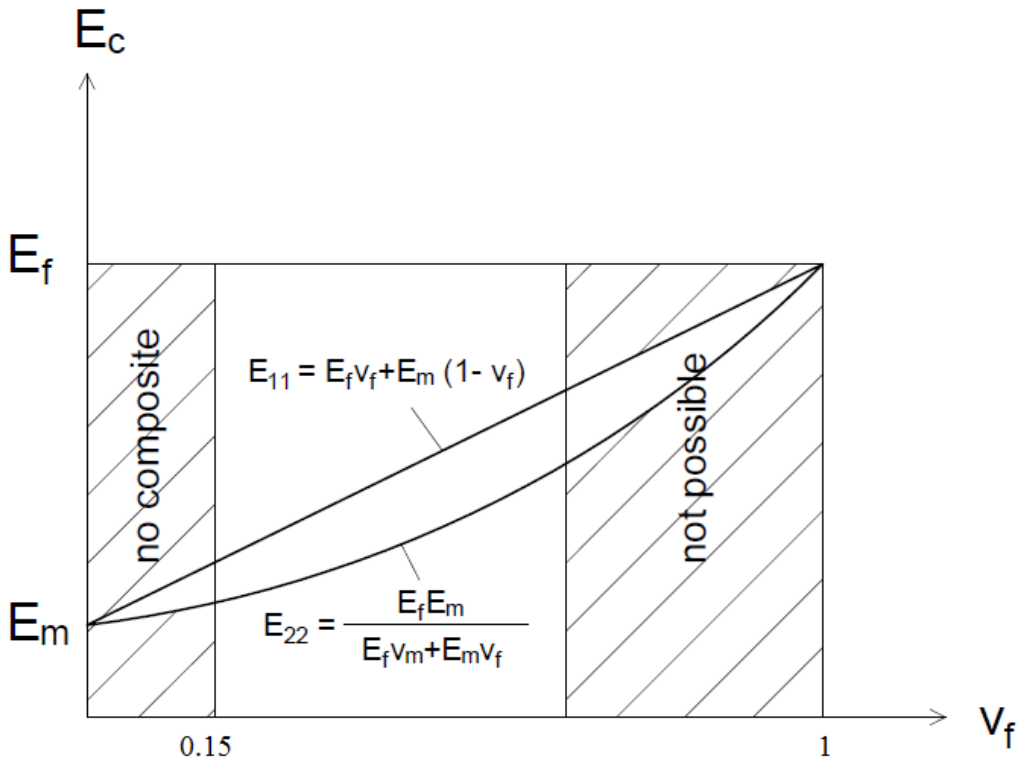

Figure 1. 4 - Upper and lower bound for the elastic modulus

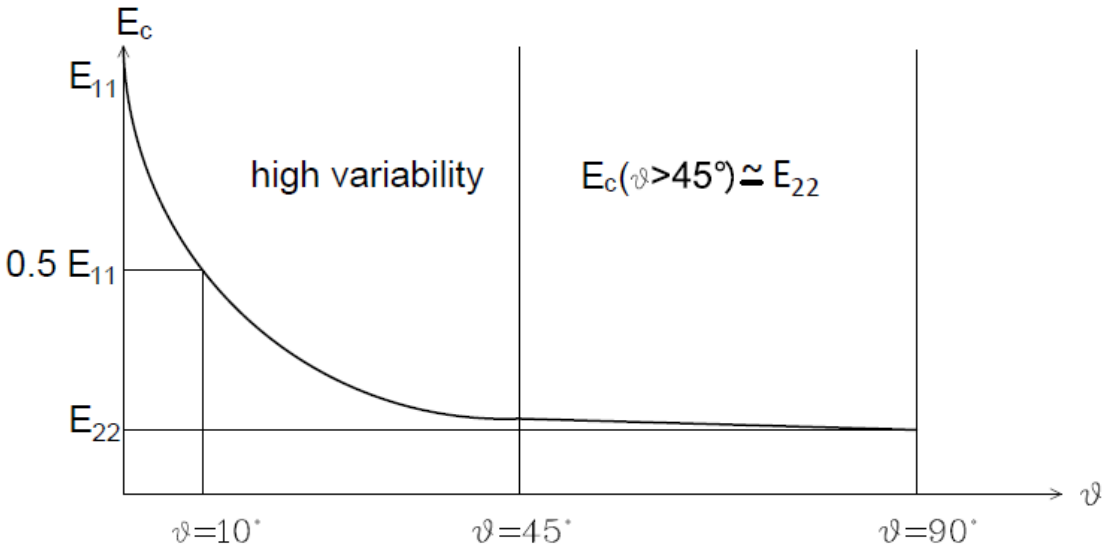

Figure 1. 5 - Elastic modulus for different direction of the load

Composite materials are widely used in the aerospace and transportation industries where low weight and high mechanical properties are required. By using them, it is possible to combine cost savings and high performance. They are also used extensively in the sport field in order to build skis, bicycles or tennis rackets, for example, and in the bioengineering to make prosthesis (Figure 1.6).

Figure 1. 6 - Example of composite material applications

In civil engineering the most commonly used composite material is steel reinforced concrete. The concrete, which is already a composite material made from aggregates and cement as a matrix, has very low tensile resistance, so it is reinforced with steel bars in order to bear tensile loading. Fabric composite materials are beginning to be used in the construction industry with the purpose of rehabilitation because of their characteristics of light weight, flexibility and simplicity of application (Figure 1.7).

Figure 1. 7 - Examples of composite material applications in civil engineering

1.3 FRCM Composite material: description and application

FRCM (Fiber reinforced cementitious matrix) is a composite material consisting of one or more layer of cement based matrix with a maximum organic content of 5%, reinforced with dry fibers in the form of open mesh or fabric (Arboleda, 2014). The organic compounds are used to ensure a proper workability and mechanical properties.

This composite is an example of brittle matrix composite material, due to the brittle characteristics of the mortar matrix, and has a very different behavior than that of a polymer matrix composite. For a polymer composite material, such as FRP, the strain limit of the matrix is higher than the strain limit of the fiber and the rule of mixtures can be applied. In the case of brittle matrix composite material, the rule of mixtures cannot be used because the strain limit of the matrix is much lower than that of the fibers. Therefore if we apply a tensile force to the FRCM before reaching the limit strength of the composite, the matrix will crack and the fiber will debond and slip, producing a pseudo-ductile behavior. In field applications, when FRCM is used to strengthen structural elements, the full strength of the fabric is not reached, and failure is slippage between fibers and the matrix, not breaking of the fibers.

FRCM was developed for rehabilitation applications, particularly for structures made of masonry or concrete. In order to be applied to the element that needs to be strengthened, the surface has to be cleaned and completely saturated. Then the excess water on the surface has to be removed in order to have a saturated-surface-dry (SSD) condition. Once the surface is ready, a first layer of mortar, prepared by mechanical mixing, is applied using a trowel. After this, the fabric (can be more than one layer) is applied on the mortar, with the orientation of the fibers in the direction of the load. Depending on the application, it is possible to apply more than one ply of fabric. A curing period of 28 days is necessary to reach the full strength of the FRCM. The process described is shown in Figure 1.8.

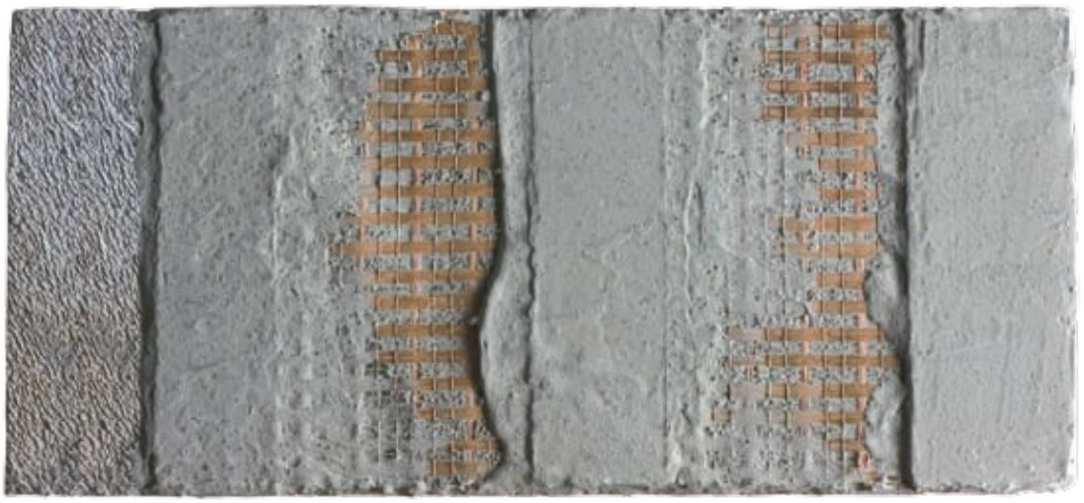

Figure 1. 8 - FRCM Application, Leardini et al. (2013)

The way in which FRCM is applied to a structure depends on the type of structural element that needs to be strengthened. Different structural elements that can be reinforced with this composite material are walls, slabs, beams and columns.

In the case of beams and slabs, it is possible to increase the flexural stiffness placing the material at the intrados of the beam, with the fibers in the direction of the tensile stress, as it is shown in Figure 1.9.

In order to perform shear reinforcement of beams the material is applied to the structural element with a U-wrap configuration, as shown in Figure 1.10. In this case, the resistance mechanism is very similar to that of stirrups.

To reinforce concrete columns, the FRCM material is wrapped around the column, with the fabric in the direction perpendicular to the axis of the column as represented

in Figure 1.11. In this way, confinement is provided and vertical elements of the structure can sustain higher axial loads.

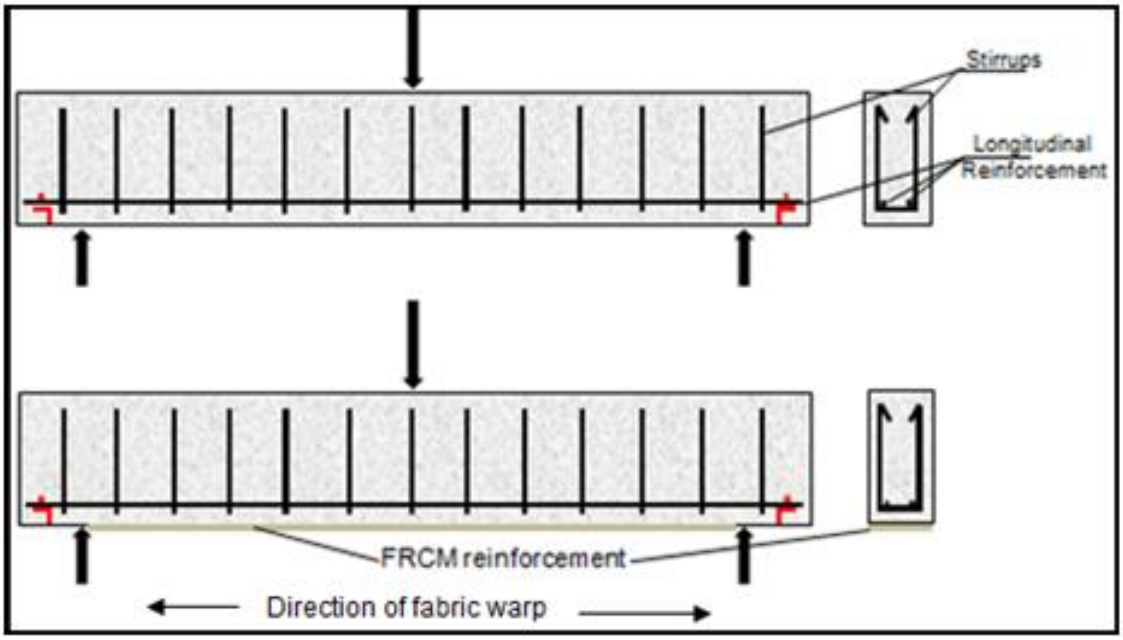

Figure 1. 9 - Flexural reinforcement with FRCM, Arboleda et al. (2014)

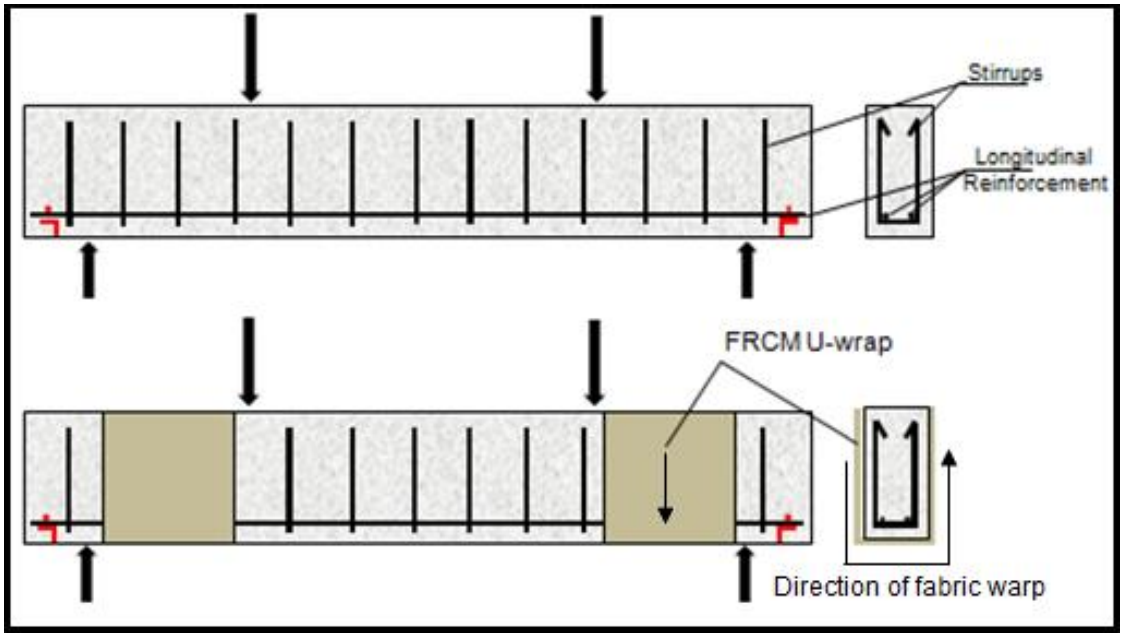

Figure 1. 10 - Shear reinforcement with FRCM, Arboleda et al. (2014)

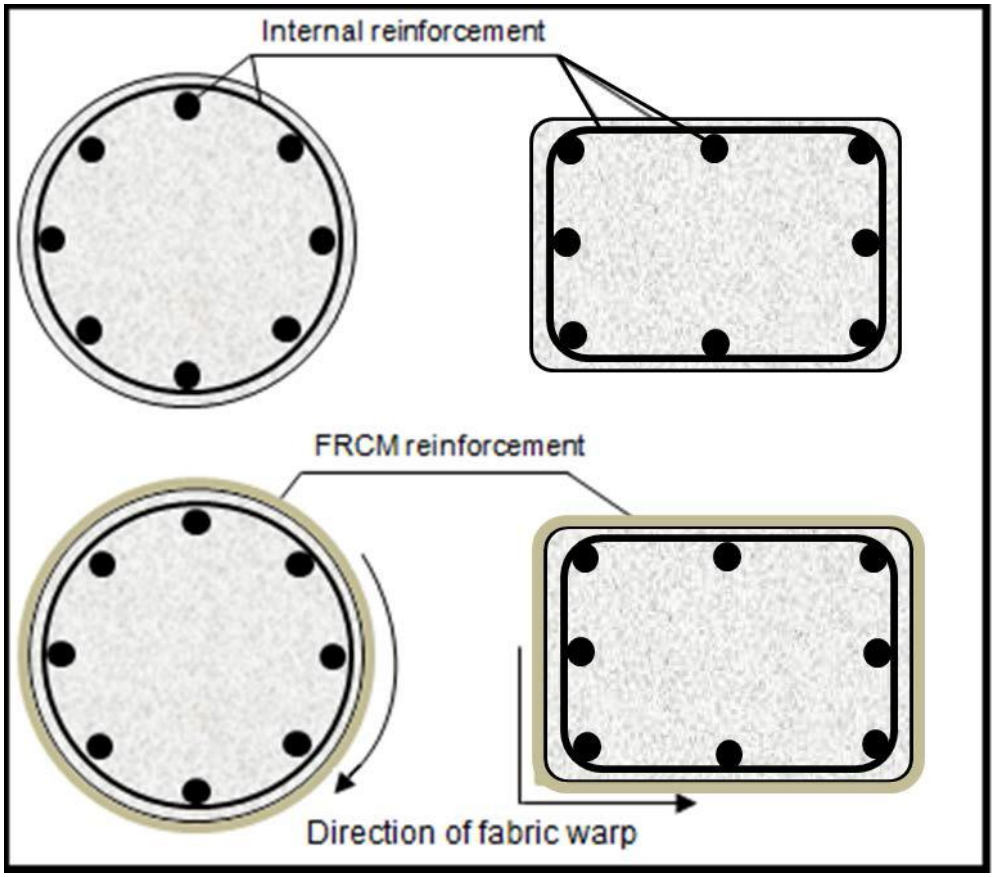

Figure 1. 11 - Column reinforcement with FRCM, Arboleda et al. (2014)

Masonry walls are strengthened using a balanced fabric mesh, which is a fabric with the same reinforcement ratio in both directions (Figure 1.12).

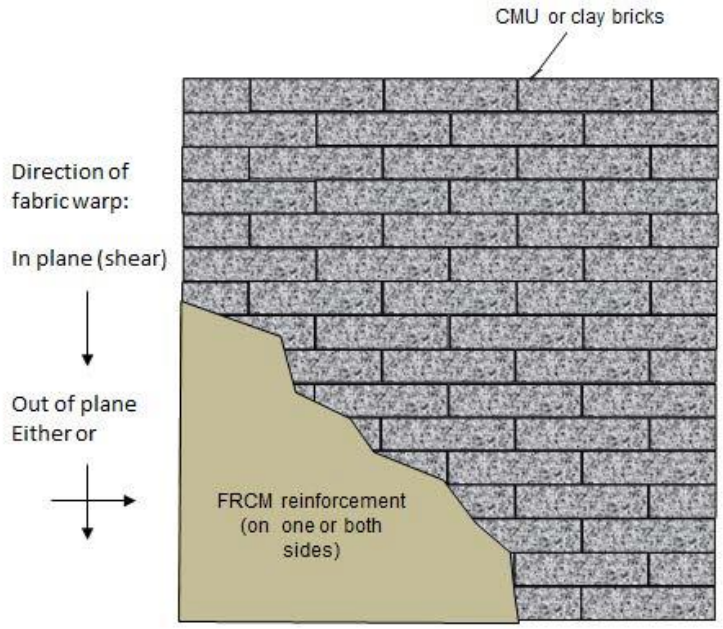

Figure 1. 12 - Reinforcement of a masonry wall with FRCM, Arboleda et al. (2014)

1.4 FRCM systems: technical specifics

The FRCM system is a combination of an inorganic matrix and a fiber mesh. Two different types of mesh were studied in this work:

- Unidirectional carbon-mesh L600: a mesh used for structural strengthening in the longitudinal direction;
- Bidirectional carbon-mesh 200/200: a mesh used for structural strengthening in both directions.

The mortar used was the same for both of the two systems. The two Carbon-FRCM systems studied are used for static retrofitting (flexural, axial, shear) of RC structures.

1.4.1 Unidirectional system

In Table 1.1 all the properties of the materials provided by the manufacturer are listed. The properties are divided into fibers properties, fabric properties and mortar properties.

Table 1. 1- Technical specifics of the unidirectional system

Carbon Fiber Properties	**Units**	**Value**
Density	g/cm^3	1.79
Tensile strength	GPa	4.00
Modulus of elasticity	GPa	240
Ultimate deformation	%	1.50

Unidirectional carbon-mesh L600 Properties	**Units**	**Value**
Weight of the fabric	g/m^2	280.8
Equivalent dry fabric thickness in the direction of the warp	mm^2/mm	0.157
Ultimate tensile strength of the warp by width unit	kN/m	628
Ultimate tensile strain of the warp by width unit	%	1.5

Mortar Properties	**Units**	**Value**
Specific weight of fresh mortar	g/cm^2	2.05 ± 0.05
Liters of water per 100 kg of MORTAR		15 - 17
Yield (dry product)	$kg/m^2/mm$	2.0 – 2.2
Compressive strength (28 days)	MPa	> 45.0

1.4.2 Bidirectional carbon system

In Table 1.2 all the properties of the materials provided by the manufacturer are listed. The properties are divided into fibers properties, fabric properties and mortar properties.

Table 1. 2 - Technical specifics of the bidirectional system

Carbon Fiber Properties	Units	Value
Density	g/cm^3	1.79
Tensile strength	GPa	4.00
Modulus of elasticity	GPa	240
Ultimate deformation	%	1.50

Unidirectional carbon-mesh L600 Properties	Units	Value
Weight of the fabric	g/m^2	80
Weight of Carbon fibers in the fabric	g/m^2	-
Equivalent dry fabric thickness in the direction of the warp	mm^2/mm	0.044
Ultimate tensile strength of the warp by width unit	kN/m	176-211
Ultimate tensile strain of the warp by width unit	%	1.5-2.0

Mortar Properties	Units	Value
Specific weight of fresh mortar	g/cm^2	2.05 ± 0.05
Liters of water per 100 kg of MORTAR		15 - 17
Yield (dry product)	$kg/m^2/mm$	2.0 – 2.2
Compressive strength (28 days)	MPa	> 45.0

1.5 Examples of FRCM application

To better understand the different ways of application of the FRCM composite material as a strengthening system, four examples of design with this material are presented in this section. Being a very new and innovative technology of structural repairing, there are only few examples of application so far.

1.5.1 Unreinforced concrete vault strengthening

This example of FRCM application regards the strengthening of a bridge along the Rome-Fornia-Naples railway in Italy (Berardi et al. 2011, Nanni 2012). The bridge deck is supported by six unreinforced concrete arches with a semicircular shape, which are supported by masonry abutments made of blocks of tuff. The span covered by the arches is approximately the same and the thickness varies between 0,7m at the crown and 1,0 m at the skewback, while the deck width is 10,5 m (Figure 1.13).

Figure 1. 13-Unreinforced concrete vault strengthening

The objective of the strengthening intervention was to change the collapse mechanism identified with a limit state analyses, increasing the safety against collapse. The FRCM was applied to the intrados surface of the arches preventing the formation of the extrados hinges. The repair intervention has the intention of modifying the ultimate behavior of the structure without changing the behavior under service loads. In order not to interrupt the use of the bridge, it was decided to strengthen the intrados instead of the extrados. In order to install the FRCM system, firstly the concrete surface of the arches was cleaned and the deteriorated portions of concrete were removed and replaced. Then, a first layer of cementitious matrix with a thickness of approximately 5 mm was applied on the concrete surface, followed by a first layer of fabric. After ensuring a good impregnation of the fibers through pressure of the fabric in the mortar, a second thinner layer of mortar was applied. Finally a second layer of fabric and the last layer of mortar were applied.

The great advantage of this intervention was the fact that was very fast and relatively easy to perform, and was possible without interrupting the train traffic.

1.5.2 Trestle bridge base confinement

This FRCM application provides confinement to the concrete support base for the trestle of a railway bridge in New York State (Nanni 2012). The pedestals that support the structure have a truncated pyramid shape and the dimension vary depending on the configuration of the ground (Figure 1.14).

Figure 1. 14- Trestle bridge base

Over the years cracking and spalling occurred significantly but, although the bad conditions, the performance of the support base is not affected (Figure 1.15). The focus of this repairing intervention was the long-term durability of the element. First of all the deteriorated concrete was removed and replaced with a fast-set concrete repair material. Then the trestle surface was prepared by grinding to provide a good bond between the concrete surface and the cementitious matrix of the FRCM system. After that, the first layer of mortar was applied to the concrete surface, followed by the fiber mesh. Ensuring a sufficient impregnation of the fabric by pressure, the final layer of mortar was troweled onto the fabric layer.

Figure 1. 15 - Trestle confinement

1.5.3 Strengthening of unreinforced masonry chimney

This example is about the strengthening of the masonry chimney part of the sawmill Francois CUNY complex located in the municipality of Gerardmer, France (Nanni 2012). The chimney made by clay bricks with sand-lime joints is 38 m high, with a diameter between 1,70 m at the top and 3,60 m at the base (Figure 1.16). The

structure was modeled as a cantilever beam subjected primarily to wind loads. The structural analyses indicated the need of a single ply FRCM strengthening.

Figure 1. 16 - Strengthening of unreinforced masonry chimney

1.5.4 Strengthening of reinforced concrete bridge pier

This FRCM repairing intervention relates the strengthening of a reinforced concrete bridge pier in Novosibirsk, Russia. The piers were reconstructed in 1958, but a severe cracks propagation was caused by temperature and shrinkage stresses. In 1991 the cracks were epoxy-injected, but inspections in 1997 revealed that the cracks had reopened, with widths ranging from 2 to 5 mm. For this reason in 2007 it was decided to make an intervention with FRCM, and the steps were the following:

- Sand-blasting the concrete surface;
- Rounding the corners to a radius of 30 mm;
- Repairing the cracks and resurfacing with single-component polymer modified cementitious mortar;
- Strengthening with FRCM;
- Surface sealing with a two-component, polymer-modified, cementitious waterproofing and protective slurry.

Figure 1. 17 - Strengthening of reinforced concrete bridge pier

1.6 Objectives

The focus of this research is the tensile characterization of two different FRCM system, composed of the same mortar but one having a unidirectional carbon fabric and the other having a bidirectional balanced fabric mesh. This characterization was done using a tensile test, following the procedure given by the Acceptance Criteria AC434. One of the variables that strongly influence the tensile performance of a FRCM system is the gripping configuration. Following AC434, clevis-type grips were used, where the load is transferred from the machine to the specimen using metal tabs that are glutted to it. The contact length is a variable of this test and the main target of this work is to understand how the tab length affects the strain-stress behavior as well as finding an optimal contact length to test this material.

In addition, this research wants to underline the different behavior of single and multiple layer systems and for this reason specimens with one and two plies of fabric were tested.

Another aspect that was studied is the effect of lap splices on the specimens, because splices are necessary in the field. The objective is to understand if these splices represent a weak section and to find the right development length to avoid any degradation of composite properties.

In the second part of the thesis, the effects of several aging procedures on the system are discussed. To do this, some specimens were tested after exposure to different environments and the results were compared with the specimens tested in controlled conditions.

2.

MECHANICAL PROPERTIES OF FRCM COMPOSITE

Every material needs to be tested in order to find parameters to describe the material's behavior under different load conditions, and these mechanical properties are fundamental for design. In this chapter a literature review will be presented, regarding the mechanical behavior of the FRCM system and the different tests performed on it, which are related to the properties under investigation.

2.1 Mechanical behavior of the FRCM system

In order to better understand how to use FRCM systems for repair applications, it is very important to know its behavior under load conditions. A good description was given by Ombres (2012): as soon as a crack is formed in the concrete because of its low tensile capacity, the tensile stresses released by the concrete are transferred to the strengthening plate, thanks to the capacity of the interfacial bond to carry shear stresses. As the applied load increases together with the required tensile strength of the plate, the cementitious-based bond between the fabric and the concrete become more critical. Finally, when the shear stress applied on the plate reaches its maximum capacity the system fails.

There are four different failure modes for an external reinforcement system, (D'ambrisi 2011), shown in Figure 2.1:

a) Fracture surface within the concrete;
b) Slippage of the fibers from the matrix;
c) Fracture surface at the matrix/concrete interface;
d) Debonding in the net layer.

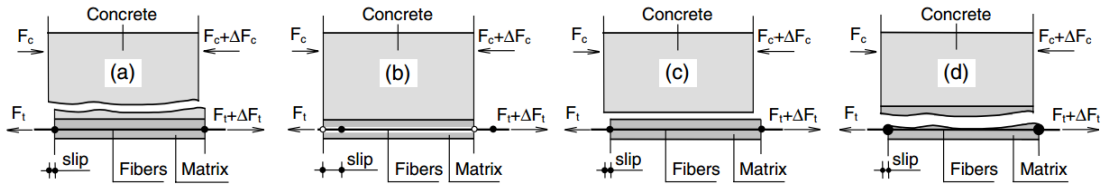

Figure 2. 1 - External reinforcement failure modes, D'ambrisi et al. (2011)

The failure modes that are more likely to occur for a beam strengthened with FRCM are the slippage of the fabric from the mortar b) and the debonding in the net layer d), and these depend on the number of plies of fabric applied, as will be explained later. We do not expect a fracture surface at the matrix/concrete interface because of the good compatibility between the mortar and the concrete substrate. This type of failure is most frequent with FRP composite materials, where the inorganic matrix cannot create a perfect bond with the concrete surface.

Moreover, due to the similar tensile resistance of the mortar and the concrete, the failure mode a) is not expected to occur in FRCM system, while it is possible with FRP because the inorganic binder has a tensile resistance that is one order of magnitude higher than the concrete.

As it was stated before, the failure modes that characterized FRCM system strongly depend on the number of plies applied to the structural element that needs to be reinforced (Ombres 2009). If a beam is reinforced using one ply of fabric with a sufficient bond length, the failure will be slippage between the fibers and the cementitious matrix (Figure 2.2) while, with a four-plies reinforcement, the system will experience a delamination of the FRCM from the beam (Figure 2.3).

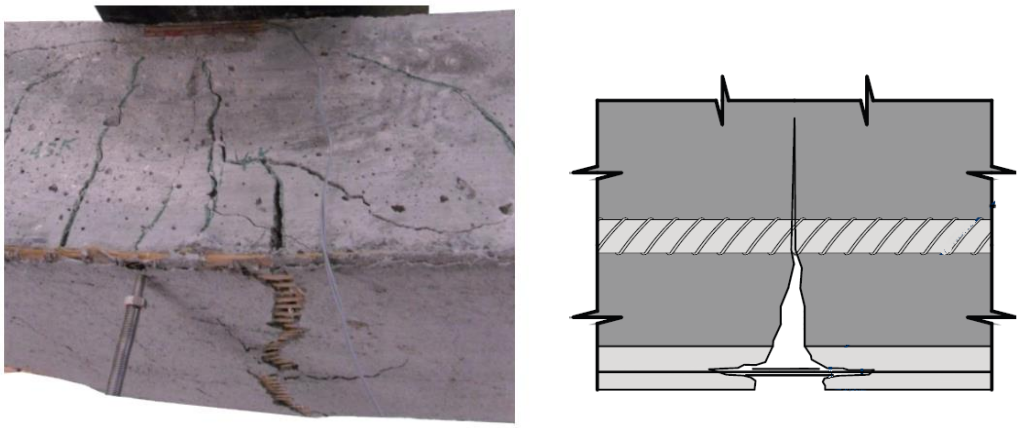

Figure 2. 2 - Slippage failure of a FRCM system, Loreto et al. (2013)

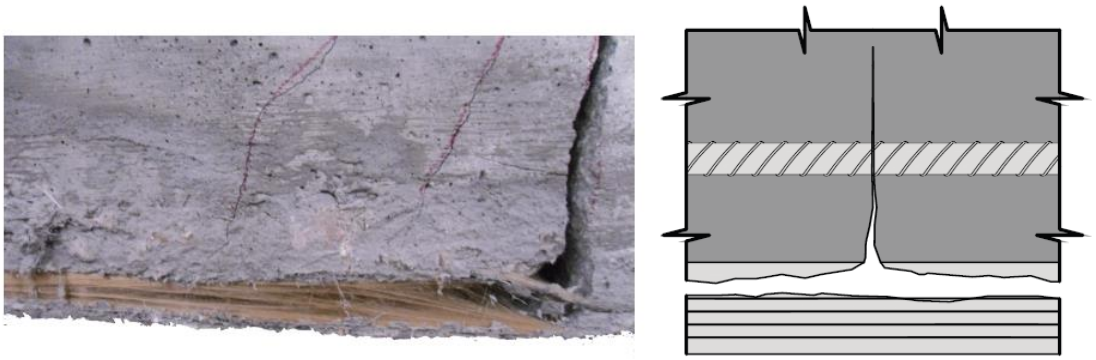

Figure 2. 3 - Delamination failure of a FRCM system , Loreto et al. (2013)

One of the big differences between FRCM and FRP is that the cementitious matrix cannot fully impregnate the fibers that remain "dry". This fact can be seen also in the slippage failure that is called "telescopic failure": the fibers impregnated by the mortar break while the core of the inner filaments of the strand slide inside the matrix leaving a void behind, as it is well represented in Figure 2.4.

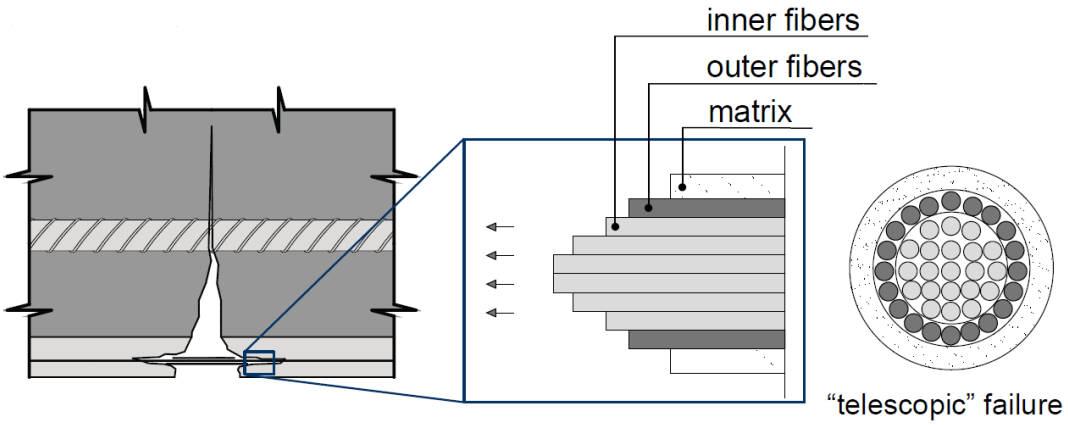

Figure 2. 4 - Telescopic failure

Researches in literature (D'ambrisi and Focacci 2011) about the flexural strengthening with one ply of FRCM show debonding of the fibers from the matrix as the failure mode. The slippage occurs in maximum bending moment regions, where the cracks propagates from the concrete substrate to the mortar exposing the fibers to the environment. The slippage phenomenon is a desirable behavior of this system because it leads to pseudo-ductility and allows for identification of the damaged regions.

After the opening of cracks in the mortar, the load is completely carried by the adhesion capacity between the fibers and the mortar. The effectiveness of the adhesion depends on different aspects:

- The chemical bond that the fiber is capable to establish with the cementicious matrix;
- The presence of fibers in the orthogonal direction;
- The friction itself between the fibers and the mortar;
- The friction itself between the fibers of the same strand.

As far as the debonding failure mode is concerned, it is defined in literature (D'Ambrisi et al 2011) as the delamination in the net layer of the FRCM plate, with a fracture surface within the matrix in the constant moment region, after a significant slippage between the fibers and the matrix (Figure 2.5). This type of failure is brittle.

Figure 2. 5 - Debonding failure occurred in a four-plies strengthened beam, Leardini et al. (2013)

After a debonding failure, was observed in most cases that a thin layer of mortar remained attached to the concrete surface, while the failure surface was in the layer with the fibers, because the fabric breaks the continuity among the matrix plate. This happens also because the fine graded mortar cannot fully impregnate the fiber strands (Banholzer 2004; Hartiget al. 2008; Hegger et al. 2006; Soranakom and Mobasher 2009; Wiberg 2003; Zastrau et al. 2008). As observed by different authors (Curbach et al. 2006; Ortlepp et al. 2004, 2006), another parameter that influences the behavior of the FRCM system is the density of the fabric net (i.e. quantity and spacing between the strands in each direction). As observed by Badanoiu and Holmgren (2003), the surface of the matrix/roving interface should be maximized because in the free spaces

present in the fabric the continuity of the matrix is ensured. Thus, a good solution is to reduce the dimension of the strands and to increase the number of strands.

2.2 Tensile properties

The tensile test on FRCM has the scope to understand the behavior of this repairing composite material in tension and to find the values necessary for the design of a strengthening system. Different types of specimen geometries and gripping mechanisms were used in the literature.

2.2.1 Different gripping mechanisms

In order to describe the tensile behavior of the FRCM systems, different gripping mechanisms and specimen geometries were used in literature. An interesting research was conducted by Stefano De Santis and Gianmarco De Felice (2014), who experimented five different clamping methods to identify the appropriate set-up. One of the results of this research is that the behavior of the specimen in tension and the measured ultimate strength are significantly influenced by the clamping method.

The five gripping mechanisms studied are divided in two groups, which reflects the different ways of application of this composite material. In the first group, three testing set-ups are analyzed, where the load is applied directly to the fabric and in this way is possible to capture the behavior of the FRCM composite in those structural application in which the load is applied to the fabric (i.e. confinement of columns or strengthening of arches and vaults with anchorages of the textile reinforcement).

The first clamping method is realized clamping the textile which come out from the free of mortar ends of the specimen. However, this way of testing the composite leads to a premature failure of the fibers at the edge of the grips, and the ultimate strength is underestimated (Figure 2.6 b). To avoid the cut of the fabric by the grips, a second gripping mechanism with aluminium tabs glutted on the fabric was developed. The aluminium was chosen for its higher deformability with respect to steel, which provides a better stress transfer. With this gripping mechanism the fabric failed at the beginning of the mortar, because of a localized variation of the axial stiffness (Figure 2.6 d). The third gripping mechanism was developed with the objective of avoiding the premature failure in proximity of the matrix ends, and for this reason a FRP reinforcement made by a bidirectional carbon fabric glutted with epoxy resin was

applied to the specimen ends. After that, the aluminium tabs were glutted. With this third gripping mechanism no premature failure was observed, and the full development of transverse crack was observed during the test (Figure 2.6 f). The three gripping mechanisms of the first group are shown in Figure 2.6 (a, c, e).

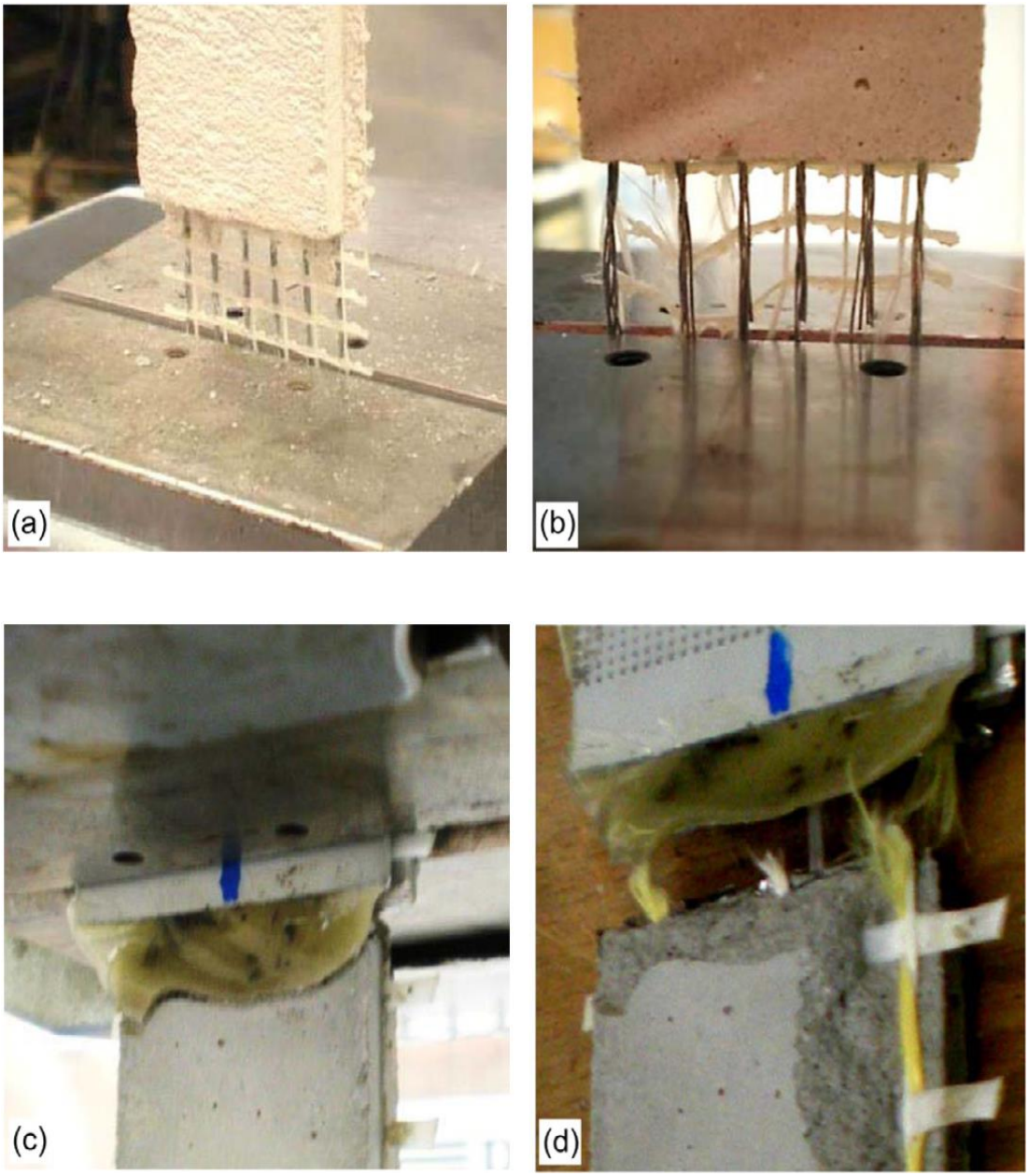

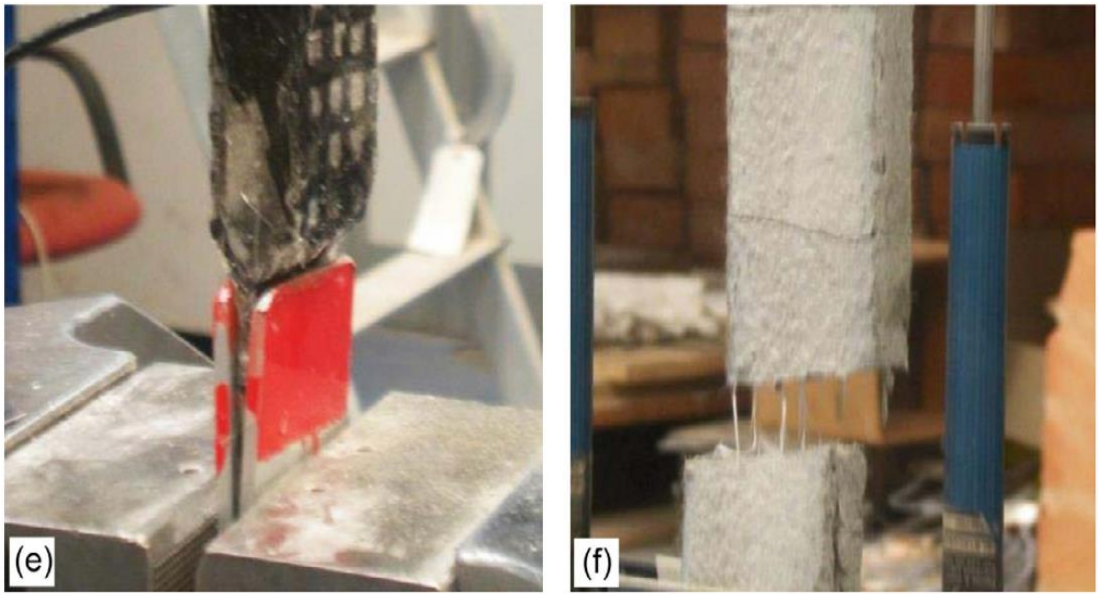

Figure 2. 6 - Gripping mechanism group one: clamping of the fabric, De Santis and De Felice (2014)

In the second group two testing set-ups were analyzed, where the load is applied to the mortar, reflecting those applications where the load is transferred from the substrate to the matrix (i.e. strengthening of masonry walls, bending reinforcement of beams, panels and jack arches).

The first gripping mechanism of this group is the clevis-type grip, in which the load is transferred to the specimen by surface shear trough metal tabs glutted on the specimen. This set-up do not clamp the specimen avoiding parastitic bending moments, and it is the set-up suggested by the US standard AC434. Testing the material in this way, the rapture of the fabric is not reached and the failure is due to slippage of the fabric within the mortar (Figure 2.7 h). In the last gripping mechanism studied in this research, the specimen is clamped directly on the mortar previously reinforced with FRP in the gripping areas, in order to prevent crushing. This gripping mechanism avoid the slippage between fabric and mortar and the failure of the specimen is due to fiber rapture (Figure 2.7 j).

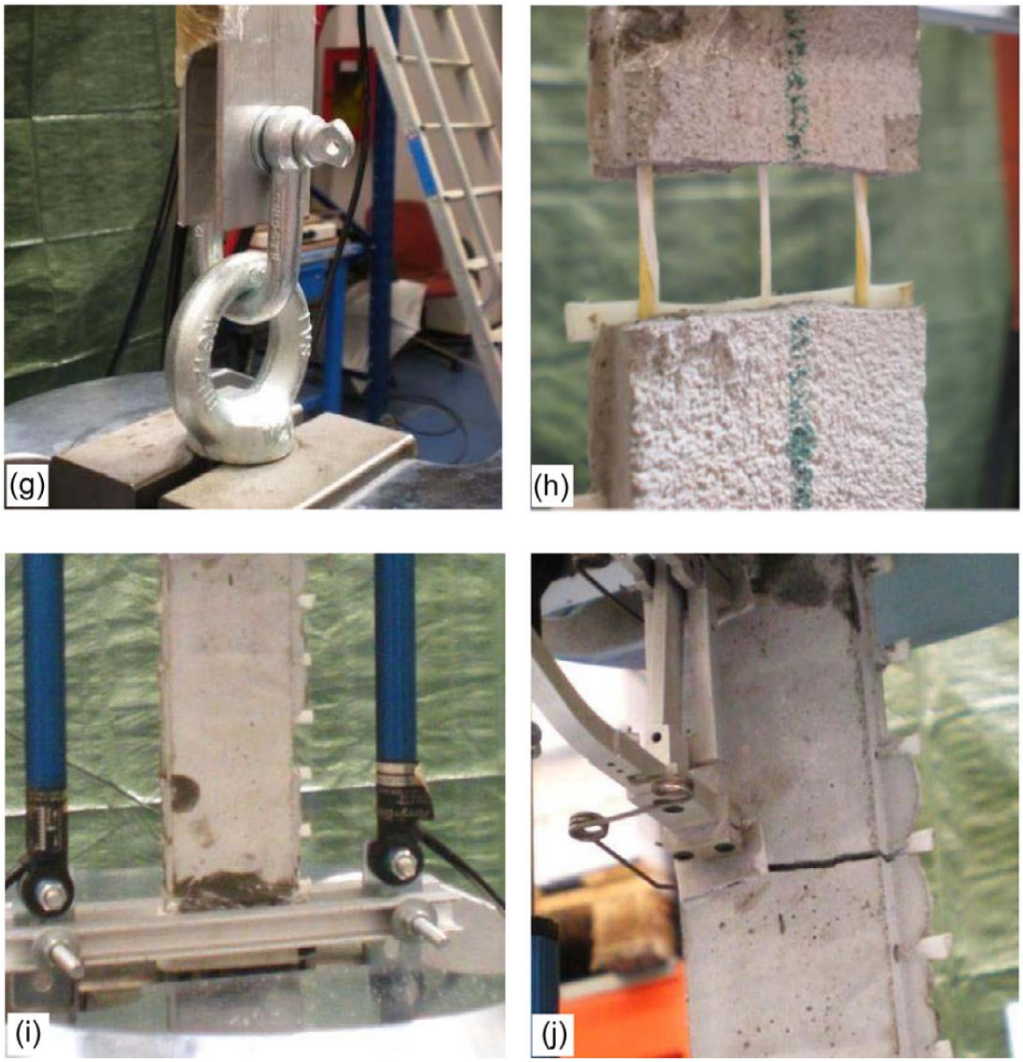

Figure 2. 7 - Gripping mechanism group two: constrain on the mortar, De Santis and De Felice (2014)

A very good summary of the different tensile tests which have already been undertaken was done by Contamine et al. (2011), who analyzed previous works on tensile test characterized by different specimen shapes, gripping mechanisms, displacement rate and procedures for measuring deformation.

Four different specimen geometries were analized by Contamine et al. :

- Rectangular parallelepiped of easy implementation (Figure 2.8 a), d), h));
- Dumbbell geometry, characterized by end sections gradually increased in thickness to ensure the transmission of the force (Figure 2.8 b));
- Bone shape specimen, where the end section gradually increase the width (Figure 2.8 e), f));
- V-notched parallelepiped, which locates the failure (Figure 2.8 c)).

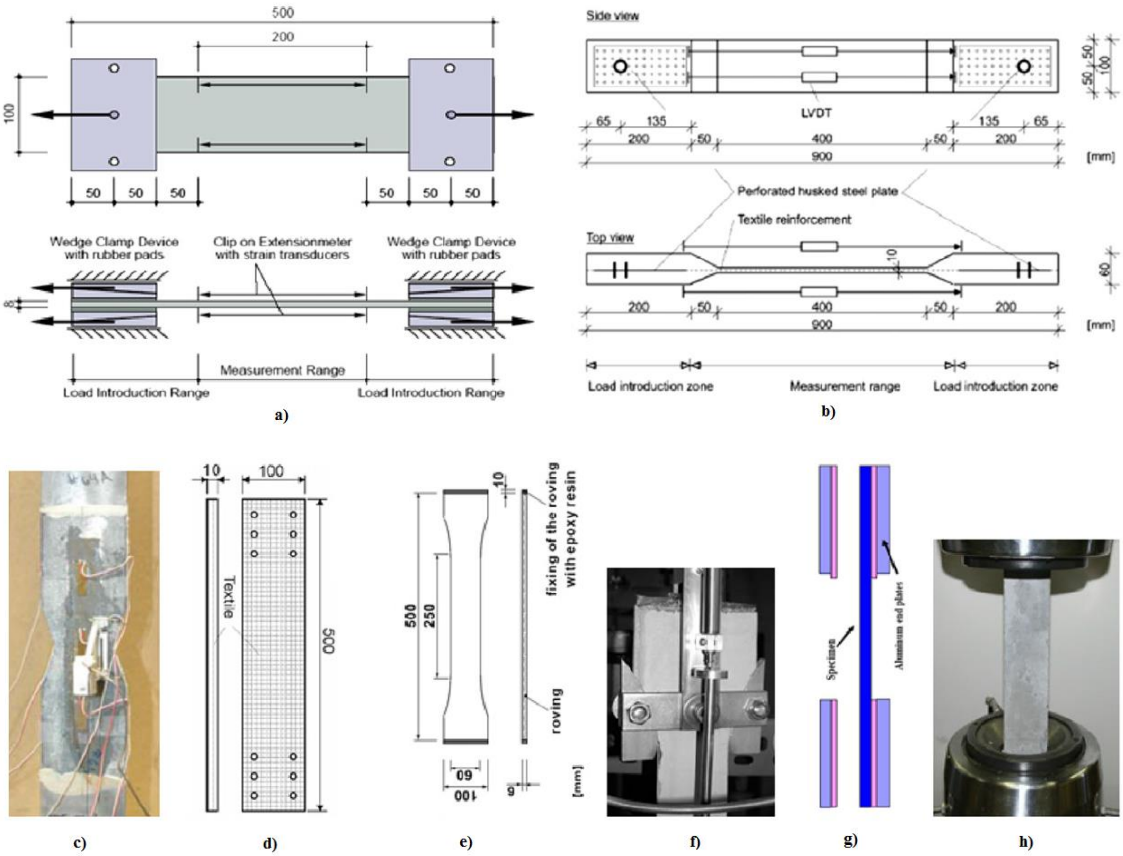

Figure 2. 8 - Different specimen shapes and gripping mechanisms, Contamine et al.(2011)

As far as the different gripping mechanisms are concerned, they were summarized in normal clamps (Figure 2.8 g), h)), clamps adapted to bone-shaped specimens (Figure 2.8 f)) and gripping mechanism were the load is transferred to the specimen through one or more steel cylinders passing through the specimen at the end plate. Contamine believes that clamps are not adequate for testing FRCM material because they introduce a parastitic compressive force that artificially increases textile-mortar interaction and, as a consequence, the ultimate strength.

Different techniques to measure the strains were used in literature, as strain gauges, LVDT (Figure 2.8 b)), extensometers (Figure 2.8 a)) and also the displacement measured by the machine.

Finally the displacement rate, constant for all the authors, ranges between 0.5 mm/min and 10 mm/min. Contamine writes in his work that speeds close to 1 mm/min are relatively more in line with static characterization.

2.3 Bond adhesion properties

In order to design a structural reinforcement with FRCM, is important to know not only the mechanical properties of the composite material itself but also its bonding resistance to the substrate. In fact, strength and adhesion are the essential properties to characterize a repairing system like FRCM. Adhesion between the strengthening system and the element that needs to be strengthen is fundamental to ensure that they work together. For this reason, appropriate test should be performed. In literature there are two main tests to determine the bonding properties of FRCM composite on concrete and masonry substrate, that are the double (or single) push-pull shear test and the pull-off test.

2.3.1 Single and double push-pull shear test

There are different push-pull shear tests in literature, performed with different set-ups. These tests are very useful to study stress-transfer mechanism of FRCM composite externally bonded to a concrete or masonry substrate. Push-pull shear test have been performed by researchers with single lap (Sneed et al. 2014, Valluzzi et al. 2012) and double laps (D'Ambrisi et al. 2012, Carozzi et al.2015, Pascucci et al. 2013). The way in which the load is applied to the FRCM system can be different.

In the study of Sneed et al. (2014) a single-lap shear test set-up, the same used to study shear debonding of FRP, was adopted. This test was performed constraining the concrete prism avoiding any possible movement (Figure 2.9), and pulling the fabric that comes out from the FRCM system bonded to the concrete. In order to constrain the concrete block, a steel frame bolted to the testing machine base was adopted. On the top of the concrete prism a steel plate was placed to distribute the pressure provided by the restrain to the specimen. The tests were performed under displacement control.

Similar to this set-up is the one adopted in other researches (D'Ambrisi et al. 2012, Carozzi et al.2015, Pascucci et al. 2013), with the difference of having two laps. In the double lap shear test "U" shape strips of fabric were applied with the mortar on two faces of concrete or masonry prisms. The load is then applied to the free strip of fabric through a steel cylinder connected to the pulling machine. Between the cylinder and the fabric, a Teflon layer is interposed to avoid stress concentration. The fixture to constrain the prism can be the same of the single lap shear test (Figure 2.10).

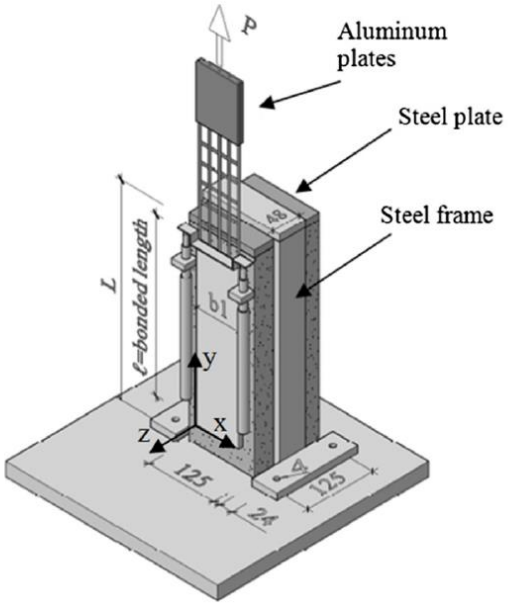

Figure 2. 9 - Single lap shear test set-up, Sneed et al. (2014)

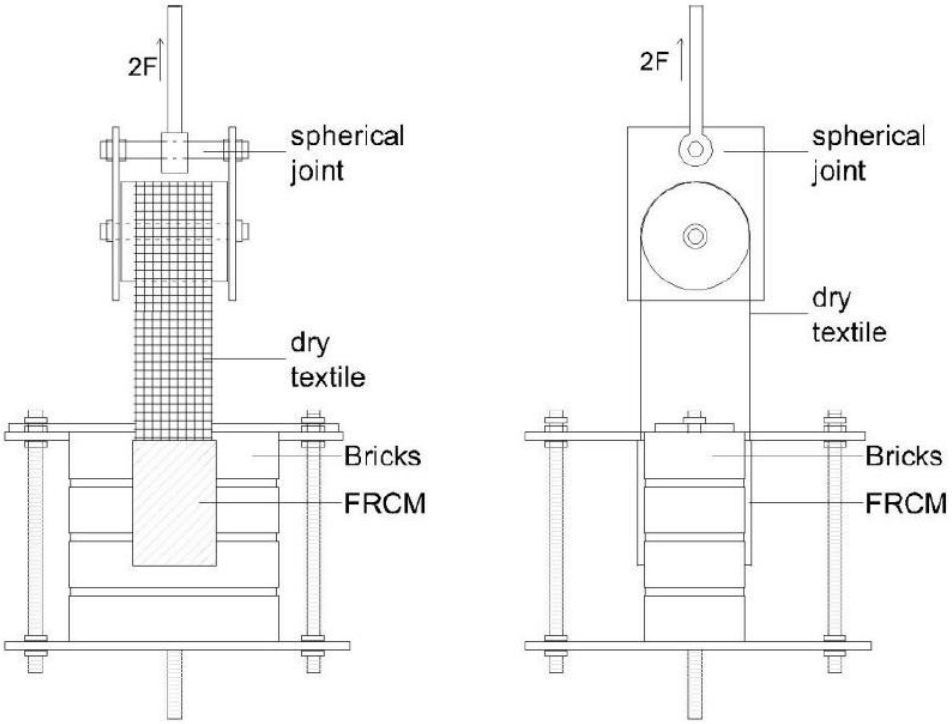

Figure 2. 10 - Double-lap shear test set-up, Carozzi et al. (2015)

The last type of push-pull shear test found in literature is the one performed by D'Ambrisi et al. (2014), where the strengthening material connects two concrete prisms. With this test set-up the tensile force in the FRCM material is transferred by pulling steel bars connected to steel plates placed at the specimen midspan (Figure 2.11). tests have been performed with one and two plies of reinforcement.

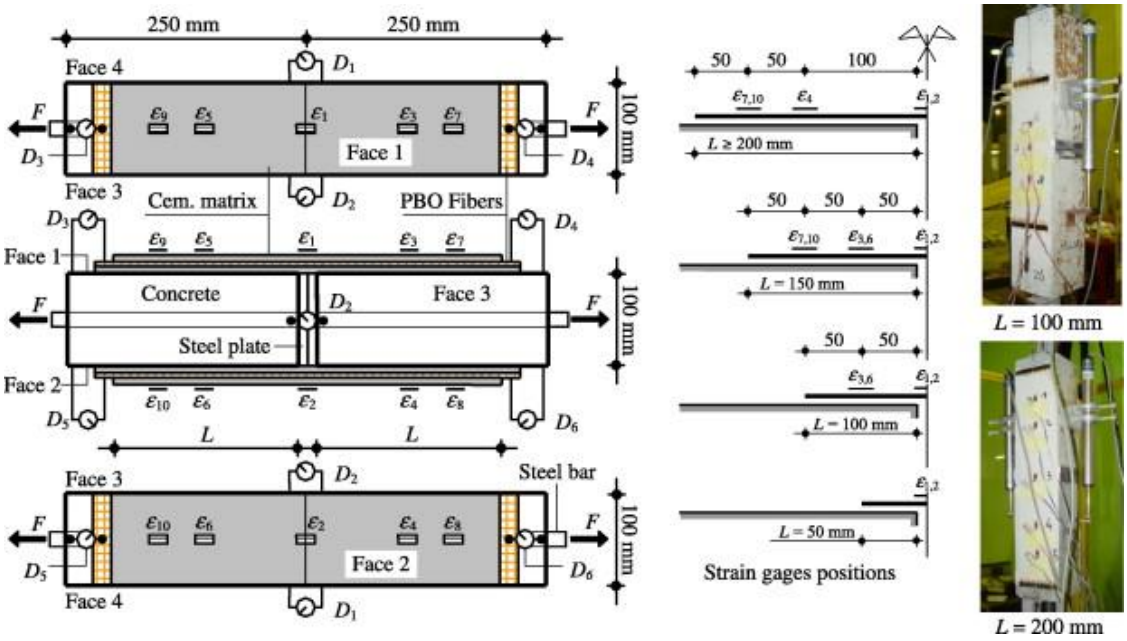

Figure 2. 11 - Push-Pull double shear test, D'Ambrisi et al. (2012)

A common aspect of these three studies is the fact that different bond lengths were tested to understand the influence of this parameter on the ultimate strength of the FRCM system. In particular, the study of D'Ambrisi et al. (2012) was performed with a PBO-FRCM material bonded to a concrete substrate with 50, 150, 200 and 250 mm of bond length. The results of this study were the starting point for the research of Sneed et al. (2014), who tested the same PBO-FRCM system with bond length ranging between 100 to 330 mm in order to confirm the findings of D'Ambrisi by examining longer composite bonded lengths and using a different set-up. In both studies the increase of the bond length produces an increase of the bond strength at a decreasing rate. This finding suggests the existence of an effective anchorage length L_{eff} , such that increasing the bond length the debonding force (maximum load at failure) remains constant. D'Ambrisi et al. (2012) identified the effective anchorage length between 250 and 300 mm, and this result was confirmed by Sneed et al. (2014) who stated that the effective bond length is longer than 250 mm but less than 330 mm. The results of this two studies are shown in Figure 2.12.

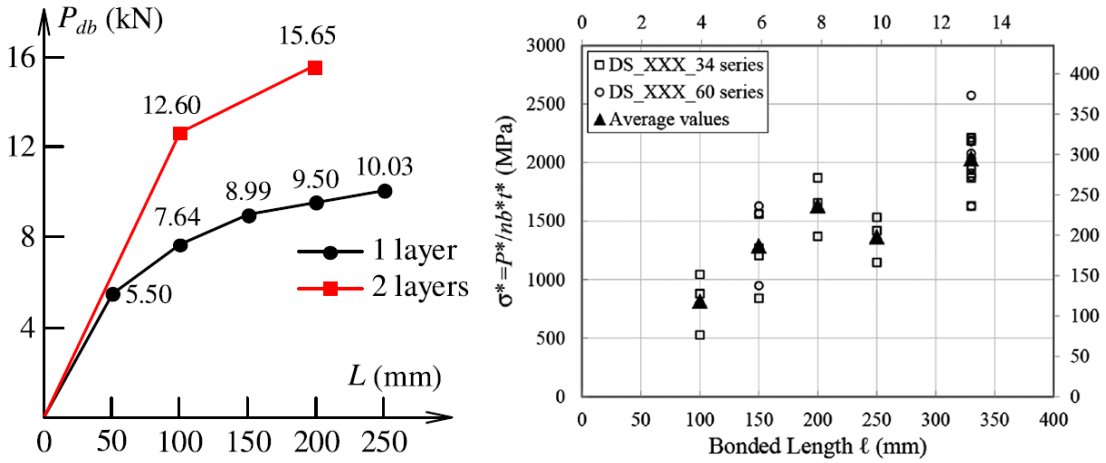

Figure 2. 12 - Peak load vs. bond length, D'Ambrisi et al. (2012) left, peak stress vs. bond length, Sneed et al. (2014) right

In the study conducted by Pascucci et al. (2013), a Carbon-FRCM system was bonded to a masonry brick with a bonded length that ranged between 51 to 152 mm. In this study the optimal bond length was not found because the bond length tested was not long enough. As can be seen in Figure 2.13, the trend of the line that represents the peak load as a function of the bond length is still linear.

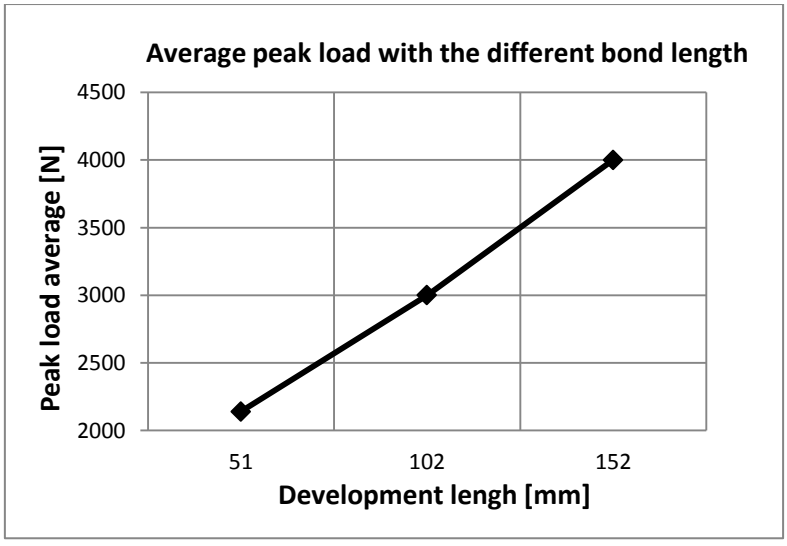

Figure 2. 13 - Force at debonding vs. bond length, Pascucci et al. (2013)

The different failure modes observed in these studies for this kind of test, are well represented in Figure 2.14.

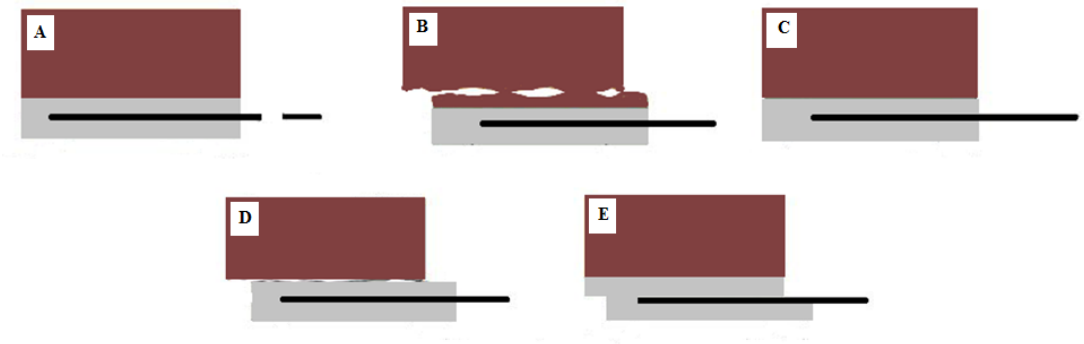

Figure 2. 14 - Possible failure modes for a Push-Pull shear test, Pascucci et al. (2013)

- Failure mode A: rapture of the fibers;
- Failure mode B: debonding in the brick surface;
- Mode of failure C: slippage of the fiber within the cementitious matrix;
- Failure mode D: debonding in the interface substrate-cementitious matrix;
- Failure mode E: debonding in the interface fiber-cementitious matrix.

The failure mode depends on different parameters: bond length of the strengthening system, interaction between the matrix and the fabric as well as the interaction between the matrix and the substrate. An interesting study of the influence of the bond length on the failure mechanism is the one of Carozzi et al.(2015). In this research different type of reinforcement (glass fabric, carbon fabric and two type of PBO fabric) bonded to a substrate made of four clay bricks were tested, with a bond length ranging between 50 to 150 mm. The results shows that the bond length has an influence not only on the failure load but also on the failure mechanism. In particular, the results of the tests performed with the glass fabric are shown in Figure 2.15. In this graph it is possible to see that the failure load increases with the bond length and that shorter bond length leads to a slippage failure of the fabric within the matrix (C). The slippage is no more the failure load for the maximum bond length of 150mm, where the specimen experienced the failure of the fabric (A).

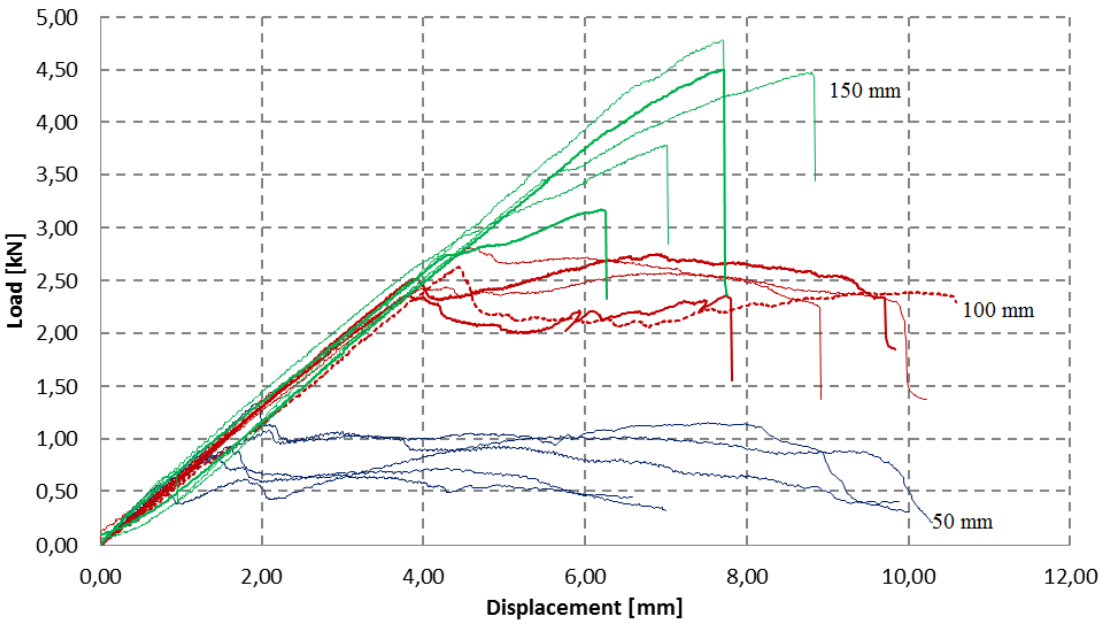

Figure 2. 15 - Load-displacement curves for G-FRCM with different bond lengths, Carozzi et al.(2015)

Bond length of 50 and 100mm show a plateau after the pick load is reached, while the longest bond length leads to a brittle failure with no slippage.

2.3.2 Pull-Off

The Pull-Off test is the easiest to perform test known to analyze the bond strength of a composite material applied on a support. In literature this test is very commonly performed with clay or concrete bricks as the substrate and it is one of the tests required by AC434. To perform this test a circular steel disc is glued with an epoxy resin to the surface of the FRCM system previously applied on the substrate. A vertical axial force is applied by a Pull-Off machine (Figure 2.16) and the force required to pull this disc out from the surface of the FRCM is registered. Before the application of the disc, the specimens are cut in the substrate block with a core drill (Figure 2.17), in order to obtain a circular cut.

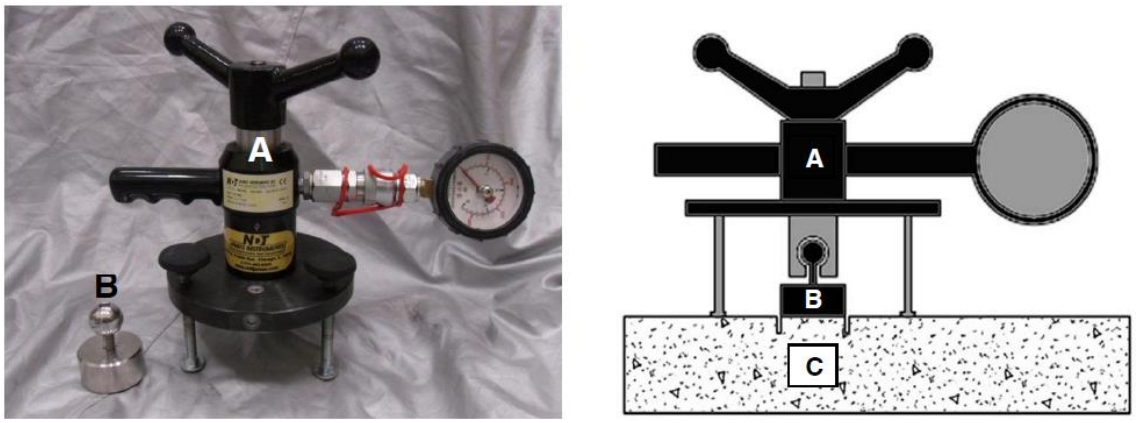

Figure 2. 16 - Pull-Off machine, Bianchi et al. (2013)

Figure 2. 17 - Core drill to cut the specimens, Bianchi et al. (2013)

Besides the maximum load applied to the disc, also the failure mode of the specimen is of great importance. According to AC434, the possible failure modes for the FRCM composite subjected to this test, are represented in Figure 2.18.

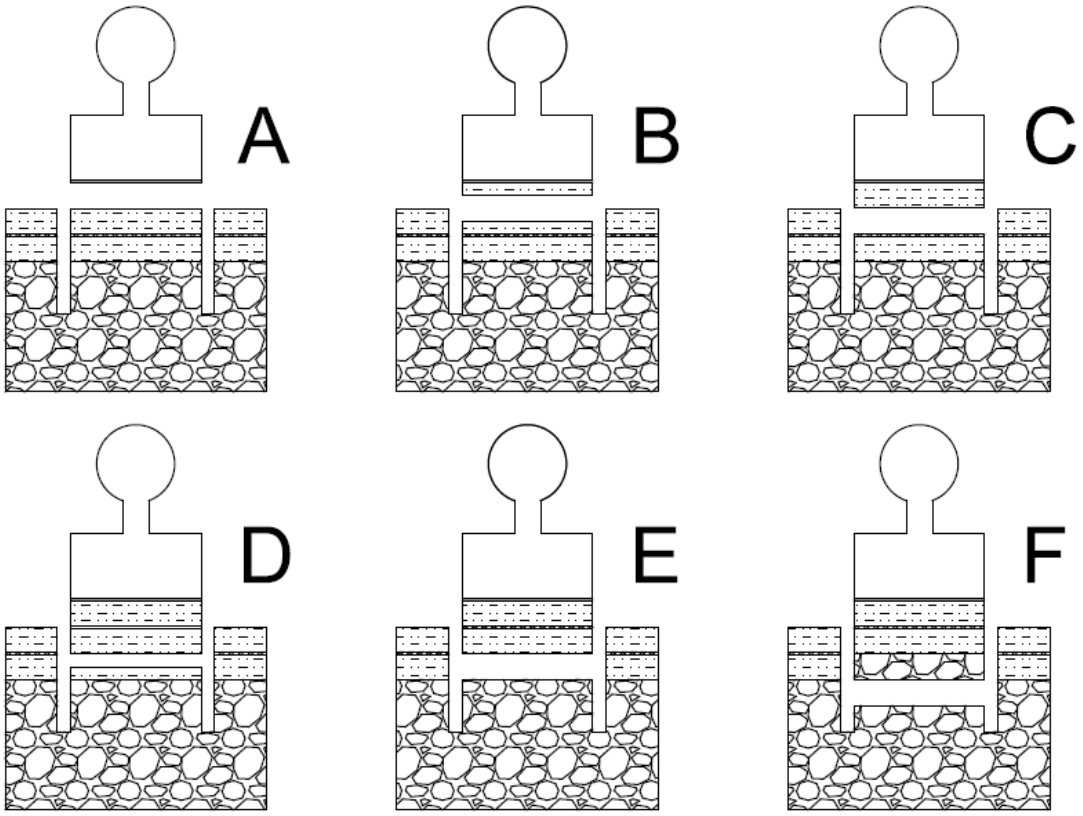

Figure 2. 18 - Possible failure mode for the Pull-Off test according to AC434, Bianchi et al. (2013)

The failure modes B), C) and D) are characterized by the failure of the repair material in different locations. The failure mode A) corresponds to the bond failure at the surface between the disc and the FRCM material. The failure mode E) corresponds to the bond failure at the concrete/overlay interface and finally the failure mode F) corresponds to the failure in the substrate.

Depending on the failure mode, there are two different ways to compute the critical stress reached at failure. For FRP systems, the ultimate stress is computed dividing the ultimate load registered by the testing machine by the area on which the load is applied. This can be correct for a continuum system like the FRP, but in the case of FRCM, if the failure occurs on the interface between the two layer of mortar, where the layer of fabric is applied, this procedure is no longer correct. Indeed, for this failure mode the peak load has to be divided by the net area, which is the entire area minus the area covered by the fabric.

In the old version of AC434 was required to have only a cohesive failure F) with a minimum stress of 1,38 MPa (experimental number). This fact was because AC434 was developed knowing FRP composite, which is able to develop an adhesion

with the substrate stronger than the bond among the support itself. Moving from FRP to FRCM, AC434 was modified because the mortar of FRCM system is not able to generate such a good bond with the substrate, and the most common failure mode occurs between the two layer of mortar (C). For this reason, two different limits are now considered in the new version of AC434: for failure modes E) and F), the limit on the stress does not change being 1,38 MPa, while for the failure mode C), for which the stress is computed dividing by the net area, the limit was set to 2,76 MPa.

2.4 Interlaminar properties

Another test required by AC434 in order to qualify a FRCM system is the composite interlaminar shear strength test, and a minimum of five specimen are required. AC434 refers to the ASTM Standard D2344 "*Standard Test Method for Short-Beam Strength of Polymer Matrix Composite Materials and Their Laminates*" for the test method. This test is a three-point bending test on short beam, where a transverse shear is induced in specimens with low support to specimen thickness (s/h) ratios. This test method determines the apparent interlaminar shear strength of high-modulus fiber-reinforced composite materials, and was commonly used to determine the short beam strength of FRP composites.

The specimen geometry and test configuration according to the ASTM Standard is shown in Figure 2.19. The upper cylinder through which the load is applied is 6.00 mm in diameter, and the two supports cylinders on the bottom are 3.00 mm in diameter.

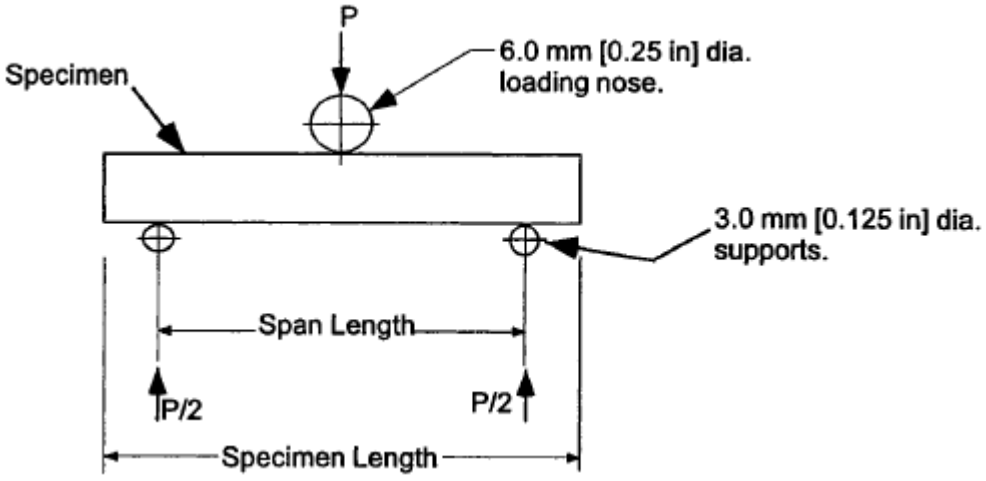

Figure 2. 19 - Short beam shear test configuration (ASTM D2344)

ASTM D2344 recommends a span to thickness (s/h) ratio of 5 for glass fiber composite materials and an s/h ratio of 4 for carbon fiber composite materials. Moreover, the standard recommends that the specimen overhang the support cylinders by at least one specimen thickness.

With this test the interlaminar shear strength of laminate composite like FRP is studied, and in order to compute the interlaminar shear strength the specimen has to exhibit an interlaminar shear failure. All the typical failure modes for this kind of test are shown in Figure 2.20.

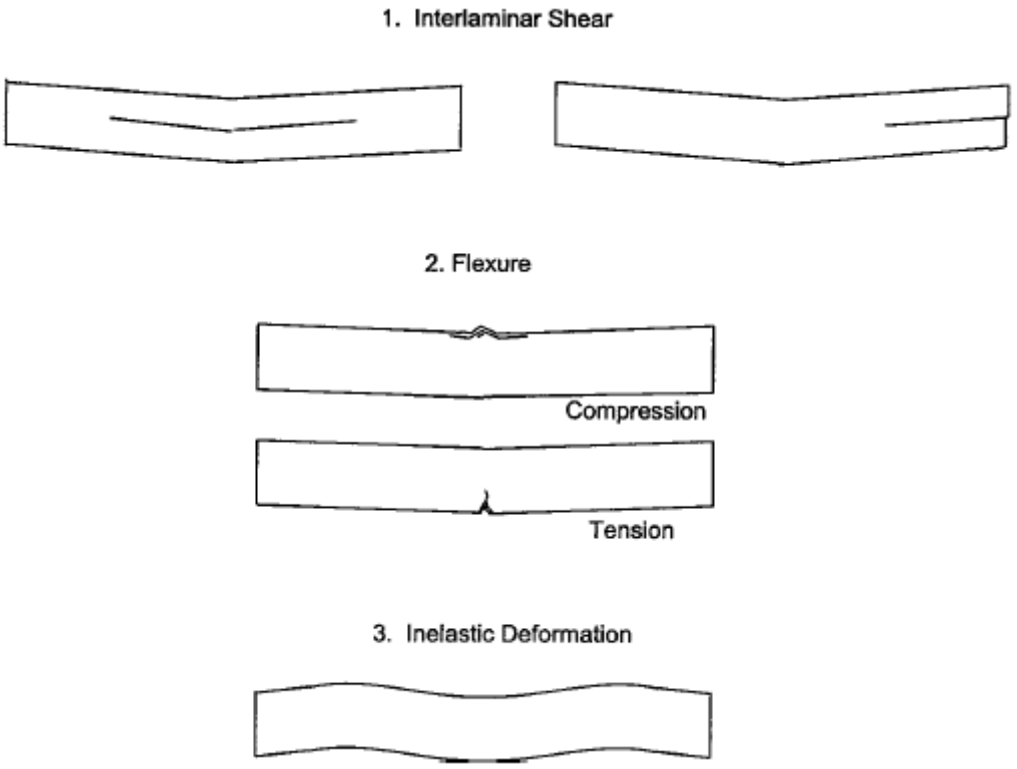

Figure 2. 20 - Possible failure modes in Short Beam Test for FRP composites

Since now this test was performed on FRCM composite only by Arboleda et al. (2014), and all the specimens showed a flexural or diagonal tension failure for which it is not possible to study the interlaminar properties of the composite. These failure modes are expected because of the low flexural strength of the cementitious matrix of FRCM system. Further studies are necessary to understand if it is possible to adapt this test to the FRCM composite material or not.

2.5 Bending & Shear reinforcement

The FRCM can be used to enhance flexural and shear strength of structural RC-element as beams or slabs. Many works were found in literature regarding bending and shear strengthening, and in this section some of them will be presented in order to understand how much the resistance can be increased and which are the parameters that influence these strengthening applications.

For this type of application four researches were studied: Brückner et al.(2006), D'Ambrisi and Focacci (2011), Ombres (2011), Leardini et al. (2013). The fibers used in these works as the reinforcement are made of: alkali-resistant (AR) glass (Brückner 2006), poliparafenilenbenzobisoxanole (PBO) (Ombres 2011, D'Ambrisi and Focacci 2011, Leardini 2013) and carbon (D'Ambrisi and Focacci 2011). In addition, D'Ambrisi and Focacci (2011) tested also some beams reinforced with carbon FRP to make a comparison between FRP and FRCM composite materials. In all these works, tests on beams and slabs strengthened for shear or bending were performed, and the results demonstrated the effectiveness of this reinforcing technology. It was found that the parameters that affect behavior and effectiveness of the reinforcement are:

- Type of fibers used as the reinforcement (carbon, glass, PBO);
- Type of binder used as the matrix;
- Number of layers of fabric;
- Strengthening configuration;

Because of the high number of parameters that influence the behavior of the strengthening system, it is not easy to compare results obtained by different researchers. D'ambrisi and Focacci (2011) studied all these aspects using different strengthening material (carbon fabric and PBO fabric), two kinds of mortar and varying the number of layers and the strengthening configuration. They found that the PBO material was most effective due the better bond that it is able to form with the mortar. In fact, the carbon has the drawback of being too smooth, while the PBO is able to establish a better bond with the binder thanks to the good adhesion properties given by the roughness of the fiber strands. Using the same amount of fiber reinforcement (same fiber cross section A_f), the carbon FRCM (C-FRCM) increased the beam's bending capacity in the range of 9-18%, for different strengthening

configuration, while the PBO-FRCM approximately of 30% with respect to the un-strengthened beams. Moreover, with PBO-FRCM the enhancement in terms of ultimate load was approximately the same of the one obtained with CFRP, although the fiber cross section A_f of the PBO-FRCM material was 75% of the one of CFRP material.

Another aspect that strongly influences the effectiveness of FRCM strengthening system is the bond between fibers and mortar. For this reason D'ambrisi and Focacci (2011) tested two different mortars with the PBO material, one (called M750) was properly designed to achieve a better bond with PBO fibers taking advantage of recent nanotechnology developments, the other (M50) was a regular mortar made of pozzolanic cement and selected silicia aggregates. The enhancement of 30% of the ultimate load obtained with PBO-FRCM with M50 mortar, increased to 38% using M750 mortar, proving the importance of having a better bond between fibers and mortar.

As far as the influence of the number of plies on the ultimate load is concerned, in all the researches analyzed different number of intrados fabric layers were compared. As it was expected, the load-carrying capacity increased as the number of reinforcement layer increased, with different magnitude of increase among the researches because of different beam geometries and strengthening configurations. For example, in the study of Leardini et al. (2013), the strength enhancement for beams strengthened for bending with one ply was approximately 32%, while using four plies the strength enhancement was 92%; these results were obtained using a low resistance concrete, with an high resistance concrete they obtained enhancements of 13%-73%. Analogous results were obtained testing slabs: 41%-105% for low resistance concrete and 35%-112% for high resistance concrete. Brückner et al.(2006), using AR glass fiber reinforcement, obtained an increase of the ultimate load with respect to the un-strengthened beam of 130% with four plies and of 195% using eight layers of reinforcement. In the study of Ombres (2012) it was observed an increase of approximately 23% with two plies and of 30% with three plies.

D'ambrisi and Focacci (2011) studied also the effect of the strengthening configuration, analyzing three different configurations (Figure 2.21):

- C beams: continuous U-shaped strips of transverse strengthening;
- D beams: U-shaped strips only at the beam ends;
- A beams: no transverse strengthening.

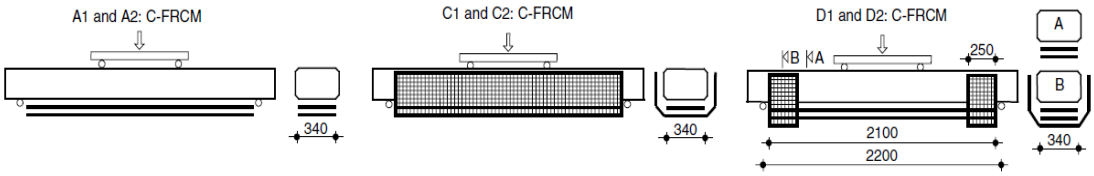

Figure 2. 21 - Different strengthening configurations, D'ambrisi and Focacci (2011)

Different failure modes were observed: for C and D beams the failure mode was slippage of the fabric within the mortar, while for A beam there was a debonding of the FRCM reinforcement because of the lack of the transverse strengthening. The best results in terms of ultimate load was achieved by C-beams, with an average increase of the ultimate load with respect to the un-strengthened beam of approximately 18%.

Also the effectiveness of PBO-FRCM material as shear strengthening was investigated in this work. Using the same flexural strengthening set-up and different shear strengthening set-up (Figure 2.22), the effectiveness of PBO-FRCM material as shear strengthening was proved.

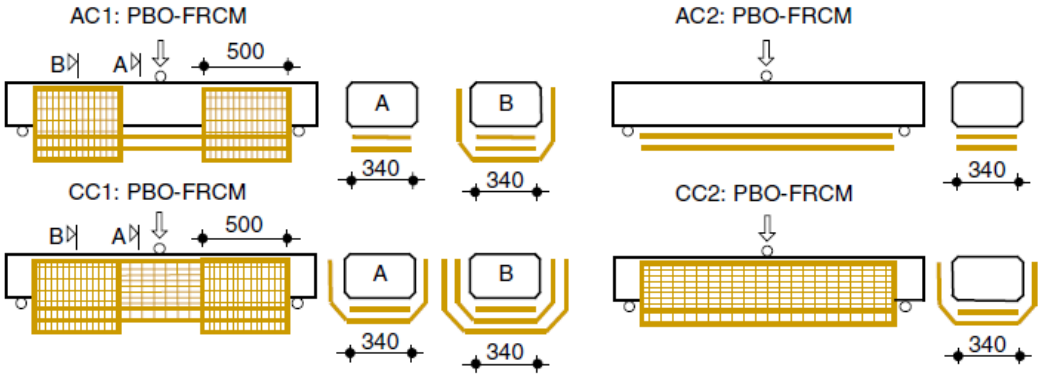

Figure 2. 22 - Shear strengthening, D'Ambrisi and Focacci (2011)

The ultimate strength of AC1 with respect to AC2 and of CC1 with respect to CC2 was higher, and the utilized shear strips allowed to modify the failure mode from shear failure mode (beams AC2 and CC2) to flexural failure mode (beams AC1 and CC1).

Similar results were obtained by Brückner (2006) who tested both rectangular section beams and T-shaped beams. For both the two types the flexural strength was

designed to be much higher of the shear strength, in order to study the effectiveness of the shear strengthening. For T-shaped beams was also studied the effect of a anchoring system that avoids fabric slippage. In the case of rectangular section beams, with two textile layers in a U-wrap configuration at beam ends, the ultimate load was 45% higher with respect to the un-strengthened beam, while using three layers the increase was 75%. Moreover, with three plies of fabric the shear capacity became higher than the flexural capacity, and the failure was due to bending. Also for the T-shaped beam the shear strengthening was found to be very effective, especially with the anchoring system which increased the ultimate load by almost 30% with respect to the strengthening system without the anchoring system.

3.

TENSILE CHARACTERIZATION

In this section the set-up (machine, extensometer, gripping mechanism) of the tensile test performed will be described, together with the material used and the specimen preparation. All the results of the tensile tests will be presented.

3.1 FRCM constitutive law: two idealized model

Depending on two different assumptions, there are two constitutive laws that can describe the idealized behavior of FRCM. If a perfect bond between the fibers and the matrix can be assumed, the material has a tri-linear stress-strain curve (Bianchi et al. 2013, Figure 3.1), while if we assume the presence of a certain grade of slippage among the fabric and the mortar, the result is a bilinear curve (Arboleda et al. 2014, Figure 3.2).

The first linear segment of the two curves is the same for both cases and represents the response of the specimen when the mortar is un-cracked, so the stress on the specimen is below the tensile resistance of the mortar and only the matrix is loaded. This is characterized by the un-cracked elastic modulus E_1 and it ends at a transition point T (f_{ft}, ε_{ft}), which is the point where the two idealized lines intersect. The second part of the graph is characterized by the elastic modulus E_2 and reflects the cracked mortar condition. The experimental curves exhibit a transition part where cracks develop which is not captured by the bilinear idealization. Considering the hypotheses of perfect bond between the fabric and the matrix is possible to recognize a third linear segment in the graph, which is characterized by the elastic modulus E_3 that is the completely cracked modulus of elasticity. In the stress-strain graph the stresses are always computed dividing the load by the area of the fabric, not the total

area of the specimen. This is primarily due to the fact that, after the cracking of the matrix, the resisting element of the system is the fabric. Moreover, the fabric area is known while the area of the matrix vary along the specimen and between different specimens. Dividing the load by the area of the fabric instead of the area of the mortar, lead to a higher accuracy on the results.

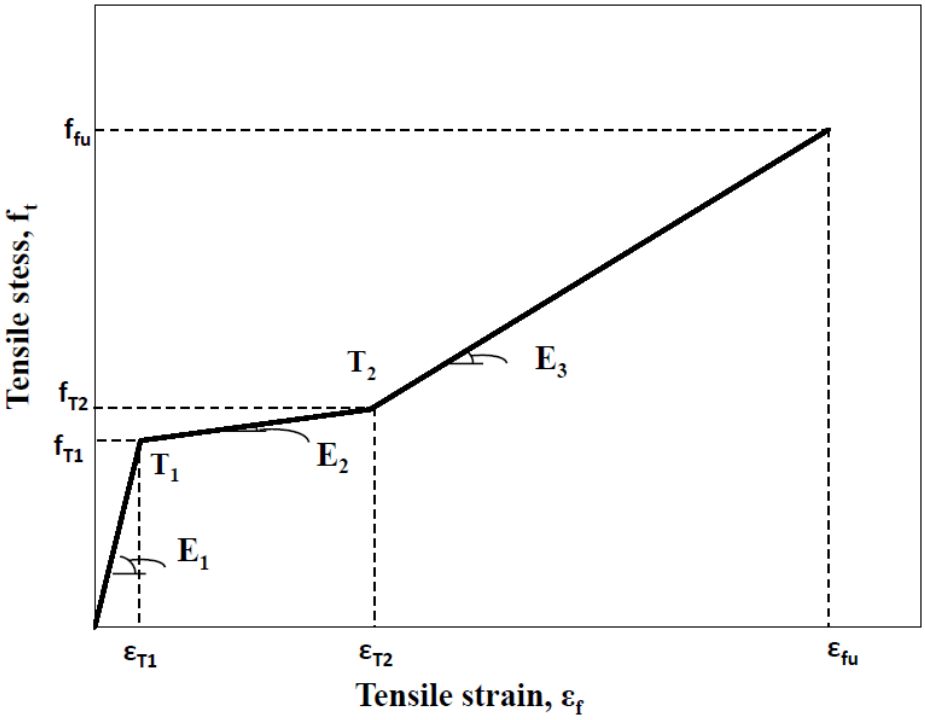

Figure 3. 1 - Tri-linear stress-strain curve, Arboleda et al. (2014)

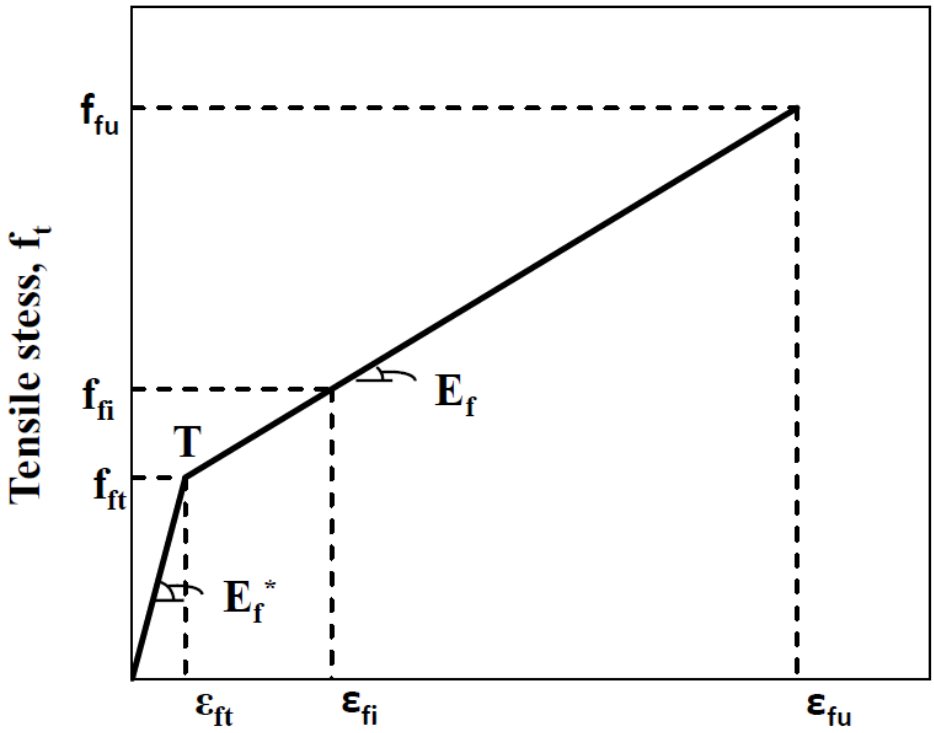

Figure 3. 2 - Bi-linear stress-strain curve, Arboleda et al. (2014)

These two different hypotheses on the base of the constitutive law are strictly related to the gripping method adopted to test the material. The two models are not in contradiction and we can obtain both for the same specimen depending on the type of gripping mechanism adopted. If the tensile test is performed constraining the fibers by clamping the edges of the specimen, the assumption of perfect bond can be applied and the result of the test will give a tri-linear curve. Using a different gripping method that does not completely constrain the fibers is possible to find the bilinear curve. The two different gripping mechanisms are shown in detail in Figure 3.3.

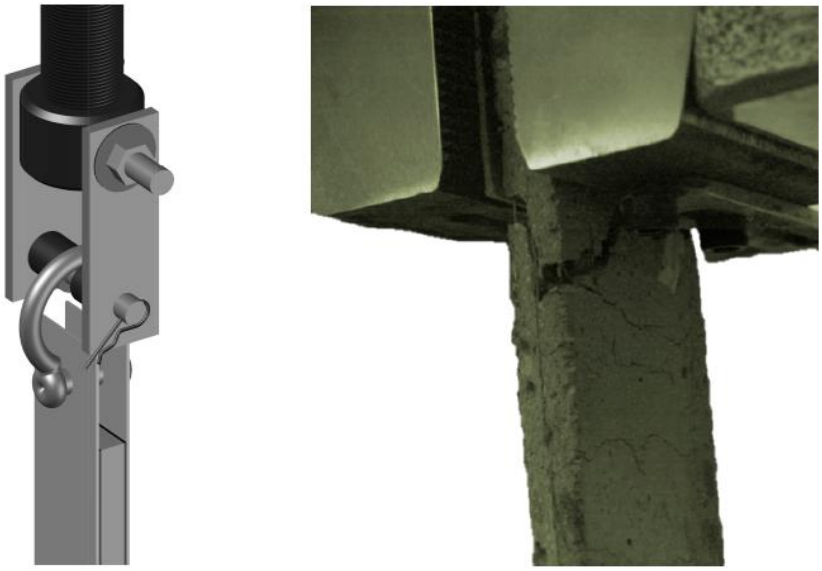

Figure 3. 3-Clevis and clamped grip

We can divide the type of gripping mechanism into clamp action type grip, that applies a transversal load to the specimen in order to fix it, and Clevis grip, which transfers the load to the specimen by surface shear (Figure 3.4).

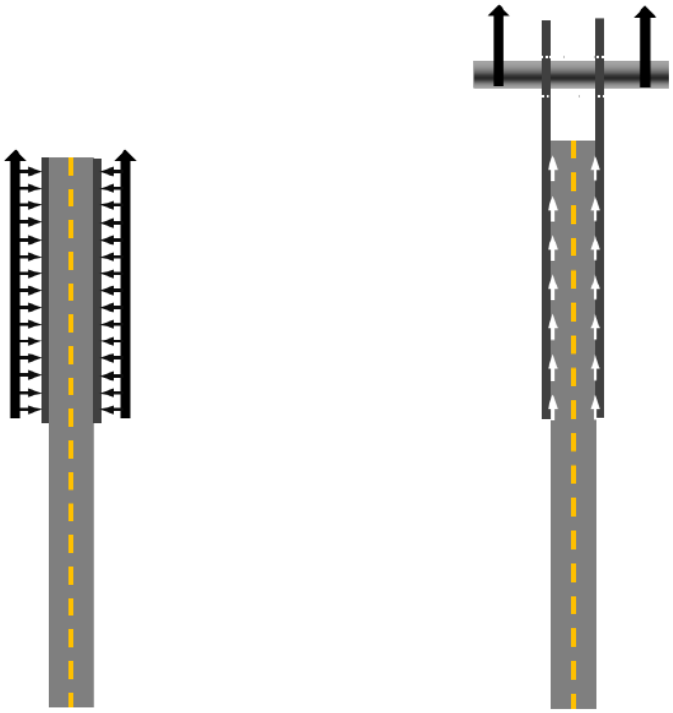

Figure 3. 4 - Different load transfer mechanisms, Arboleda et al. (2014)

Research has shown (Bianchi et al. 2013) that the first gripping mechanism leads to higher results for the ultimate load because the failure happens for the breaking of the fibers, as it is shown in Figure 3.5. On the other hand, when the

specimen is tested with a clevis-type grip, a different failure mechanism is observed and is given by slippage of the fabric within the mortar.

This second type of gripping mechanism represents the boundary condition in the field application of FRCM, where the fabric is not anchored at its ends and the failure mode of the FRCM in tension is the slippage of the fibers. For this reason, it was selected the Clevis grip for this study, that leads to results more representative of the repair application.

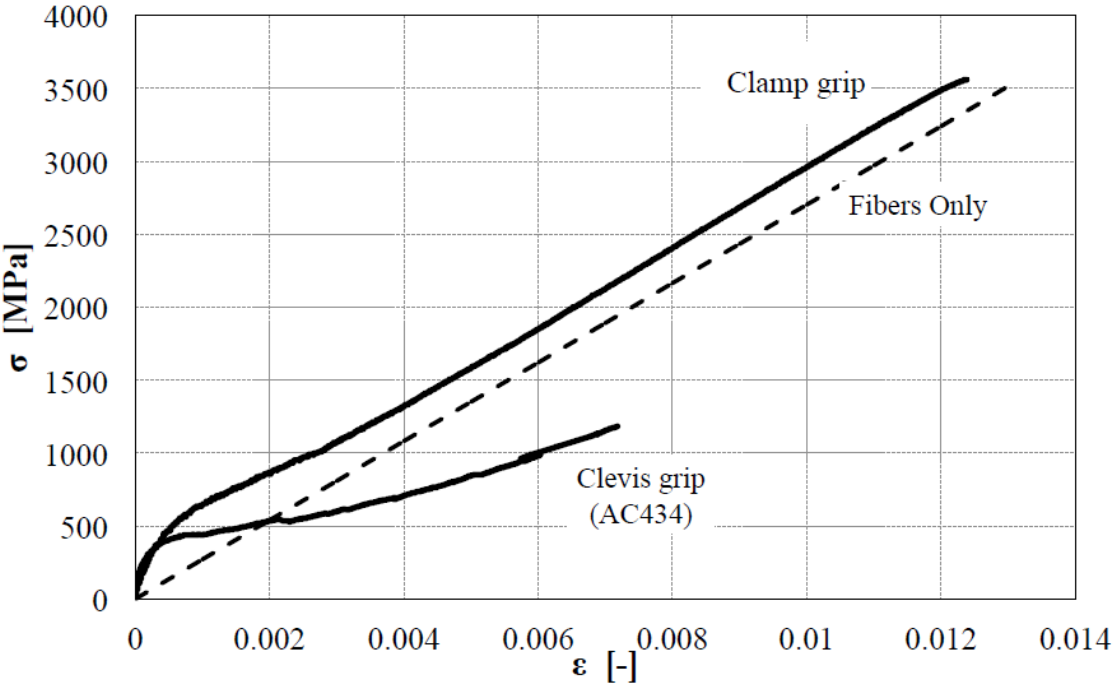

Figure 3. 5-Comparison of the results with different grips, Bianchi et al. (2013)

The goal of this experimental campaign is to find the parameters that describe the constitutive load of the material. Using a Clevis type grip, and obtaining therefore a bilinear curve, the parameters that are obtained from each test are:

- E_1: the un-cracked modulus of elasticity;
- E_2: the cracked modulus of elasticity;
- f_{fu}: the ultimate tensile stress at failure;
- ε_{fu}: the strain related to the ultimate tensile stress;
- f_{ft}: the stress at the transition point;
- ε_{ft}: the strain at the transition point.

With these parameters, it was possible to compare:

- The results with two different FRCM system (described in Section 3.3);
- The different behavior of multi-layer system (specimens with 1, 2 and 3 plies of fabric were tested);
- The effect of overlapping (specimens with a lap splice were tested);
- The effect of several aging process (specimens were tested after exposure to different environments described in Section 5).

3.2 Test setup

3.2.1 Machine

A Universal Test Frame with a maximum capacity of 130kN was used to perform the uniaxial tensile test. The tests were performed under displacement control at a rate of 0.25 mm/minute. The set-up of the test is given by the Annex A of the Acceptance criteria AC434 for masonry and concrete strengthening using fabric-reinforced cementitious matrix (FRCM) composite system.

3.2.2 Extensometer

To measure axial deformations a clip-on extensometer with a 100 mm gauge length was used, because the cross head displacement measurement is not very precise and is influenced by the machine compliance. In literature, there are several studies (Bianchi et al.2013, De Santis et al. 2015, De Felice et al. 2014) where the extensometer was put directly on the surface of the specimen. This way of application leads to a problem that is difficult to solve. In fact, if cracks generate outside the length covered by the extensometer, or there is a slippage of the fabric under the tabs, the instrument will not read this deformation. For this reason in this study the extensometer was place on the surface of the tab (Figure 3.6).

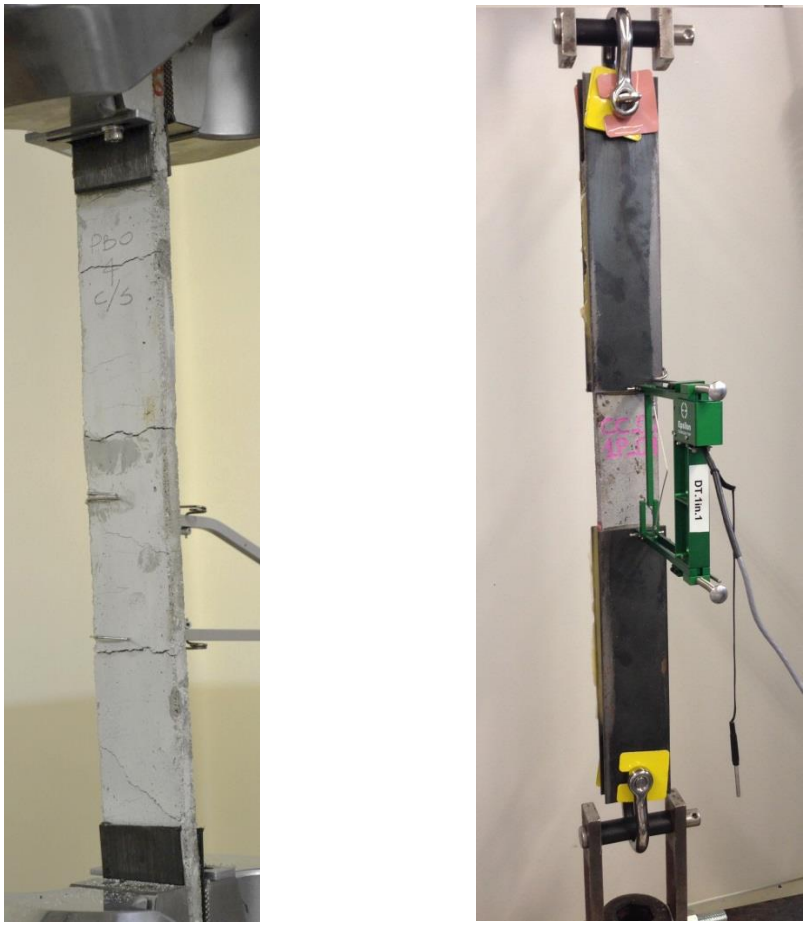

Figure 3. 6 - Extensometer application: on the specimen and on the tabs

By Appling the extensometer on the tabs, during the test the deformation of the epoxy is also measured and this fact must be taken into account. For this reason the compliance of the epoxy was measured for some test with an image analysis.

3.2.3 Gripping mechanism

As suggested by AC434 a Clevis type gripping mechanism (Figure 3.7) was used where the load is applied to the specimen by surface shear, which more closely represents rehabilitation application in which the fabric is not constrained at its ends. In this way, there are multiple degrees of freedom and the rotation is allowed in two perpendicular planes.

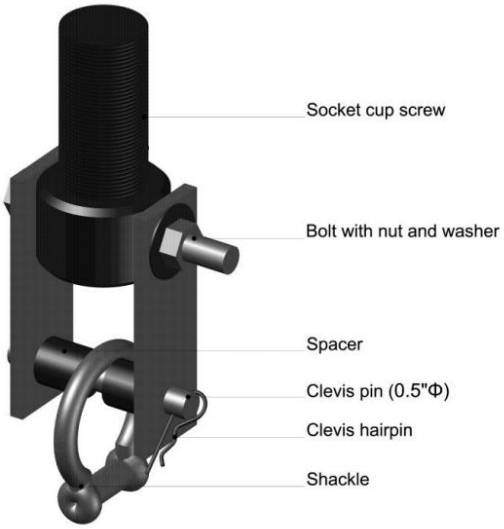

Figure 3. 7 - Clevis-type gripping mechanism according to AC434

Metal tabs of the same width of the specimen are glutted on it, in order to transfer the load from the machine to the specimen by shear. In this way, damages to the specimen are avoided.

3.3 Material description

3.3.1 Fabric

3.3.1..1 Geometry and characteristics

The two different type of fabric used in this research are shown in Figure 3.8. All the technical properties of the fibers and the fabric are listed in Section 1.4.

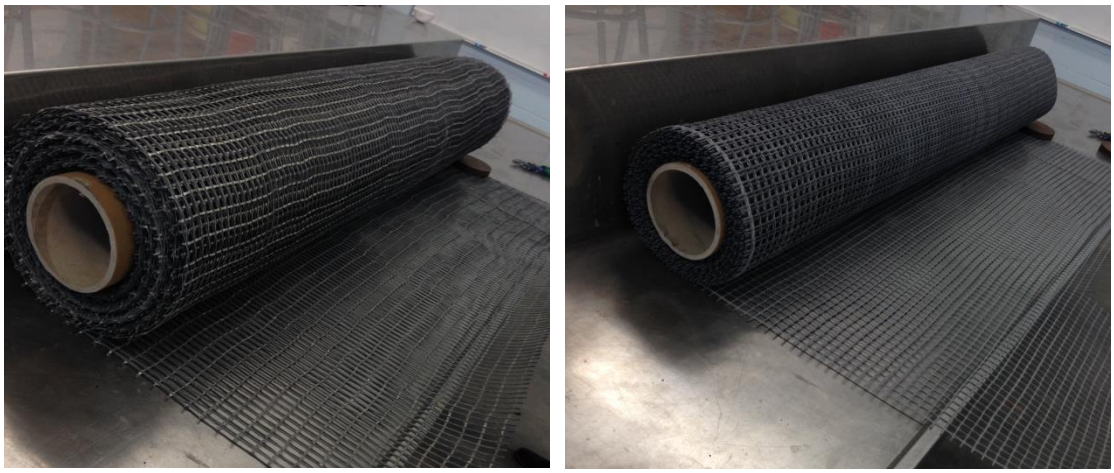

Figure 3. 8 - Unidirectional carbon-mesh (left) and bidirectional carbon mesh (right)

The unidirectional fabric is composed by carbon fibers in the longitudinal direction and glass fibers in the orthogonal direction, just as a support. An epoxy coating of the fibers is provided to improve the adhesion between the mortar and the yarns. The spacing between the yarns is 12 mm in the longitudinal direction and 28 mm in the orthogonal direction and the nominal thickness is 5 mm and 3 mm (Figure 3.9).

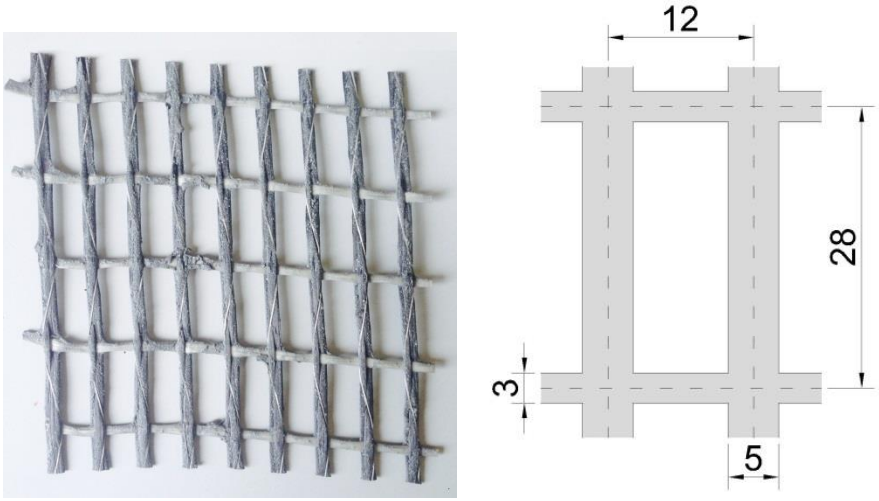

Figure 3. 9 - Unidirectional fabric

The bidirectional fabric is composed by carbon fibers in both the directions. A epoxy coating of the fibers is provided to improve the adhesion between the mortar and the yarns. The spacing between the yarns is 14 mm in both the directions and the nominal thickness is 3 mm and 3 mm (Figure 3.10).

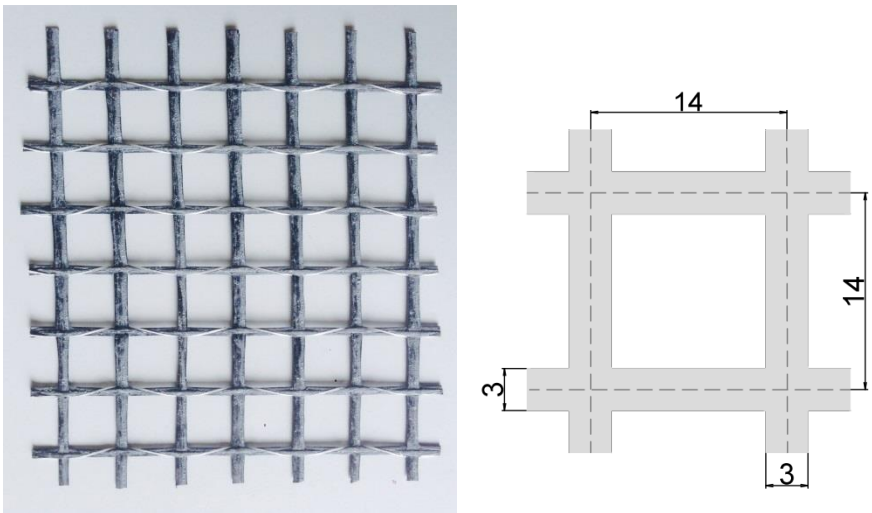

Figure 3. 10 - Bidirectional fabric

3.3.1..2 Tensile strength

The certified tensile strength is 4 GPa and the elastic modulus is 240 GPa for both the materials, that are typical values for carbon fibers.

3.3.2 Mortar

The properties of the mortar used in FRCM composite material as the matrix that need to be computed according to AC434 are:

- Specific weight and void content;
- Compressive strength at 7 and 28 days that has to be at least 17,0 and 24,0 MPa respectively.

These parameters were computed and are presented in this section.

3.3.2..1 Composition and properties

The mortar used is the same for both FRCM systems and it is a one-component product based on inorganic binders, fibers, selected aggregates, admixtures and polymer. A special reactive component is added in order to have a better bond behavior with the carbon-fabric.

3.3.2..2 Specific weight and void content

Specific weight and void content are two of the most important parameters to characterize a cementitious material as the mortar. The durability of the matrix is strongly influenced by the void content as well as the distribution and dimension of the voids. Oxygen and water can easily propagate in presence of a high void content and a good interconnection of the voids. On the other hand, many small and not interconnected voids help against the deterioration caused by freezing and thawing processes. Looking at the mortar also as a component of the FRCM composite material, it is very important also to underline that its role is to provide a good adhesion between the fibers and the support. In this sense, a high void content can affect bond with the fibers, decreasing the effectiveness of the FRCM system.

In order to obtain these parameters, three ASTM (American Society of Testing Materials) procedures were followed:

- ASTM C138/C138M-10b Standard Test Method for Density (Unit Weight), Yield, and Air Content Gravimetric) of Concrete;

- ASTM C185-08 Standard Test Method for Air Content of Hydraulic Cement Mortar;
- ASTM C188-09 Standard Test Method for Density of Hydraulic Cement.

According to the manufacturer's indications, the mortar was mixed. The fresh mortar was insert in the mold and weighted. Knowing the weight, the specific weight was obtained dividing the net weight by the container volume. The void content (V.C.) is defined by the following equation:

$$V.C. = \frac{V_v}{V_t} = \frac{V_t - V_{m+w}}{V_t} = 1 - \frac{V_{m+w}}{V_t}$$

Where:

- V_v is the void volume;
- V_t is the total volume;
- V_{m+w} is the dry mortar plus water volume.

Writing the volume as the ratio between the weight and the specific weight, the previous equation can be rewritten as follow:

$$V.C. = 1 - \frac{W_{m+w}/SW_{m+w}}{W_t/SW_t}$$

Where:

- W_{m+w} is the weight of the dry mortar and the water;
- W_t is the total weight;
- SW_{m+w} is the specific weight of dry water and water together;
- SW_t is the total specific weight.

Being W_{m+w} equal to W_t, they can be simplified and the final equation to compute the void content V.C. is:

$$V.C. = 1 - \frac{SW_t}{SW_{m+w}} = 1 - \frac{SW_t}{W_{m+w}/V_{m+w}} = 1 - \frac{SW_t}{\left[\frac{W_m + W_w}{\left(\frac{W_m}{SW_m} + \frac{W_w}{SW_w}\right)}\right]}$$

Where:

- W_m is the weight of dry mortar;
- W_w is the weight of the water;
- SW_m is the dry mortar specific weight;
- SW_w is the water specific weight.

All the elements to compute the void content are known, except for the dry mortar specific weight. Five test were performed to compute the void content at Supermix quality laboratory, and the result are shown in Table 3.1.

Table 3. 1 - Void content

	Weight measured [g]	**Weight mortar [g]**	**Total specific weight [g/cm^3]**	**Dry mortar specific weight [g/cm^3]**	**Void content [%]**
Sti-CM-VC-01	7568	5740	2,03	2,45	3,94
Sti-CM-VC-02	7576	5748	2,03	2,45	3,80
Sti-CM-VC-03	7533	5705	2,01	2,45	4,52
Sti-CM-VC-04	7569	5741	2,03	2,45	3,92
Sti-CM-VC-05	7560	5732	2,02	2,45	4,07
Average	7561,2	5733,1	2,02	2,45	4,05
Std. Dev.	16,754	16,754	0,006		0,280
C.O.V. (%)	0,222	0,292	0,292		6,925

The mold used has a weight of 1828,1 g and a volume of 2831,7 cm^3. The total weight of the mortar is 22 Kg and the water used is 2,75 l.

3.3.2..3 Compressive strength

In order to obtain the compressive strength of the mortar, simple uniaxial compressive tests were performed on cube specimens. After following the manufacturer's indication to mix the mortar, ten cube specimens were cast. The cubes were cured in control environment (19-21°C and 65-70% of humidity).

The uniaxial compressive tests were performed using a screw type universal test frame (Figure 3.11) under displacement control at a rate of 0,635 mm/minute. The ultimate strength was obtained dividing the maximum load by the area of the face of the cube.

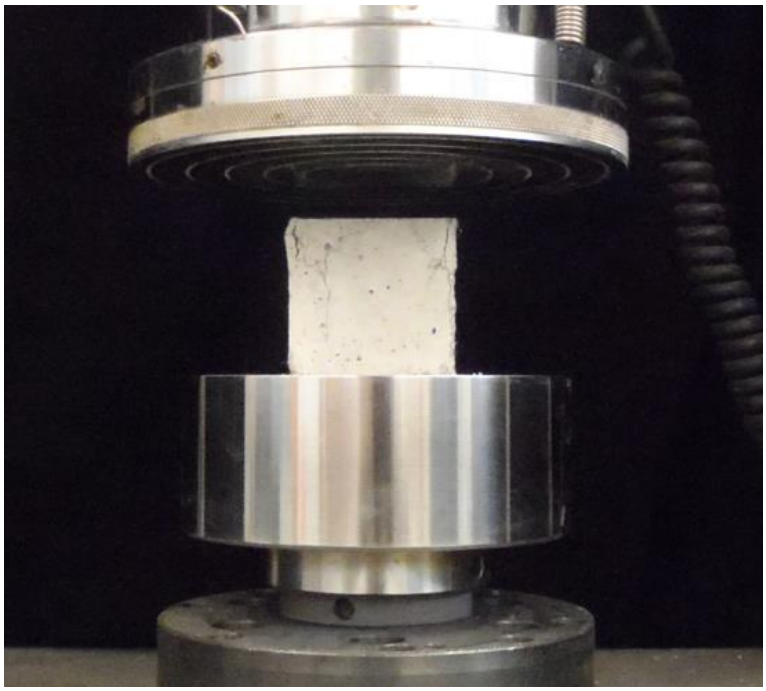

Figure 3. 11 - Uniaxial compressive test on the mortar

The tests were performed after a curing period of 7 and 28 days. All the results are listed in Table 3.2 d Table 3.3.

Table 3. 2 - Strength after 7 days

	Area [mm^2]	**Peak Load [kN]**	**Strength [MPa]**
Sti-CM-CSM-7-01	2580	55,09	21,35
Sti-CM-CSM-7-02	2580	50,37	19,52
Sti-CM-CSM-7-03	2580	53,22	20,63
Sti-CM-CSM-7-04	2580	68,31	26,48
Sti-CM-CSM-7-05	2580	56,03	21,72
Average		56,60	21,94
Std. Dev.		6,89	2,67
C.O.V. (%)		12,17	12,17

Table 3. 3 - Strength after 28 days

	Area [mm^2]	**Peak Load [kN]**	**Strength [MPa]**
Sti-CM-CSM-7-01	2580	84,95	32,93
Sti-CM-CSM-7-02	2580	85,53	33,15
Sti-CM-CSM-7-03	2580	84,91	32,91
Sti-CM-CSM-7-04	2580	88,64	34,36
Sti-CM-CSM-7-05	2580	89,45	34,67
Average		86,69	33,60
Std. Dev.		2,18	0,84
C.O.V. (%)		2,51	2,51

3.4 Specimen preparation and geometry

Following the manufacturer's instruction, 22 Kg of mortar and 2,75 l of water were mixed. 90% of the water was put at the beginning in the mixing bucket while the mortar was added continuously during the mixing. At the end, the last 10 % of water was added, as suggested by the indication of the manufacturer. Once the mix is ready, panels of the dimension of 580x450 mm and 660x580 mm (two different tab lengths) were manufactured by applying a first thin layer of mortar using a trowel on a flat surface, while monitoring a to have constant thickness using a marked instrument. After the first layer of mortar, one ply of fabric was placed on top of it, followed by another layer of mortar. The coated fabric was provided by the company in large rolls, so the shape was curved. For this reason after the cutting with the dimension of the panel, the fabric was put in the oven to make it flat. The temperature of 60°C and the time of 15 minutes were set in order to soften the coating to make the surface flat, but at the same time to not damage the material.

In addition to the one ply specimen, there were also manufactured panels with two plies, following the same procedure. Panels with a lap splice with an overlap of 120 mm were also manufactured, in order to understand if the lap can be a weak section with respect to continuous fabric. This kind of study is very important because in field application there is always the need for lap sections.

After a curing period of 28 days at laboratory conditions of 20°C and 70% relative humidity, the panels were cut to obtain coupons of 400x40 mm and 500x40 mm. All the procedures are shown in Figure 3.12.

It is very important to pay attention to some aspect during the casting of the specimens. First of all it is crucial to have the fabric in the middle plane of the panel, in order to avoid bending during the tensile test due to the dissymmetric position of the reinforcement. For this reason the thickness of the two layers of mortar where monitored in order to be the same with a marked instrument. Secondly, there is the need to have straight specimens, thus the panels were cured with a plastic sheet on them in order to avoid differential shrinkage which can cause a curvature in the panel. Finally, it is crucial to cut the specimens from the panels with the same amount of carbon fibers, three yarns in the case of this work.

Figure 3. 12 - Specimens preparation

3.5 Tab application

In order to test the specimen, two metal tabs were glutted on each side of the coupon using an epoxy resin, after cleaning them with aceton. Two different sizes of metal tabs were used: one that provides a contact length of 150mm and one of 200mm, in order to understand how this difference can affect the results. Both the cases are in agreement with the acceptance criteria AC434 which recommends a minimum contact length of 75mm. The coupon can be tested after a curing period of 24 hours, fundamental to reach the full strength of the epoxy. The fixture shown in Figure 3.13 was made to keep the tabs in place on the specimen during the curing period of one day. Before applying the tabs, the surface of the specimen and of the tabs were roughen in order to increase the mechanical bond between the epoxy and the two surfaces. This was done after some nonperforming test with two plies specimens, where the delamination of the tabs was observed due to the smoothness of the surfaces.

Figure 3. 13 - Tabs application

3.6 Matrix of the specimens tested

Several kinds of specimens were cast and tested in order to compare different FRCM systems and different test set-ups. The main objective of this study was to investigate how the contact length between the specimen and the metal tab influences the results of the tensile test, so specimens with different contact lengths were tested.

The second objective of the study addressed the effect of exposure for 1000 hours to different environments (alkaline, sea water, water vapor, and freezing and thawing). The third objective concerned the study of multiple plies and lap splices. The total number of specimens tested was 104 as summarized in Table 3.4.

Table 3. 4 - Matrix of the specimens tested

FRCM system	Contact length [mm]	Specimen type	Repetitions
Unidirectional fabric	100	One ply control condition	6
	150	One ply control condition	10
		Two plies control condition	10
		Lap splices	10
		Sea water environment	7
		Alkaline environment	7
		Water vapor environment	7
		Freezing and thawing	7
	200	One ply control condition	10
		Two plies control condition	10
Bidirectional fabric	150	One ply control condition	10
		Lap splices	10
			Total number 104

3.7 Parameter calculation

In order to compute the stresses, the loads obtained by the test frame were divided by the area of the carbon strands included in the specimen cross-section. The strains were recorded using an Epsilon 100 mm extensometer. The data presented in the previous section was calculated following Annex A of AC434.

The modulus of elasticity of the uncracked specimen E_1 was computed from the graph with a linear interpolation of the data from the start to the first crack. Being that the specimen is uncracked, this elastic modulus should represent the modulus of the mortar that controls the stiffness of the first part of the test. Nevertheless, since E_1 is computed dividing the load by the fabric area, this value is meaningless and the only way to compare this modulus to the modulus of the mortar is dividing the load by the gross cross-sectional area of the specimen.

As far as E_2 is concerned, a linear interpolation of the experimental curve between two preselected points was done. The two points are given by AC434 and correspond to the stress values $0.90f_{fu}$ and $0.60f_{fu}$. The strain values associated with these stresses are $\varepsilon_{f@0.90ffu}$ and $\varepsilon_{f@0.60ffu}$, so the modulus of elasticity of the cracked specimen according to the AC434 is:

$$E_f = \frac{\Delta f}{\Delta \varepsilon} = \frac{(0.90f_{fu} - 0.60f_{fu})}{(\varepsilon_{f@0.90ffu} - \varepsilon_{f@0.60ffu})}$$

This equation was first proposed by Bianchi et al.(2013) and later adopted by AC434 as the way to compute E_2 from the graph in an unequivocal way, avoiding inconsistency. Before choosing these points, other intervals were investigated in order to produce the most accurate value of E_2. In Figure 3.14 is shown the interpolation interval chosen in the AC434.

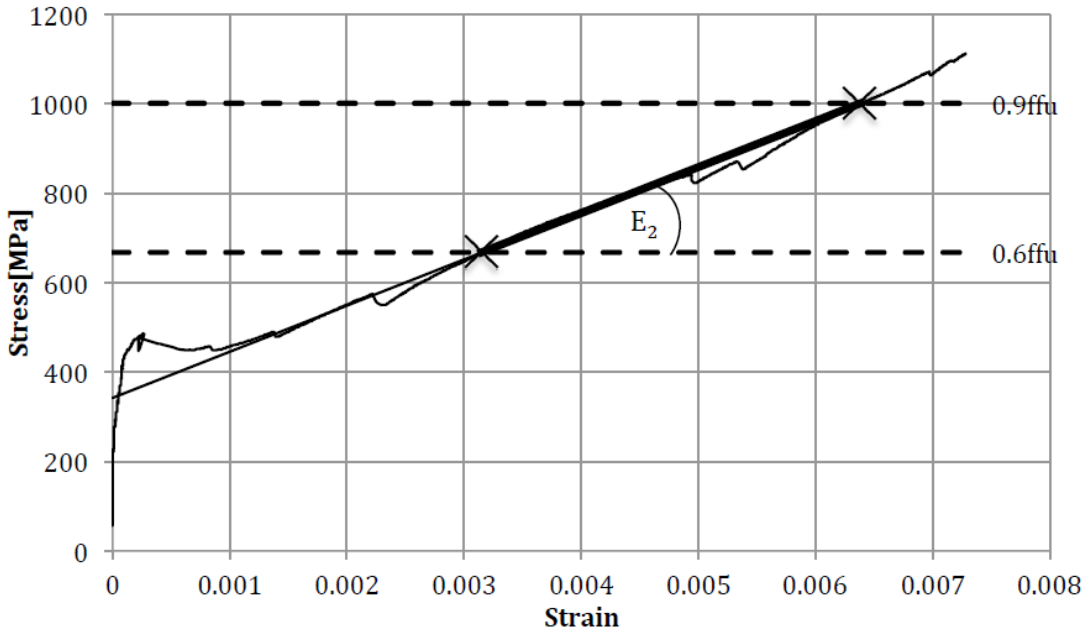

Figure 3. 14 - Interpolation of the AC434, Bianchi et al. (2013)

Bianchi et al. (2013) ended out with this interval doing a research on PBO-FRCM composite, thus it is not valid a priori for every FRCM system. For this reason the author verified the applicability of this formula to his results on the carbon-mesh FRCM before applying it. Also for the two systems object of this research the idealization proposed by Bianchi et al. (2013) is reasonable and for this reason will be used to compute the elastic modulus of the cracked specimen.

The ultimate strain ε_{fu} was calculated according to AC434 as the abscissa of the point on the E_2 line at which corresponds the f_{fu} value.

Finally, the transition point T of coordinates f_{ft}, ε_{ft} was computed as the intersection point of the two straight lines of E_1 and E_2. In this way the transition point T does not coincide with the point of the first crack C, which belong to the experimental curve and not to the idealize one. This aspect will be explained more in details in Section 4.2.

3.8 Problems related with the data analysis

As it was underline in the introductory section, one of the drawbacks of the FRCM strengthening system is the high coefficient of variance and the difficulty related to material characterization. There are different aspects that can condition the results of a tensile test. One of them is that it is not easy to cast panels with a constant thickness and to cut specimens of the same width. This problem affects the results in the first part of the graph until the first crack, where the load is carried by the mortar. Dividing the load by the area of the fabric in order to obtain the stress, the difference in the dimension of the specimen cannot be seen, consequently the parameters E_1, ε_t and f_t shows a high variability. In section Sections 4.1 and 4.2 this aspect is treated more in details.

Another problem related with the fabrication of the specimens is the dissymmetric reinforcement distribution, which cause an error in the extensometer recording. The dissymmetry can be both in the thickness and in the width of the specimen. If the reinforcement is not symmetric in the thickness, performing the tensile test causes a warping of the specimen. This warping generates a different crack opening in the two sides of the specimen and the recording of the extensometer is different if it is applied on the convex or concave face. (Figure 3.15). The same problem occurs in the case of dissymmetry of the reinforcement in the width. As can be seen in Figure 3.16 the crack opening is wider near the edge without reinforcement and tighter on the other edge. If the extensometer is not centered in the specimen its position influences the results.

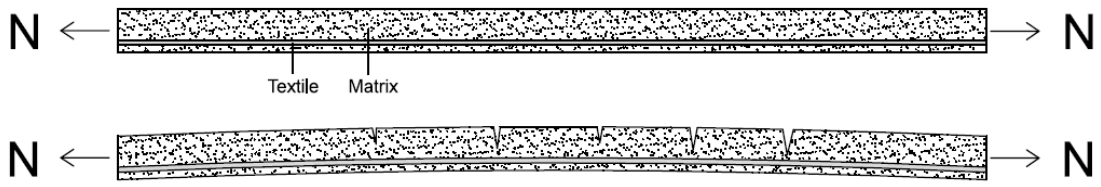

Figure 3. 15 - Dissymmetry of the reinforcement in the thickness of the specimen, Carozzi et al. (2015)

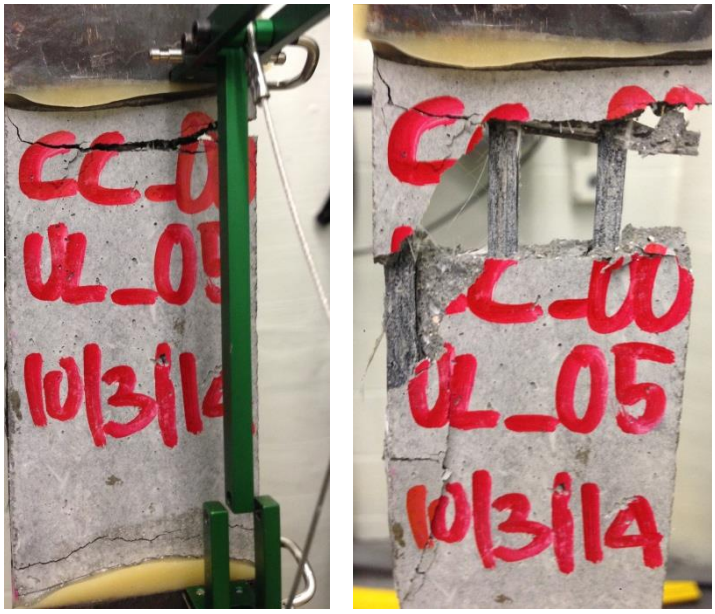

Figure 3. 16 - Dissymmetry of the reinforcement in the width of the specimen

Another aspect that can affect the extensometer recording is a warping of the specimen. The non-planarity of the specimen induce a parastitic bending moment and the crack opening is different on the two sides of the specimen, as can be seen from Figure 3.17. As in the case of a dissymmetric reinforcement in the thickness of the specimen, the side on which the extensometer is applied conditions the deformation recording: if the extensometer is applied on the convex side it will read a fictitious compression until the specimen becomes straight.

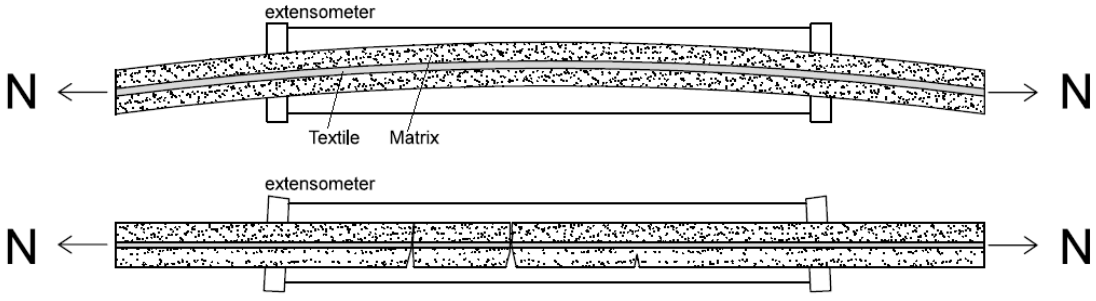

Figure 3. 17 – Effect of the warping of the specimen, Carozzi et al. (2015)

The last parameter that affects the results is the position of the cracks, that is something that cannot be predicted. As will be described in Section 4.2, the failure occurs after the opening of one of the cracks formed in the cracking phase. The position of this crack changes the anchorage length, that is equal to the tab length plus the distance between the end of the tab and the position of the crack that opens, that is variable (Figure 3.18). Testing the material with the clevis-type grip, the anchorage length is a parameter that change the ultimate strength (Section 4.6).

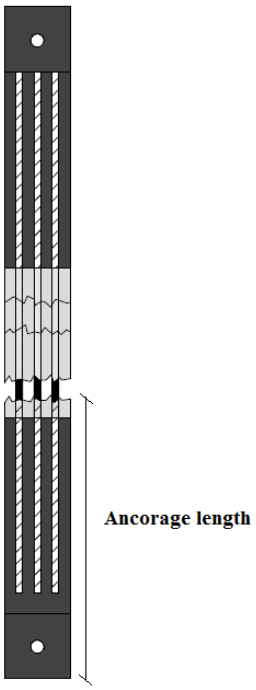

Figure 3. 18 - Anchorage length

3.9 Experimental results

This section summarizes the test results and graphs. How the parameters were computed is explained in the Section 3.7.

3.9.1 Unidirectional system

This section presents the outcomes from the tensile tests on the unidirectional FRCM system.

3.9.1..1 Control condition one ply 100 mm tab length

For the control condition of the one-ply specimens with a tab length of 100 mm 6 specimen were tested. The graphs are shown in Figure 3.19 and the results in terms of ultimate strength are presented in Table 3.5.

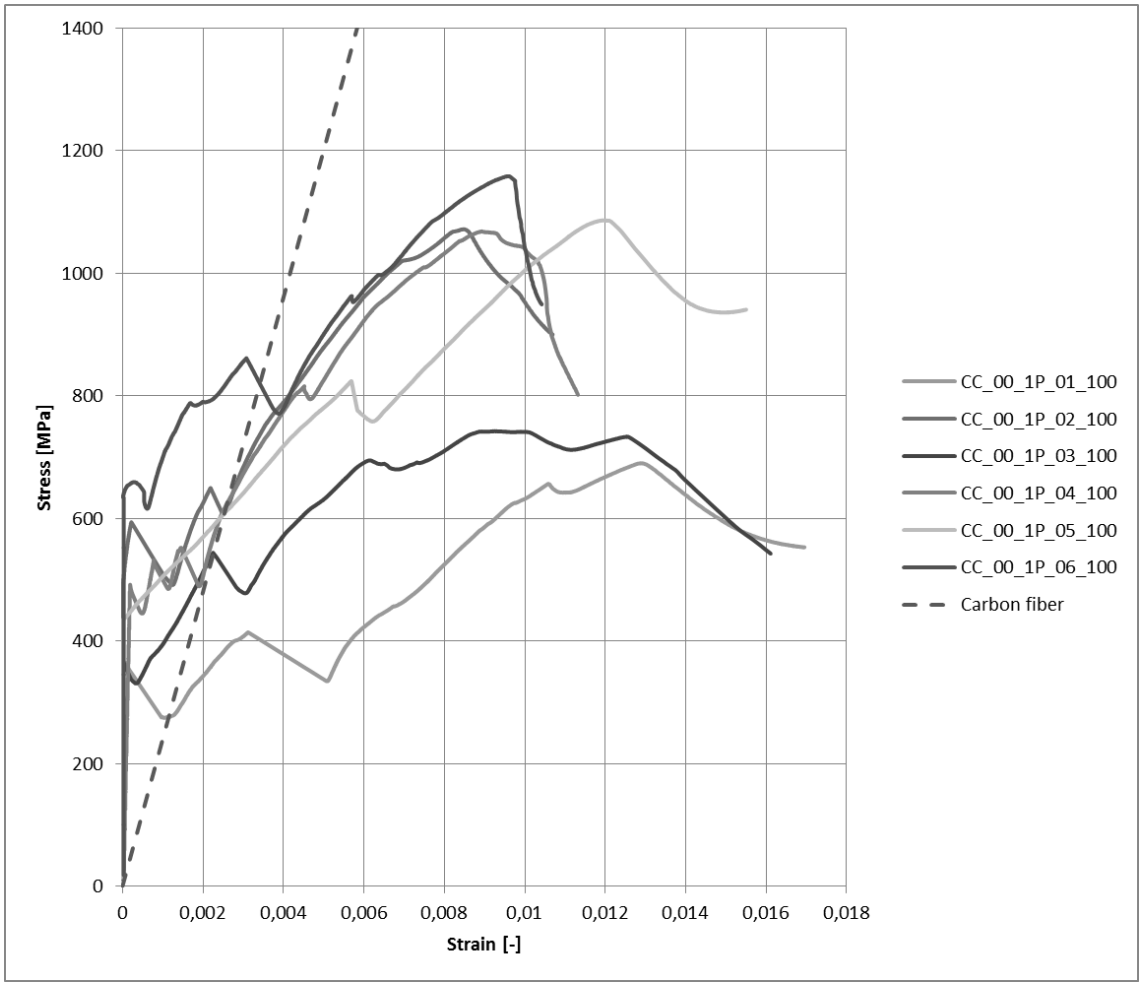

Figure 3. 19 - Control specimens one-ply with 100mm tab length

These specimens were tested only to compare the ultimate stress with the specimens with a tab length of 150 mm and 200 mm. For this reason only the outcomes from the ultimate strengths are listed in Table 3.5.

Table 3. 5 - Ultimate strength for one-ply specimens with 100 mm tab length

	f_{fu} [MPa]
CC_01	690
CC_02	1072
CC_03	742
CC_04	1068
CC_05	1086
CC_06	1158
Average	969
Stand.Dev.	200
C.o.V.	20,59%

The variance on the results is significant if compared with the results from the other specimens. This is due to the fact that these specimens are less precise, because they are coming from the first casting when the experience in making panels was less. As can be seen in Figure 3.15, the variability of the stress of the first crack is very high, because there is a significant variation in the thickness of the specimens. Being the stress computed with respect to the area of the fabric, that is the same in all the specimens, different thickness. The first part of all the graphs is vertical, because the specimens were warped. The failure mode was slippage of the fabric from the mortar within the tabs for all the specimens, after the formation of three or four macro cracks. All these aspects will be discussed more in details in the data analysis section.

3.9.1..2 One-ply 150 mm tab length

For the control condition of the one ply specimens with a tab length of 150 mm, 10 specimen were tested. Specimen CC_01 was discarded because of faulty condition during testing. The graphs are shown in Figure 3.20 and the parameters obtained are presented in Table 3.6.

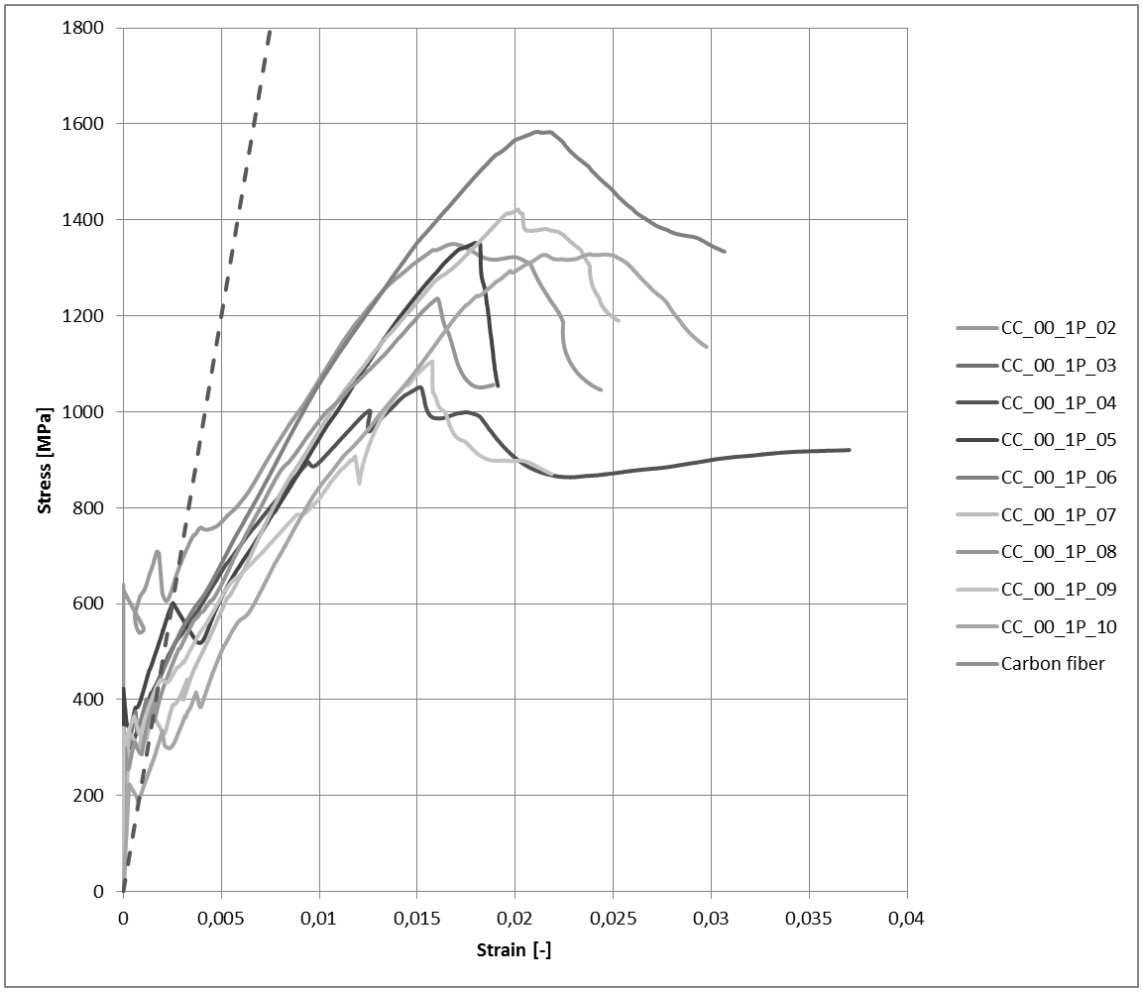

Figure 3. 20 - One-ply with 150mm tab length

Table 3. 6 - Parameters for one-ply with 150 mm tab length

	E_1 [MPa]	E_2 [MPa]	f_{ft} [MPa]	ε_{ft} [-]	ε_{fu} [-]	f_{fu} [MPa]
CC_02	-	62110	-	-	0,014643	1350
CC_03	2164358	70861	230	0,000106	0,014360	1240
CC_04	-	47157	-	-	0,013390	1052
CC_05	-	62878	-	-	0,016620	1352
CC_06	1178098	59100	470	0,000399	0,019240	1584
CC_07	1216993	54902	413	0,000340	0,018710	1422
CC_08	-	53518	-	-	0,015470	1236
CC_09	-	45918	-	-	0,015667	1105
CC_10	750870	52321	333	0,000444	0,019470	1329
Average	1327580	56529	362	0,000322	0,016397	1297
Stand. Dev.	596480	8010	104	0,000150	0,002252	162
C.o.V.	44,93%	14,17%	28,82%	46,62%	13,74%	12,46%

As can be seen in Figure 3.20, the graphs of these specimens are more regular and this is visible also in the lower coefficient of variation listed in Table 3.6. The variability on the outcomes is quite low except for the modulus of elasticity E_1 and

the strain at the transition point. This is due to the fact that these parameters depend on the mortar which carries the load in the first part of the test until the first crack. Different dimension of the specimens lead to a fictitious variability because the stresses are computed dividing the area of the fabric. For some specimens, it was not possible to compute the modulus E_1 and consequently the coordinates of the transition point, because of an accuracy issue of the extensometer. For all the specimens the failure mode was slippage of the fabric from the mortar within the tabs, after the formation of three or four macro cracks.

3.9.1..3 Two plies 150 mm tab length

For two-ply specimens with a tab length of 150 mm, 10 specimen were tested. Four specimens (CC_01, CC_02, CC_04, CC_08) experienced a debonding of the metal tabs from the mortar as the failure mode. For these specimens the outcomes of the ultimate stress f_{fu}, the ultimate strain ε_{fu} and the modulus of elasticity E_2 could not be computed and, consequently, the transition point. Looking at these specimens after the debonding of the tabs, it was noticed that the surfaces of the specimens and of the metal tabs were too smooth, thus the failure occurred in between them. In order to avoid this problem the mortar and steel surfaces were roughen, increasing the adhesion between the tab and the specimen (Figure 3.21). The graphs of the other six specimens are shown in Figure 3.22 and the parameters obtained are presented in Table 3.7.

Figure 3. 21 - Tab debonding and solution

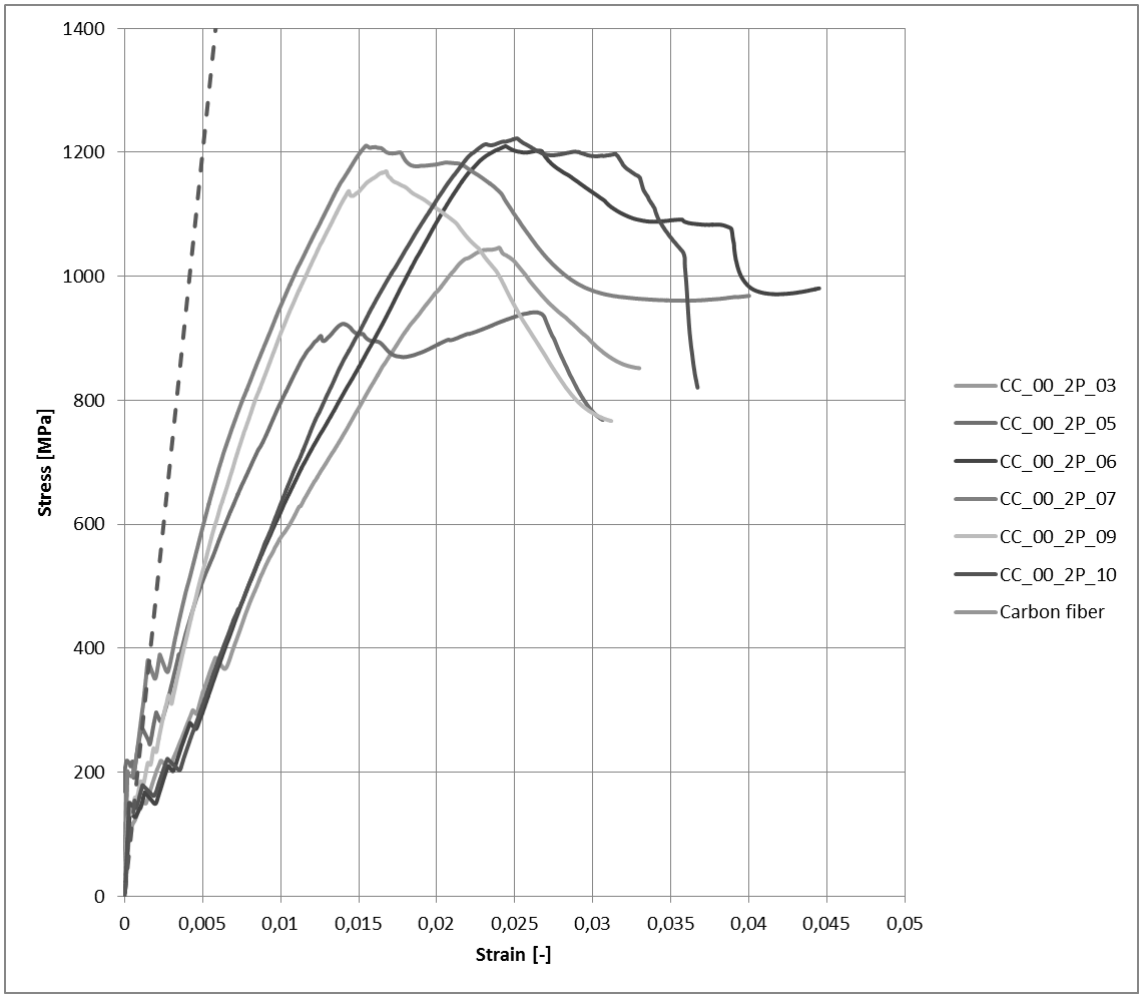

Figure 3. 22 - Control condition tests for two plies with 150mm tab length

Table 3. 7 - Parameters for control tests for two plies with 150mm tab length

	E_1 [MPa]	E_2 [MPa]	f_{ft} [MPa]	ε_{ft} [-]	f_{fu} [MPa]	ε_{fu} [-]
CC_01	463617	-	-	-	-	-
CC_02	-	-	-	-	-	-
CC_03	321281	40388	201	0,000627	1046	0,021540
CC_04	485890	-	-	-	-	-
CC_05	-	55622	-	-	942	0,012693
CC_06	385129	45708	197	0,000510	1210	0,022677
CC_07	-	59540	-	-	1211	0,014633
CC_08	-	-	-	-	-	-
CC_09	645358	63666	280	0,000433	1169	0,014407
CC_10	489881	47256	202	0,000412	1222	0,022007
Average	465193	52030	220	0,000496	1133	0,017993
Stand. Dev.	110110	8978	40	0,000097	114	0,004536
C.o.V.	23,67%	17,26%	18,17%	19,59%	10,08%	25,21%

The variability on the outcomes is quite low except for the modulus of elasticity E_1 and the strain at the transition point. For some specimens, it was not

possible to compute the modulus E_1 and consequently the coordinates of the transition point, because of an accuracy issue of the extensometer. As can be seen in Figure 3.22, the variability on the stress at the first crack is lower with respect to one ply specimens because the dimensions of these six specimen were more similar.

For all the specimens the failure mode was slippage of the fabric from the mortar within the tabs after the formation of three or four macro cracks, except for the specimens in which a delamination of the tabs occurred.

3.9.1..4 One-ply 200 mm tab length

For the one-ply specimens with a tab length of 200 mm, 8 specimen were tested. The graphs are shown in Figure 3.23 and the parameters obtained are presented in Table 3.8.

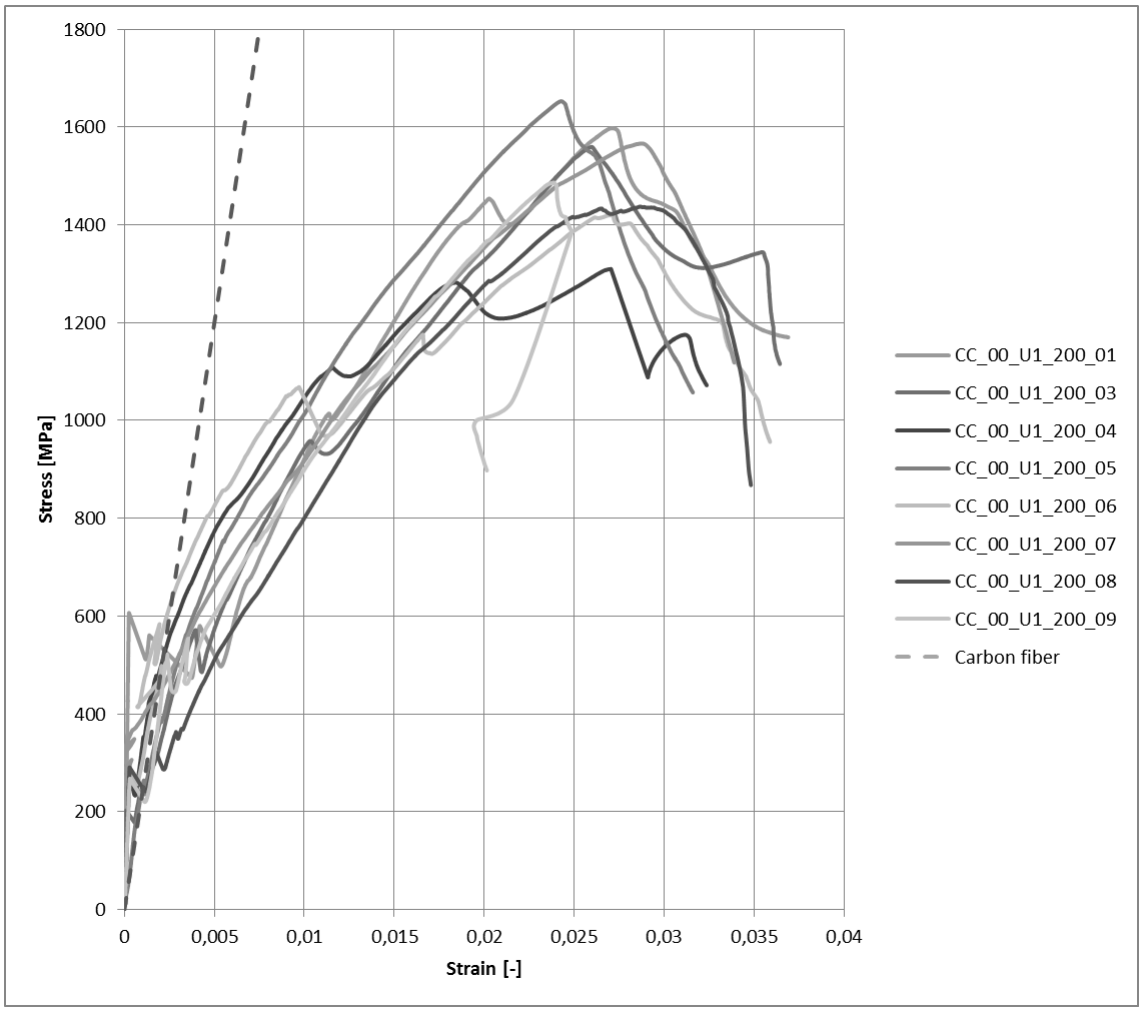

Figure 3. 23 - One-ply with 200mm tab length

Table 3. 8 - Parameters for control tests for one ply with 200mm tab length

	E_1 [MPa]	E_2 [MPa]	f_{ft} [MPa]	ε_{ft} [-]	f_{fu} [MPa]	ε_{fu} [-]
CC_01	-	39100	-	-	1598	0,026817
CC_02	-	-	-	-	-	-
CC_03	-	45201	-	-	1559	0,025330
CC_04	999294	39611	605	0,000605	1310	0,018407
CC_05	-	49990	-	-	1653	0,022847
CC_06	950799	35857	726	0,000764	1420	0,021230
CC_07	-	41189	-	-	1567	0,025633
CC_08	1001852	44328	391	0,000391	1438	0,023993
CC_09	887574	46847	453	0,000510	1487	0,022583
CC_10	-	-	-	-	-	-
Average	959880	42765	544	0,000567	1504	0,023355
Stand. Dev.	53621	4642	151	0,000158	112	0,002708
C.o.V.	5,59%	10,85%	27,80%	27,78%	7,43%	11,60%

The variability on the outcomes is quite low except for the strain at the transition point. For some specimens, it was not possible to compute the modulus E_1 and consequently the coordinates of the transition point, because of an accuracy issue of the extensometer. The stress at the first crack is between 200 and 300 MPa for all the specimen except for CC_01, for which is higher. This is due to the fact that this specimen was wider with respect to the others, and the area of the cross section of this specimen is 546 mm^2 while the average of the others is 460 mm^2. The graph of specimen CC_05 does not show a clear changing in the slope, probably because this specimen was pre-cracked. This fact does not affect the ultimate tensile strength of the specimen. For all the specimens the failure mode was slippage of the fabric from the mortar within the tabs, after the formation of three or four cracks.

3.9.1..5 Two-ply 200 mm tab length

For the control condition on the one ply specimens with a tab length of 200 mm, 8 specimen were tested. Specimens CC_01 and CC_07 were not tested because some problems with the gluing of the tabs arose. The graphs are shown in Figure 3.24 and the parameters obtained are presented in Table 3.9

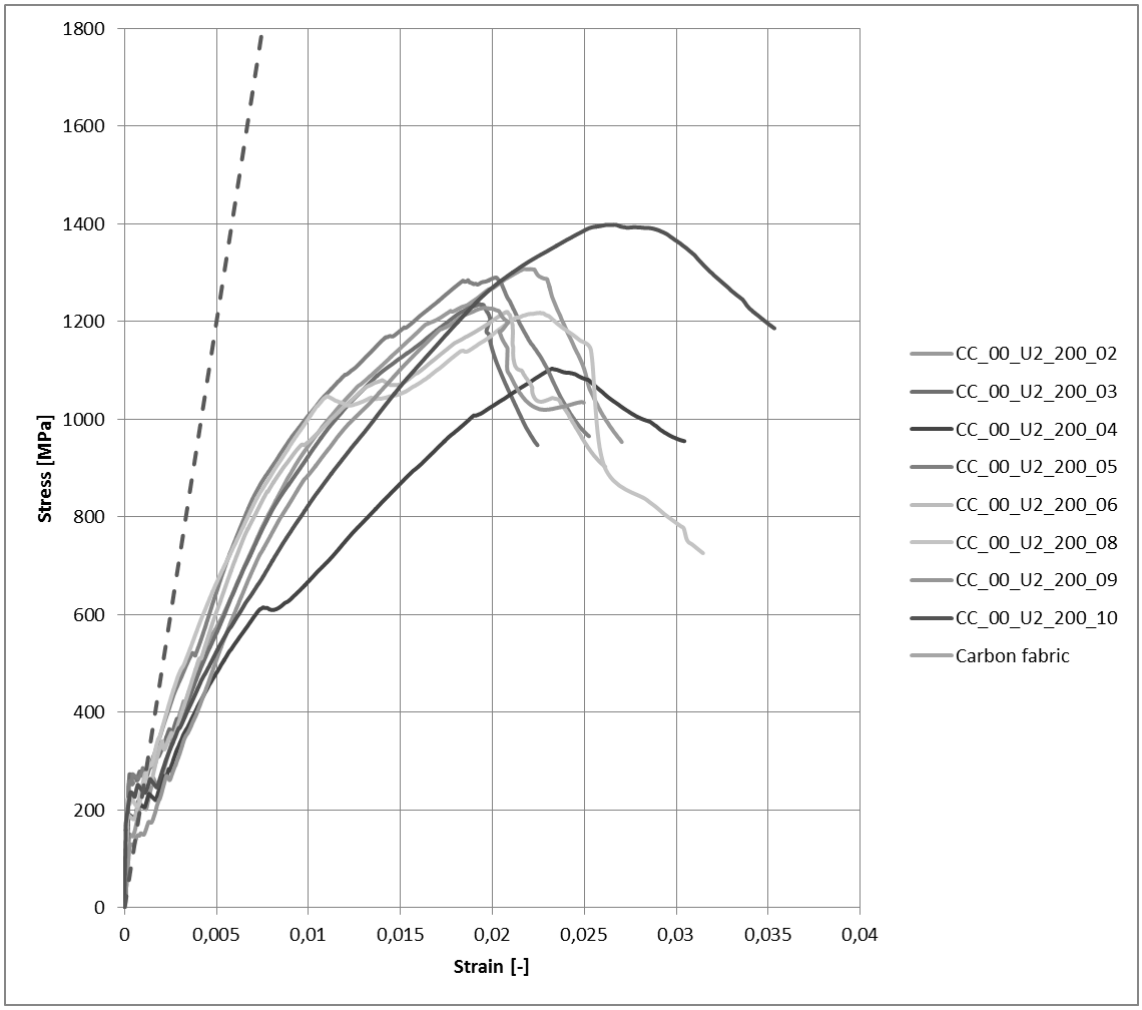

Figure 3. 24 - Two-ply with 200mm tab length

Table 3. 9 - Parameters for control tests for two plies with 200mm tab length

	E_1 [MPa]	E_2 [MPa]	f_{ft} [MPa]	ε_{ft} [-]	f_{fu} [MPa]	ε_{fu} [-]
CC_01	-	-	-	-	-	-
CC_02	529562	47029	471	0,000890	1307	0,018670
CC_03	1012895	49756	410	0,000405	1236	0,017003
CC_04	918762	38012	300	0,000327	1104	0,021463
CC_05	1146543	49995	482	0,000421	1290	0,016570
CC_06	1160779	37221	517	0,000446	1220	0,019317
CC_07	-	-	-	-	-	-
CC_08	459703	49120	409	0,000889	1228	0,017570
CC_09	-	33186	-	-	1218	0,020510
CC_10	-	44666	-	-	1398	0,022780
Average	871374	43623	432	0,000563	1250	0,019235
Stand. Dev.	305960	6574	77	0,000256	85	0,002215
C.o.V.	35,11%	15,07%	17,88%	45,51%	6,82%	11,51%

The variability on the outcomes is quite low except the strain at the transition point, but these results will be discussed later. For some specimens, it was not possible to compute the modulus E_1 and consequently the coordinates of the transition point, because of an accuracy issue of the extensometer. The graph of specimen CC_04 shows a little step at a stress of about 600 MPa, followed by a slight chance in the slope. This can be caused by the loss of adhesion of one of the yarns. For all the specimens the failure mode was slippage of the fabric from the mortar within the tabs after the formation of three or four macro cracks.

3.9.1..6 Lap specimens

For the control condition on the lap specimens with a tab length of 150 mm, 9 specimen were tested. The overlap length in the middle was equal to 100 mm. The outcomes from the specimens CC_03, CC_04, CC_05, CC_06, CC_08 are not considered because there were problems in the test setup. All the problems related with the testing of these specimens is explained in Section 3.9.3, critical analysis of the results of the lap specimens. The graphs are shown in Figure 3.21 and the parameters obtained are presented in Table 3.10

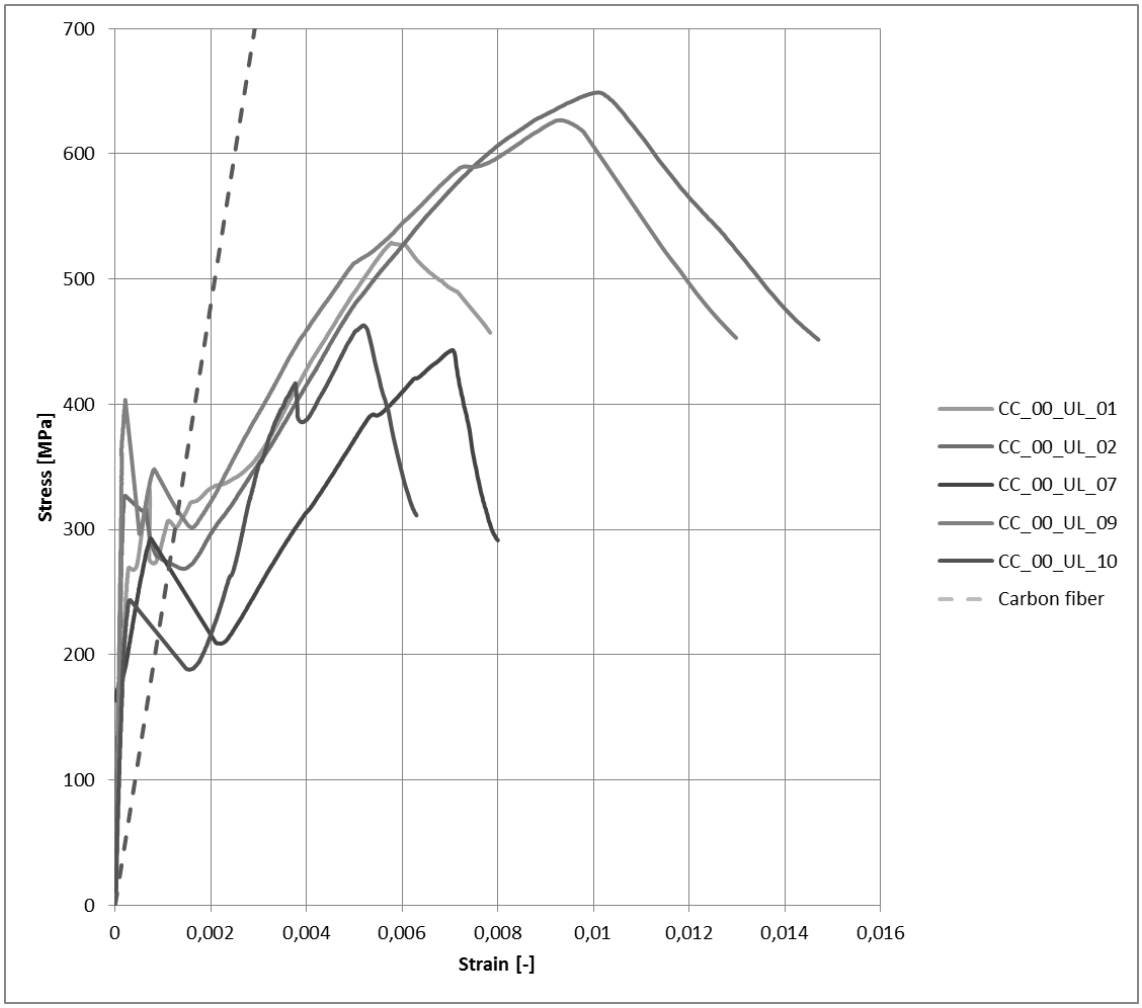

Figure 3. 25 - Control condition tests for lap with 150mm tab length

Table 3. 10 - Parameters for control tests for lap specimens with 150mm tab length

	E_1 [MPa]	E_2 [MPa]	f_{ft} [MPa]	ε_{ft} [-]	f_{fu} [MPa]	ε_{fu} [-]
CC_01	1174506	48834	253	0,000216	529	0,00586
CC_02	2026869	52058	207	0,000102	649	0,00860
CC_03	-	-	-	-	-	-
CC_04	-	-	-	-	-	-
CC_05	-	-	-	-	-	-
CC_06	-	-	-	-	-	-
CC_07	-	52153	-	-	443	0,00659
CC_08	1225962	-	-	-	-	-
CC_09	2377448	49751	244	0,000216	627	0,00780
CC_10	1120030	73503	97	0,000444	463	0,00507
Average	1584963	55260	200	0,000244	542	0,006784
Stand.Dev.	578107	10300	72	0,000144	93	0,001427
C.o.V.	36,47%	18,64%	35,87%	58,75%	17,20%	21,03%

Except for the ultimate load, the coefficient of variance is quite high for all the parameters computed. The high variability of the results of these tests is due to a bad

manufacture of the lap specimens. For many of them the external yarns were not confined, and this problem affect significantly the performance of the specimen. All these aspects will be explained more in detail in the data analysis section. The failure mode was in all the cases slippage in the overlap section.

3.9.2 Bi-directional system

This section presents the outcomes from the tensile tests on the Bidirectional FRCM system.

3.9.2..1 Control condition one ply 150 mm tab length

For the control condition of the one ply specimens with a tab length of 150 mm, 9 specimen were tested. The outcomes from specimens CC_08 and CC_09 were discarded because of faulty conditions during testing. The graphs are shown in Figure 3.26 and the parameters obtained are presented in Table 3.11.

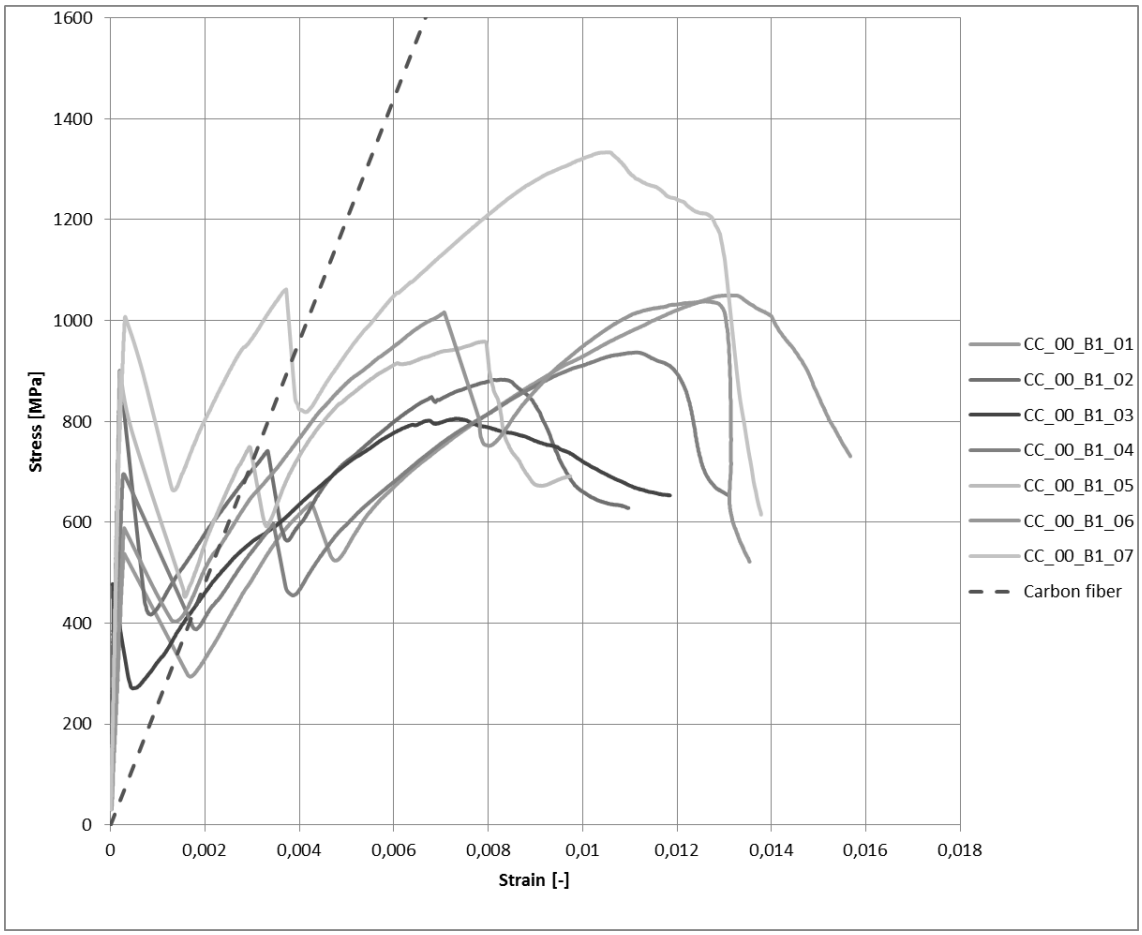

Figure 3. 26 - Control condition one ply 150 mm tab length

Table 3. 11 - Parameters for control tests for bidirectional specimens

	E_1 [MPa]	E_2 [MPa]	f_{ft} [MPa]	ε_{ft} [-]	f_{fu} [MPa]	ε_{fu} [-]
CC_01	689102	66476	287	0,000416	1050	0,011900
CC_02	-	107211	-	-	901	0,007000
CC_03	-	81943	-	-	806	0,006123
CC_04	963432	73778	235	0,000244	937	0,009760
CC_05	-	-	-	-	959	0,005887
CC_06	762637	103143	388	0,000508	1038	0,006817
CC_07	762637	100799	468	0,000614	1334	0,009203
CC_08	-	-	-	-	-	-
CC_09	-	-	-	-	-	-
Average	794452	88892	344	0,000446	1003	0,008099
Stand.Dev.	117866	17086	104	0,000157	168	0,002239
C.o.V.	14,84%	19,22%	30,20%	35,20%	16,71%	27,65%

The variability on the outcomes is quite low except for the coordinates of the transition point. For some specimens, it was not possible to compute the modulus E_1 and consequently the coordinates of the transition point, because of an accuracy issue of the extensometer. For all the specimens the failure mode was slippage of the fabric from the mortar within the tabs after the formation of two or three macro cracks. After failure, in correspondence to the cracks that opened, it was noticed that yarns lost the coating. The behavior shown by these specimens is different from the one that characterize the unidirectional material. Less macro crack are formed and the drop in the stress caused by a macro crack is more pronounced. The comparison between the two different FRCM system will be treated more in details in the data analysis section. Specimens CC_010 was not tested.

3.10 Failure mode

For all the specimens tested, without considering the specimens that experienced tab debonding and the lap specimens, the failure mode was consistently slippage of the carbon fabric from the cementitious matrix within the tabs. This kind of failure occurred after multiple cracking perpendicular to the length of the specimen, located in gage length of the coupon. The position and the number of cracks varies among the different specimens, and it is influenced by the unpredictable distribution of the voids in the matrix.

The phenomenon called “crack propagation” is divided in different phases. At the beginning the specimen is uncracked and all the load is carried by the mortar. Increasing the load micro cracks occur until the formation of a macro crack orthogonal to the direction of the load. During cracking there is a release of energy that causes a sudden drop in stiffness and load that can be seen in the graphs. The number of macro cracks varied from two to four and their spacing was not constant. After the formation of all the macro cracks, one of them starts opening and the load is transferred by friction from the mortar to the fabric. For this carbon fabric, the slipping involves the whole strands and the telescopic effect cannot be seen. This may be due to the resin coating of the carbon fabric, that impregnates the external fibers of the strands. The three strands that compose the fabric inside the specimen slip from the side where the tab is closer to the crack that opens.

The resin coating strongly increased the adhesion between the carbon and the mortar and the resulting FRCM system is efficient. The difference between coated or not-coated fabric can be seen only testing the material using a clevis type grip, because the failure is governed by slipping. The graphical representation of Figure 3.27 shows the tensile test behavior until failure.

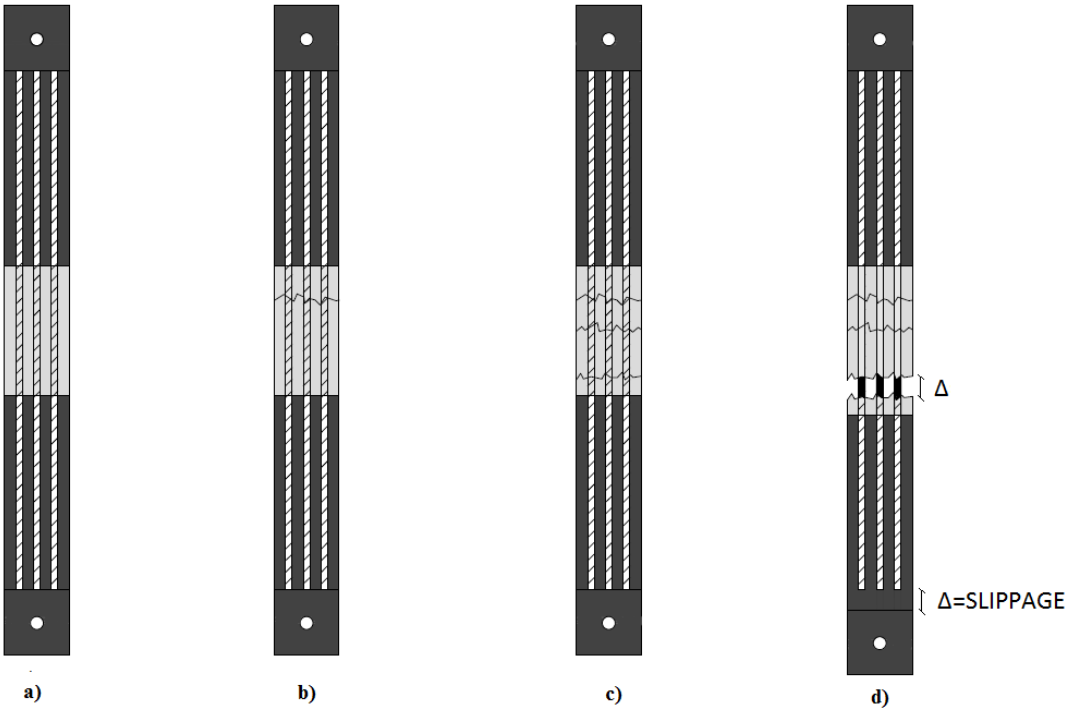

Figure 3. 27 – a) virgin specimen, b) first macro-crack, c) cracked specimen, d) opening of one of the cracks and slippage of the fabric within the tabs

4.

ANALYSIS OF THE RESULTS

Several aspects of the results are discussed in this section. Since this material is new as they are the testing procedures and parameter calculations are not yet standardize, the goal is to provide a critical analysis that can help to better understand how to study this composite material and open the window for future studies and researches.

4.1 Uncracked elastic modulus E_1

With respect to others parameters, the elastic modulus and the coordinates of the transition point T ($\varepsilon_T,\ f_t$) yield higher variability.

In the first part of the graph, before the matrix cracks, the load is carried only by the mortar. As explained in the Section 3.8, all the stresses are computed with respect to the fabric area, so E_1 is a fictitious value that represent a transformed cross section. The real comparison between elastic modulus should be done computing E_1 with respect to the cross section of the specimen. Moreover, there is a variability in the dimensions of the specimens that can affect the behavior of the FRCM in the first part of the test that is mortar dependent. For example, this computation is shown for the specimens with one ply and tab length of 150 mm, and the results are presented in Table 4.1:

Table 4. 1 - -Cross section of the specimens with one ply and the tab length of 150mm

	Width_1	Width_2	Average width	Thickness_1	Thickness_2	Average thickness	Area
	[mm]	[mm]	[mm]	[mm]	[mm]	[mm]	[mm^2]
CC_03	48,65	48,78	48,72	11,77	12,47	12,12	590,43
CC_06	50,08	49,58	49,83	9,58	9,27	9,43	469,65
CC_07	49,56	50,17	49,87	9,45	9,64	9,55	475,96
CC_10	48,79	48,41	48,60	9,32	9,53	9,43	458,06

Dividing the load by the cross section of the mortar instead of the cross section of the fabric enables the computation of the tensile strength on the mortar and its elastic modulus. The results are listed in Table 4.2.

Table 4. 2 - Uncracked modulus with respect to the cross section of the specimen

	$E_{1mortar}$
	[Mpa]
CC_03	22911
CC_06	18814
CC_07	19177
CC_10	12294
Average	18299
Stand. Dev.	44101
C.o.V	24,10%

The order of magnitude of E_1 given in Table 4.2 is in agreement with what we expected from a cementitious material. This is a very important validation of the test results.

The coefficient of variance for the elastic modulus drops from 44.93% when computed considering the fabric area, to 24.10% when computed with respect to the cross section of the coupon. Considering the intrinsic variability of a tensile test of a brittle material, this is considerably a good outcome.

At times, the measurement of elongation during the uncracked phase is not reliable particularly when the extensometer is installed on the convex surface of the coupon, that leads to fictitious compression recording. For this reason, if this was the case, the first part of the graph was not considered, and the deformation was assumed equal to zero until the first crack.

4.2 Transition point and point of the first crack

The transition point T is defined as the point in which the two linear segments of the idealized bi-linear curve intercept. This point is not the point of the first crack C. This can be seen in Figure 4.1, which represents the superposition of the real graph with its idealization according to AC434.

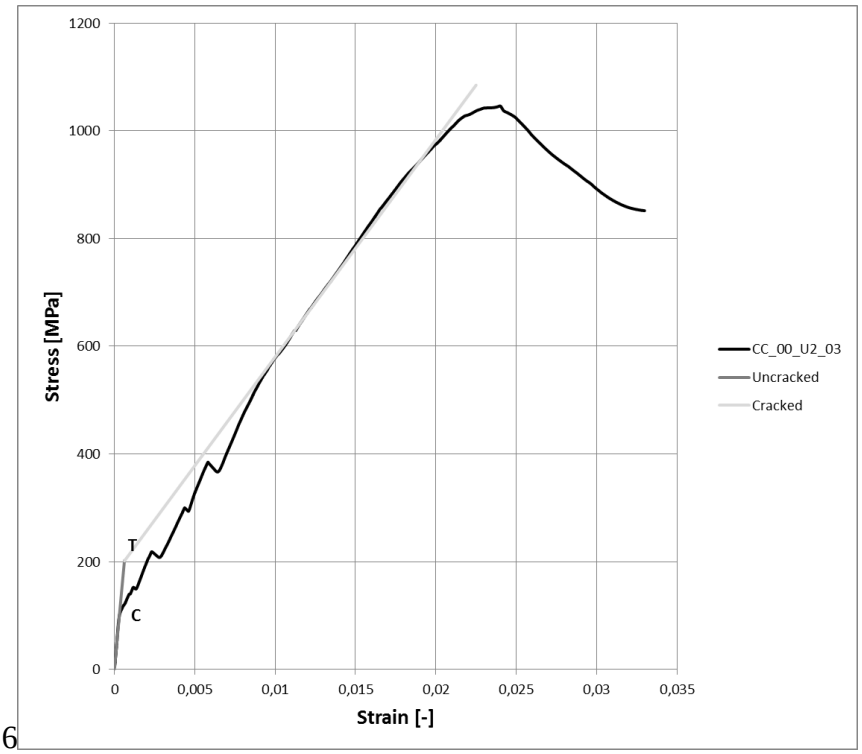

6

Figure 4. 1 - AC434 idealized curve

In order to understand the difference between C and T points, the outcomes from four one ply-specimens are presented. In Table 4.3 are listed the results coming from the specimens: CC_03, CC_06, CC_07 and CC_010.

Table 4. 3 - Comparison between transition point and point of the first crack

	Transition point-Fabric		**First crack-Fabric**		**First crack-Mortar**	
	f_T	ε_T	f_C	ε_C	f_C	ε_C
	[MPa]	**[-]**	**[MPa]**	**[-]**	**[MPa]**	**[-]**
CC_03	230	0,000106	523	0,000220	5,5	0,000220
CC_06	470	0,000399	336	0,000290	5,4	0,000290
CC_07	413	0,000340	332	0,000300	5,2	0,000300
CC_10	334	0,000444	224	0,000310	3,7	0,000310
Average	362	0,000322	354	0,000280	5,0	0,000280
Stand. Dev.	90	0,000130	108	0,000035	0,8	0,000035
C.o.V	24,96%	40,37%	30,40%	12,63%	15,17%	12,63%

As in Figure 4.1 shown and confirmed by Table 4.3, the transition point is an overestimation of the point of the first crack. However, it is not important from a design perspective because in concrete strengthening application, calculations are based on the second part of the graph (i.e. ultimate strain and E_2) the second part of the graph, and ultimate strain and stiffness are the parameters sought. The first part of the idealized constitutive law is important to ensure quality control.

Another aspect that has to be taken into account in order to understand why the first part of the FRCM behavior is less important than the second, it is that in the actual application, the substrate prevent cracking and there is less energy released by the system. This is due to the fact that the cracks are dictated by the structural element the FRCM is applied on. If, for example, the FRCM system is put on the bottom of a beam as a flexural reinforcement, the cracks will form where the concrete opens in the beam. In this way, the cracking pattern of the FRCM alone studied in the tensile test is different from the one in strengthening applications. However, in both the cases there is slippage, and the tensile test captures the behavior of the FRCM system in the second part, when the fabric slips from the cementitious matrix.

The first crack is identified as the point in which the load drops significantly for the first time. The coordinates of this point, as the uncracked modulus of elasticity E_1, is a characteristic of the mortar and depends on its tensile resistance. The values of f_c and ε_c based on gross cross section are shown in the last two columns of Table 4.3.

The coefficient of variance for the first crack strength computed with respect to the area of the mortar is half of the one computed with the fabric area

The first crack strength computed with respect to the area of the mortar (5,0 MPa average value) is close to the value that the manufacturer gives as the tensile resistance of the mortar (4,5 MPa). This result is important to ensure quality control during tensile testing, as in the case of the uncracked elastic modulus computed with respect to the area of the mortar.

4.3 Lap splices

For all the specimens, the failure was slippage from the overlapping section, at an ultimate stress that is half of the maximum stress of the specimens with continuous fabric. The objective of this kind of test is to understand if the overlapping length is enough to avoid a loss of strength in the specimen and, looking at the results obtained,

the conclusion is that 100 mm of superposition of the fabric is not sufficient to guarantee load transfer. The slippage occurred always in the central part of the specimens so the lap section is actually a weak section for the coupon. The reason is that testing an overlap of 100 mm with a tab length of 150 mm causes the slippage to be in the middle and the ultimate stress will be lower than the ultimate stress with continuous fabric. Is evident from the graphs that a lap of 100 mm with a tab length of 150 mm is not enough and the minimum overlap should be equal to the tab length. If AC434 moves to standardize a tab length of 150 mm, the recommendation is that a minimum lap length of 150 mm is needed.

In the study of Arboleda et al. (2014) on the PBO-FRCM material, the lap splices did not form weak areas because the specimens in Arboleda's study were tested with a tab length of 100 mm and a lap of 120 mm. This confirms the hypothesis that the lap has to be at a minimum equal to the tab length.

Regarding the accuracy of the results, it was underlined previously that the coefficients of variance for the outcomes of this test are considerably high. Unlike the specimens with continuous fabric, the presence of an offset in the overlap made it more difficult to cut the specimens without damaging the fabric. For example, the external yarns were not always confined by the mortar, as can be seen in Figure 4.2, and this affected a few results.

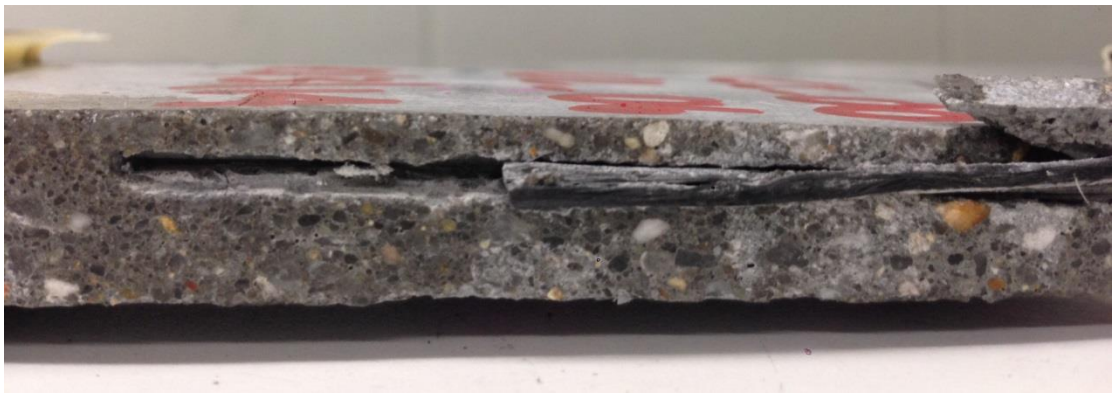

Figure 4. 2 - Lateral view of a tested lap specimen

4.4 Single ply vs. two plies specimens

Specimens with one and two plies were tested in order to investigate the different behavior of a multiple ply system with respect to a single ply one. What can be expected with more than one ply is that the interaction between the plies affects the ultimate resistance of the system. The results obtained meet the expectation in terms of performance, but it is interesting to observe that the loss of efficiency is limited. There is a slight decrease of the ultimate strength as well as the ultimate strain. In the ultimate strength, there is a decrease of 13% for the specimens tested with 150 mm tab length and 17% for 200 mm tab length, while for the ultimate deformation the differences are 9% and 17% respectively. That's means that the efficiency of the multiple ply system is good. Table 4.4 shows the parameter's comparison for one and two plies for both of 150 and 200mm tab lengths studied.

Table 4. 4 - Comparison between one ply and two plies system

		One ply			Two plies		
		E_2 [MPa]	f_{fu} [MPa]	ε_{fu} [-]	E_2 [MPa]	f_{fu} [MPa]	ε_{fu} [-]
150 mm	Average	56529	1297	0,016397	52030	1133	0,017993
	Stand.Dev.	8010	162	0,002252	8978	114	0,004536
	C.o.V.	14,17%	12,46%	13,74%	17,26%	10,08%	25,21%
200 mm	Average	42765	1504	0,023355	43623	1250	0,019235
	Stand.Dev.	4642	112	0,002708	6574	85	0,002215
	C.o.V.	10,85%	7,43%	11,60%	15,07%	6,82%	11,51%

An important aspect that can be highlighted is that for both the tab lengths studied, the elastic modulus of the cracked specimen remains the same as can be seen in Figure 4.3, in which are shown two representative curves of specimens with one and two plies tested with a tab length of 150 mm..

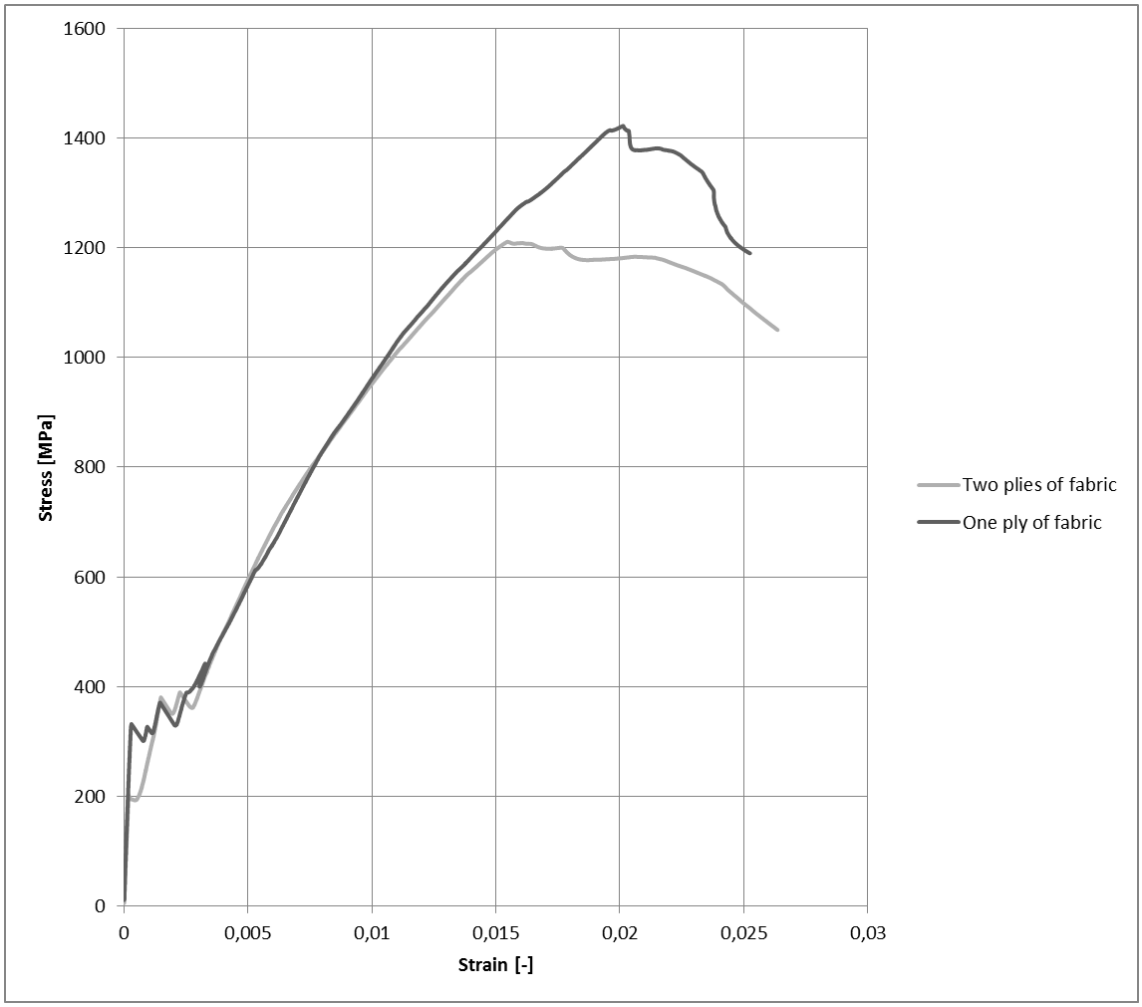

Figure 4. 3 - One ply and two plies systems tested with 150 mm tab length

4.5 Comparison of bi-directional and unidirectional systems

Two FRCM fabric architectures were studied. Looking at the graphs presented previously, it is possible to recognize that the behavior of the two systems is fairly different. It was observed during the test that, in the case of the unidirectional system, the number of cracks at failure was three or four, while in the case of the bi-directional system the cracks at failure are always two. This can be seen by counting the number of drops in the graphs of the two systems. Figure 4.4 compares the behavior of the specimens CC_U1_06 and CC_B1_01, and the number of cracks in the specimens.

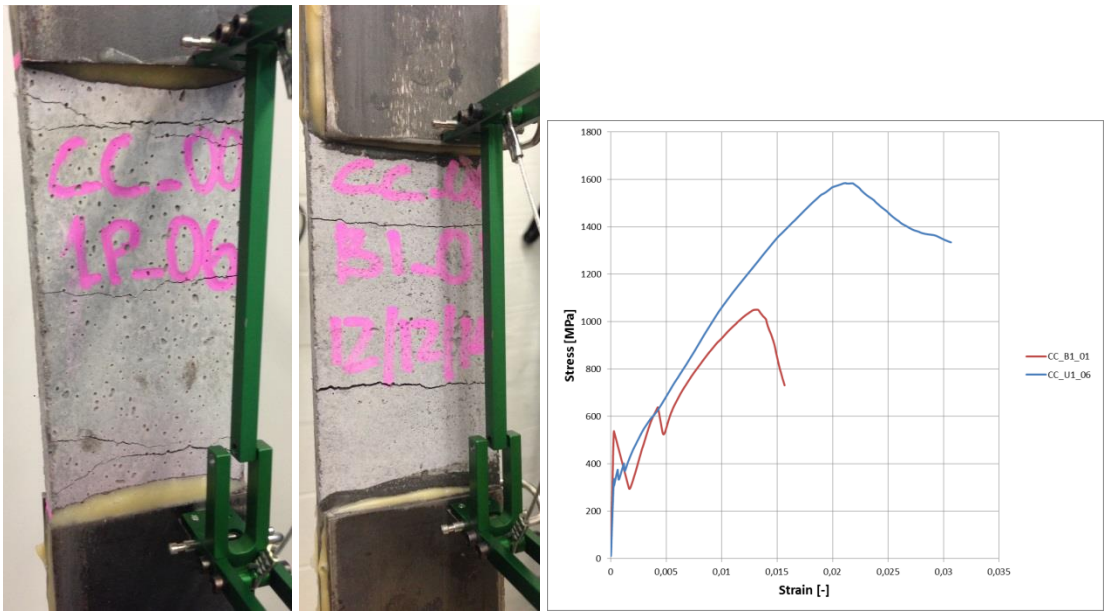

Figure 4. 4 - Cracking pattern behavior: unidirectional and bi-directional systems

Another distinction between the two systems is the amplitude of the drops in the graphs caused by crack formations, which is much more pronounced in the case of the bidirectional system. The bidirectional system is characterized by a fabric area that is only one third of the one of the unidirectional system (i.e. 1,5% vs. 0,5%). For this reason the energy that is released by the mortar when it cracks is not carried by the fabric immediately.

In terms of ultimate strength, the unidirectional system is stronger than the bi-directional one with an increment equal to 23%. This can be due to the better coating

of the first system, that in the case of a slipping failure plays a fundamental role in the efficiency of the composite material.

Looking at the graphs obtained (Figure 4.5), the two systems are very different also in terms of stiffness, and the cracked modulus E_2 of elasticity of the bi-directional system is higher by 36%.

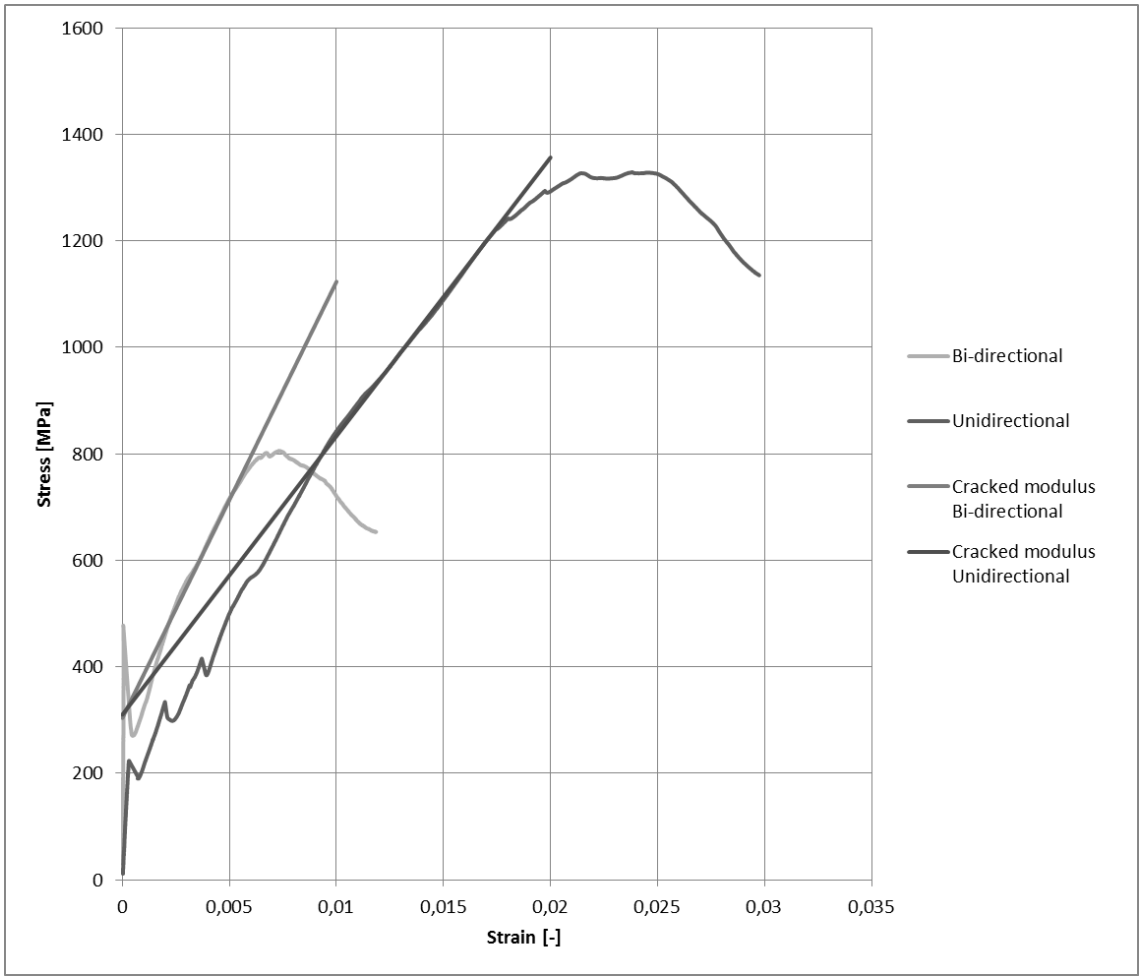

Figure 4. 5 - Unidirectional and Bi-directional comparison : stiffness

4.6 Tab length comparison

The most important aspect studied in this research is the influence of tab length on the results obtained from the tensile test. As expected, increasing the contact length between the metal tabs and the specimens increases the apparent tensile strength. This is due to the fact that, with a clevis-type grip which allows slippage of the strands at failure, a higher anchoring length cause a higher ultimate stress. This is in accordance with the study of Arboleda on PBO. In this experimental campaign, one ply specimens with three different tab lengths (100 mm, 150 mm, 200 mm) were tested and two in the case of two plies (150 mm and 200 mm). Table 4.5 summarizes the results obtained in terms of ultimate stress with the different tab lengths in one and two plies.

Table 4. 5 - Tab length comparison: ultimate stress

	One ply		Two plies	
	f_{fu} [MPa]	Increase [%]	f_{fu} [MPa]	Increase [%]
100 mm	969	N/A	-	-
150 mm	1297	25%	1133	N/A
200 mm	1504	14%	1250	9%

An interesting trend can be seen in the results for the one ply, which show a decreasing rate of the increase of the ultimate stress. These results are not far from the study of Arboleda on PBO, in which there is also a significant difference between the increase in the ultimate stress obtained moving from 100 mm to 150 mm and from 150 mm to 200 mm of tab length. Based on these results it is possible to predict that longer tabs will not produce significant higher strengths. This indicates that there is an ideal tab length for testing the material that lead to the characteristics ultimate stress and after which no further differences can be found in terms of ultimate stress.

Additional observations can be made by analyzing the rest of parameters computed for the different tab lengths, remembering that for the 100 mm tab length the only ultimate stress was computed. Table 4.6 summarizes the different outcomes.

Table 4. 6 - Parameters comparison for different tab length

		One ply			Two plies		
		E_2 [MPa]	f_{fu} [MPa]	ε_{fu} [-]	E_2 [MPa]	f_{fu} [MPa]	ε_{fu} [-]
150 mm	Average	56529	1297	0,016397	52030	1133	0,017993
	Stand.Dev.	8010	162	0,002252	8978	114	0,004536
	C.o.V.	14,17%	12,46%	13,74%	17,26%	10,08%	25,21%
200 mm	Average	42765	1504	0,023355	43623	1250	0,019235
	Stand.Dev.	4642	112	0,002708	6574	85	0,002215
	C.o.V.	10,85%	7,43%	11,60%	15,07%	6,82%	11,51%

These tabulated results show also that the coefficient of variance decreases from a 150 mm tab length to a 200 mm tab length, and this trend is valid both for the one and two plies of fabric. So the longer the contact length, the lower the variability of the test results.

The cracked modulus of elasticity E_2, for one ply as well as for two plies decreased from the 150 mm to the 200 mm tab length specimens. This result was not expected and needs to be further investigated.

Figure 4.6 are shows three representative graphs of specimens from the different families of tab lengths together with the graph of the carbon fiber alone.

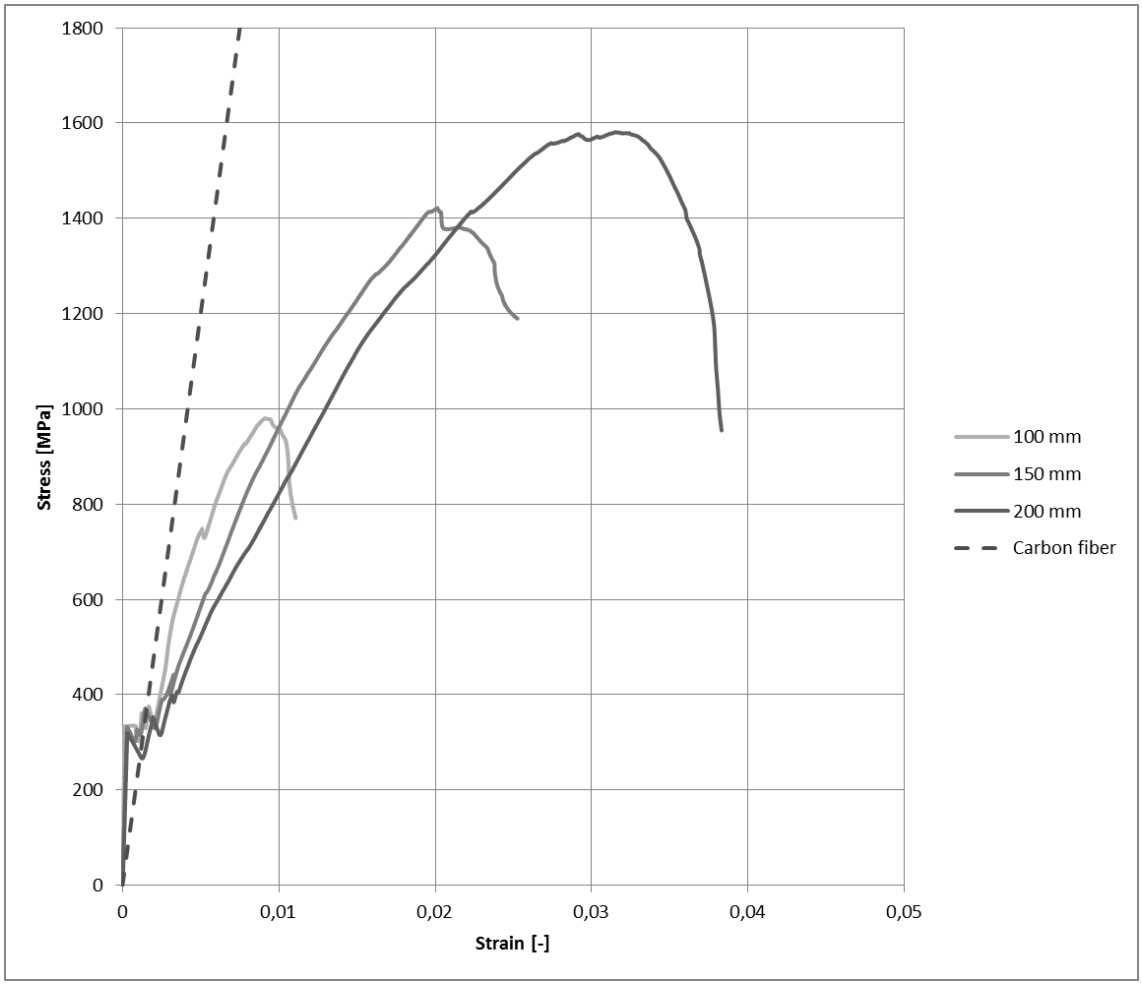

Figure 4. 6 - Representative graphs for the three different tab lengths

From Figure 4.6 it is also visible the increasing of the ultimate strength for longer tab length, with a decreasing rate. This result is similar to the results presented in Section 2.3 regarding the push-pull shear tests found in literature, and the trend suggest the existence of an effective tab length. In Figure 4.7 the graph of the ultimate strength for different tab length is shown, together with the error related to this parameter. In this way it is visible the trend of the ultimate strength varying the tab length but at the same time the decreasing of the error is visible. In this sense Figure 4.7 can be seen as the summary of section 4.6.

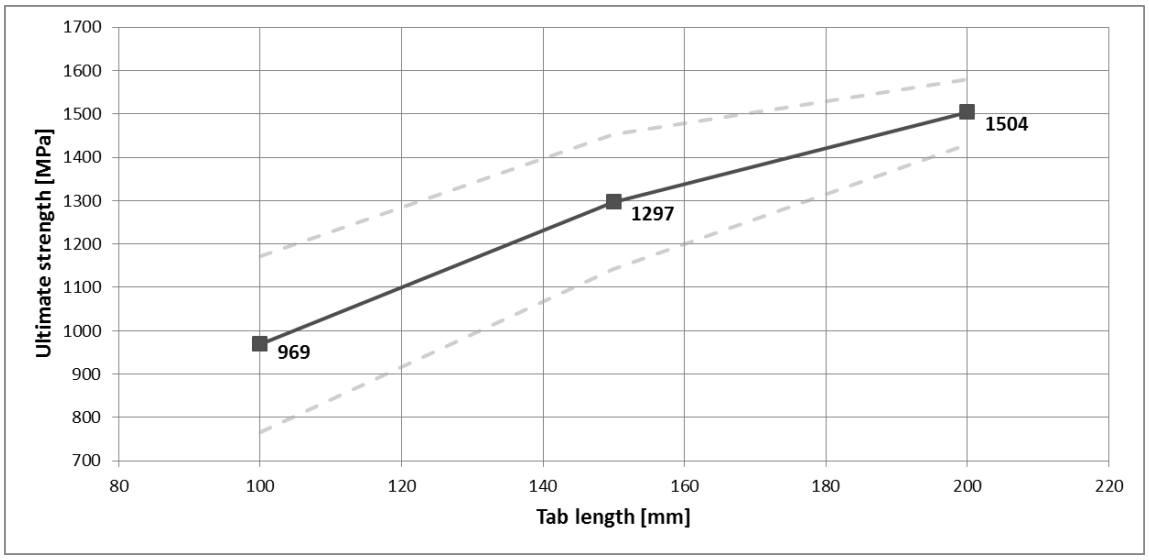

Figure 4. 7 - Ultimate strength with error band for different tab length

5.

DURABILITY

5.1 Durability on FRCM system: introduction

Durability is one of the key aspects in engineering. A construction material should have the ability to maintain required performance over time under the effect of external actions. A deterioration of the structural components affects the performance of the building and it can cause an earlier failure. A good design can prevent future costs for maintenance and repair. For all these reason it is crucial to test the durability properties of the FRCM composite, after exposure to environments that most likely it will experience in the field. Being the proposed FRCM an alternative to FRP, it seems reasonable to study exposure to the same environments. For this reason, this study focused on environments known to be dangerous for the components of these repairing systems. The exposure environments selected for this study are: freeze/thaw (known to be detrimental for cementitious material), alkalinity solution, seawater and water vapor exposure because these environment are problematic for composite with glass fibers and organics, both present in the mortar used. Moreover, chemical reactions that produce compounds of higher volume can be very critical for the mortar and they can strongly affect the adhesion between the fabric and the matrix. The freezing of the water present in the voids of the mortar produces internal cracks generated by volume expansion. The alkali-aggregate reaction is the reaction between the alkali, sodium and potassium (Na_2O and K_2O), present in the cement and the silicia present in certain aggregates. The alkali, that after the hydration generates sodium and potassium hydroxide ($2Na(OH) and\ 2K(OH)$), and the aggregates react with the hydroxyl ions (OH^-) associated with the alkali, generating compounds characterized by a higher volume.

The durability study of a composite material such as the FRCM, should consider the effect of the environments on all the components of the system and their interface. These are the cementitious matrix, the fabric and the two interfaces fabric-matrix and matrix-substrate. Since this study focuses on the tensile test characterization, the interface between the composite and the substrate outside the scope of the work. The effect of the environment exposure was evaluated by analyzing the changes in tensile strength of the specimens before and after the exposure.

5.2 Environment description

Different environment conditions were considered in this research, and the relative results were compared with the results of the control condition, characterized by a temperature of 22°C and relative humidity of 50%. In order to understand the durability performance of FRCM, tensile tests were performed after exposure to determinate the residual strength of the composite system. The durability study was limited to one-ply specimens of the unidirectional system after an exposure of 1000 hours. The environments considered in this work are four.

For the freezing and thawing conditioning, specimens were subjected to 20 freeze-thaw cycles after a week in a humidity chamber at a temperature of 37.7°C and 100% relative humidity. Each cycle consists of four hours at a temperature of -18°C, followed by twelve hours in the humidity chamber (37.7°C, 100% relative humidity).

Specimens were also subjected to three different kinds of aging processes. In the first, water vapor, the specimens were put in a humidity chamber at 100% relative humidity and 37.7°C for 1000 hours. The second consists of submerging the specimens in saltwater obtained from the Atlantic Ocean (Key Biscayne Bay, Florida) and replaced monthly. The third kind of aging process consists of submerging the specimens in an alkaline environment (pH>9.5 and temperature equal to 22°C), where the solution consists of a composition of calcium hydroxide (Ca(OH)2), sodium hydroxide (NaOH) and potassium hydroxide (KOH).

5.3 Experimental results

This section summarizes all the test results and the graphs from the durability study. Parameters were computed is explained in Section 3.7.

The durability study was conducted only on unidirectional FRCM with a tab length of 150 mm. For this reason the outcomes are compared with the results of the control condition test done on the same specimens with tab length of 150 mm.

5.3.1 Alkaline resistance

For the alkaline resistance of the-one ply specimens with a tab length of 150 mm, six specimen were tested. The graphs are shown in Figure 5.1 and the results in terms of ultimate strength are presented in Table 5.1.

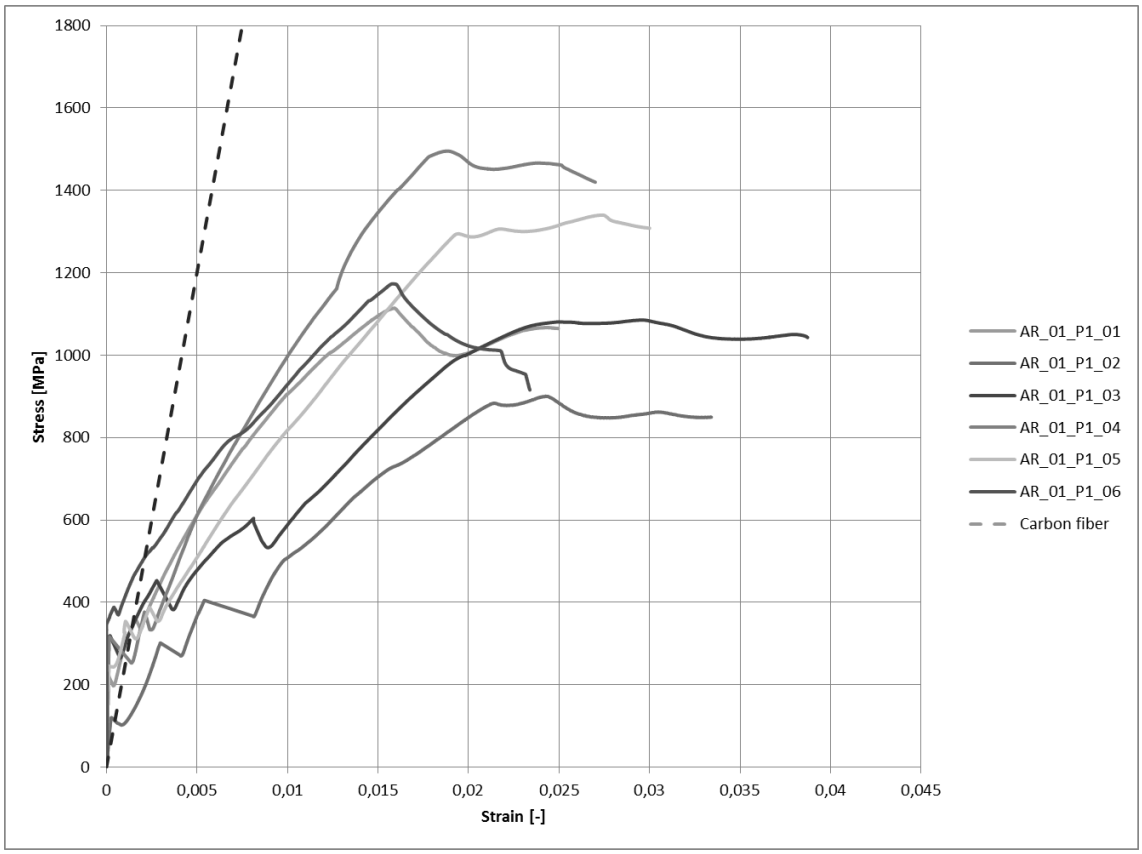

Figure 5. 1 - Alkaline resistance

Table 5. 1 - Parameters for Alkaline resistance tests

	E_1 [MPa]	E_2 [MPa]	f_{ft} [MPa]	ε_{ft} [-]	f_{fu} [MPa]	ε_{fu} [-]
AR_01	-	52248	-	-	1115	0,014403
AR_02	-	34853	-	-	900	0,021343
AR_03	-	42744	-	-	1086	0,02144
AR_04	-	65049	-	-	1496	0,017797
AR_05	-	52355	-	-	1340	0,01997
AR_06	-	46260	-	-	1173	0,015277
AR_07	-	-	-	-	-	-
Average	-	48918	-	-	1185	0,018372
Stand.Dev.	-	10258	-	-	208	0,003048
C.o.V.	-	20,97%	-	-	17,56%	16,59%

The variability on the outcomes is quite low. For all the specimens was not possible to compute the modulus E_1, and consequently the coordinates of the transition point, because of an accuracy issue of the extensometer. The graph of specimen CC_04 shows a discontinuity in the slope at a stress of about 1200 MPa. This is due to the fact that during the test a problem occurred with the machine and the author had to interrupt the test and restart it. For all the specimens the failure mode was slippage of the fabric from the mortar within the tabs after the formation of three or four macro cracks. The behavior of the specimens after the exposure to the alkaline environment was the same observed with the control specimens, and also the parameters computed are similar. The only difference with the control specimen was the white residual from the solution, deposited on the specimen surface.

5.3.2 Sea water resistance

For the sea water resistance of the one ply specimens with a tab length of 150 mm, seven specimens were tested. The graphs are shown in Figure 5.2 and the parameters obtained are presented in Table 5.2.

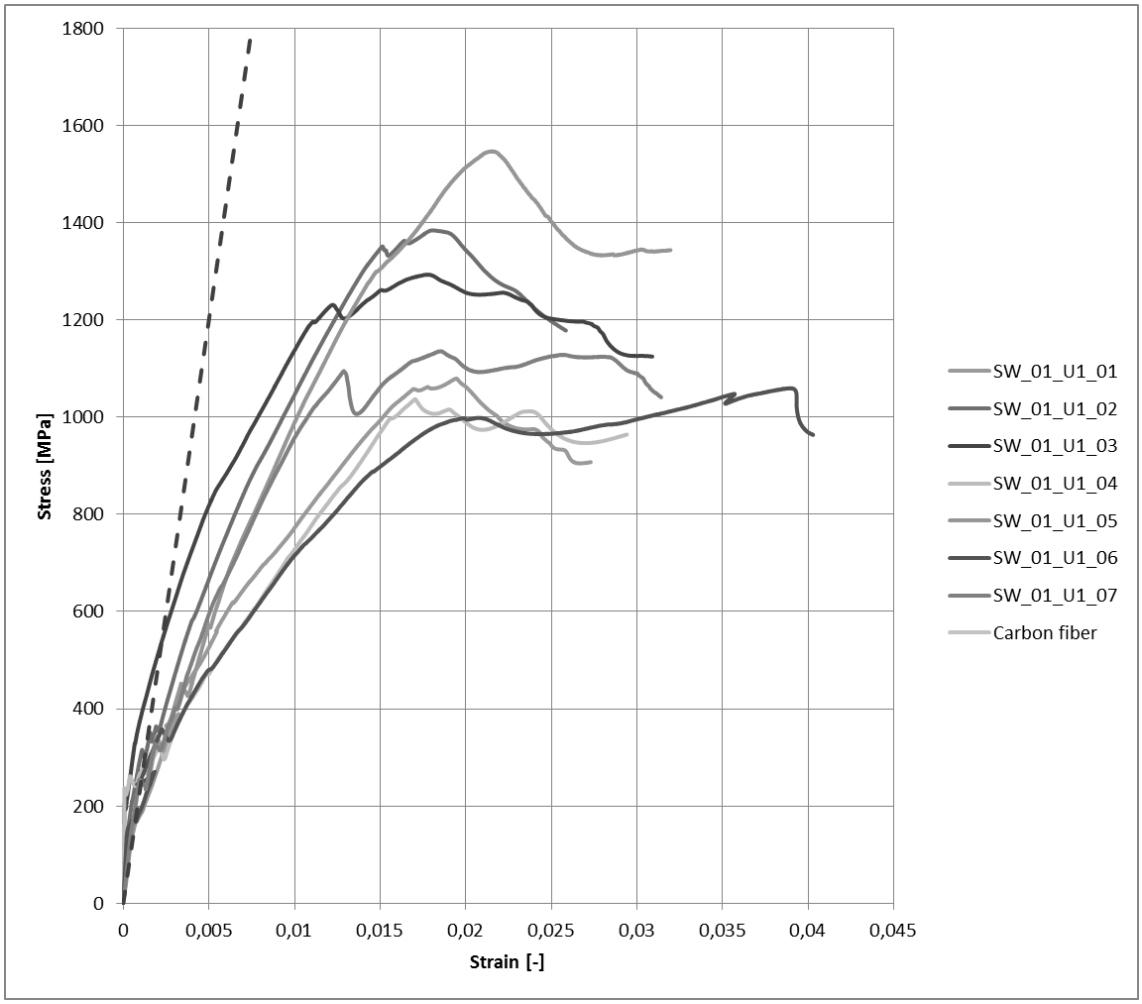

Figure 5. 2 - sea water resistance

Table 5. 2 - Parameters for Sea Water resistance tests

	E_1 [MPa]	E_2 [MPa]	f_{ft} [MPa]	ε_{ft} [-]	f_{fu} [MPa]	ε_{fu} [-]
SW_01	279488	49661	428	0,001532	1079	0,014643
SW_02	557123	67077	419	0,000751	1384	0,015143
SW_03	-	65745	-	-	1293	0,012397
SW_04	-	48904	-	-	1037	0,01647
SW_05	535394	57570	444	0,000829	1547	0,019987
SW_06	-	36449	-	-	1059	0,019947
SW_07	289234	67871	341	0,001180	1136	0,012883
Average	415310	56183	408	0,001073	1219	0,015924
Stand.Dev.	151519	11787	46	0,000358	194	0,003080
C.o.V.	36,48%	20,98%	11,17%	33,39%	15,89%	19,34%

The variability on the outcomes is quite low except the uncracked modulus of elasticity and the deformation at the transition point, and the reason was explained in the Section 3.9. For some specimens was not possible to compute the modulus E_1, and consequently the coordinates of the transition point, of an accuracy issue of the extensometer. For all the specimens the failure mode was slippage of the fabric from the mortar within the tabs after the formation of three or four macro cracks. The behavior of the specimens after the exposure to sea water was the same observed with the control specimens, and also the parameters computed are similar.

5.3.3 Water vapor resistance

For the water vapor resistance of the one ply specimens with a tab length of 150 mm, six specimen were tested. The graphs are shown in Figure 5.3 and the parameters obtained are presented in Table 5.3.

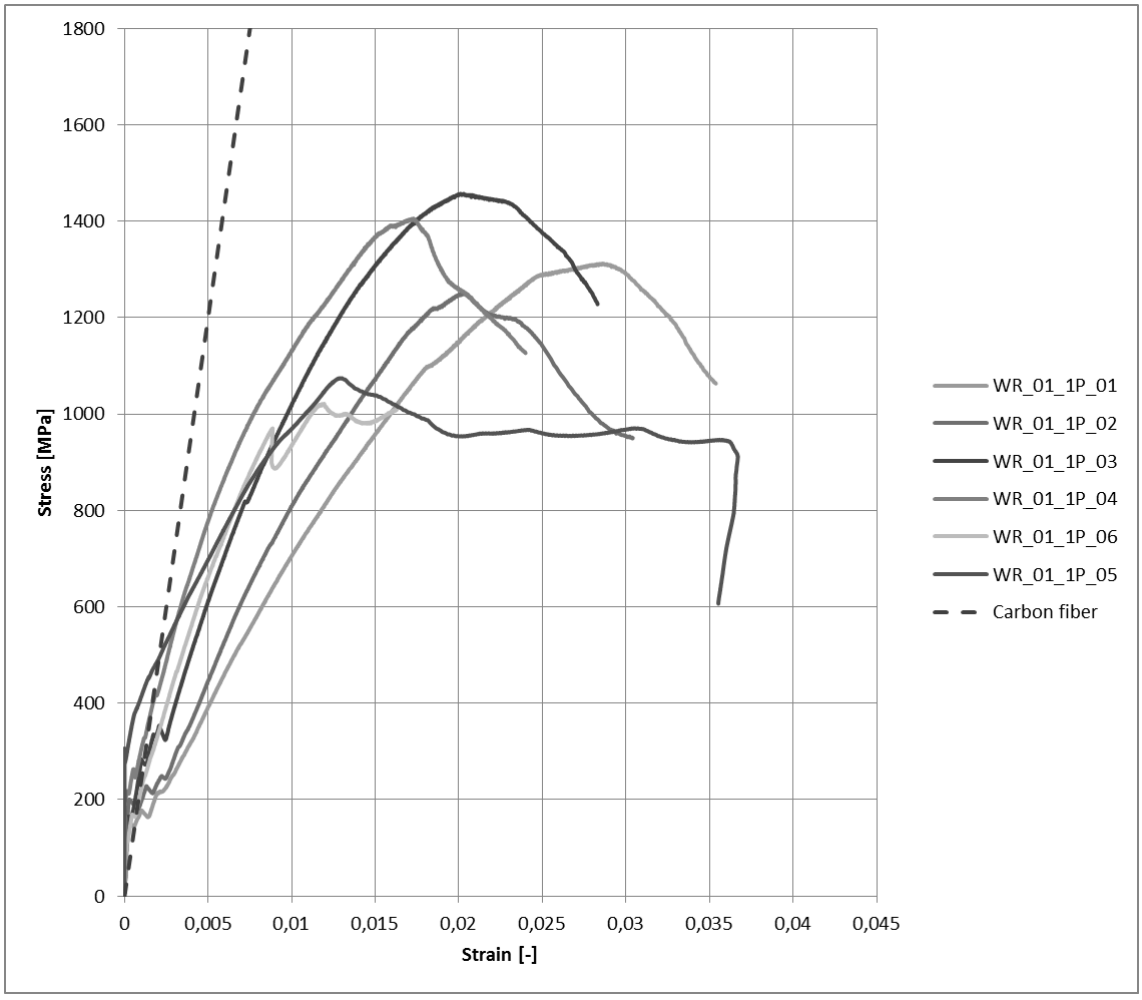

Figure 5. 3 - Water vapor resistance

Table 5. 3 - Parameters for Water Vapor resistance tests

	E_1 [MPa]	E_2 [MPa]	f_{ft} [MPa]	ε_{ft} [-]	f_{fu} [MPa]	ε_{fu} [-]
WR_01	652856	42012	324	0,000496	1312	0,024023
WR_02	852794	53895	278	0,000326	1250	0,01837
WR_03	985569	62351	397	0,000403	1457	0,017397
WR_04	-	60146	-	-	1405	0,015057
WR_05	-	56154	-	-	1074	0,011843
WR_06	955595	85810	250	0,000261	1021	0,00925
Average	861704	60061	312	0,000372	1253	0,015990
Stand.Dev.	150394	14473	64	0,000101	175	0,005209
C.o.V.	17,45%	24,10%	20,64%	27,21%	14,00%	32,58%

The variability on the outcomes is quite low except the ultimate strain and the deformation at the transition point, and the reason was explained in the Section 3.9. For some specimens was not possible to compute the modulus E_1, and consequently the coordinates of the transition point, because of an accuracy issue of the extensometer. For all the specimens the failure mode was slippage of the fabric from the mortar within the tabs after the formation of three or four macro cracks. The behavior of the specimens after the exposure to water vapor was the same observed with the control specimens, and also the parameters computed are similar.

5.3.4 Freezing and thawing resistance

For the Freezing and thawing resistance of the one-ply specimens with a tab length of 150 mm, six specimen were tested. The graphs are shown in Figure 5.4 and the parameters obtained are presented in Table 5.4.

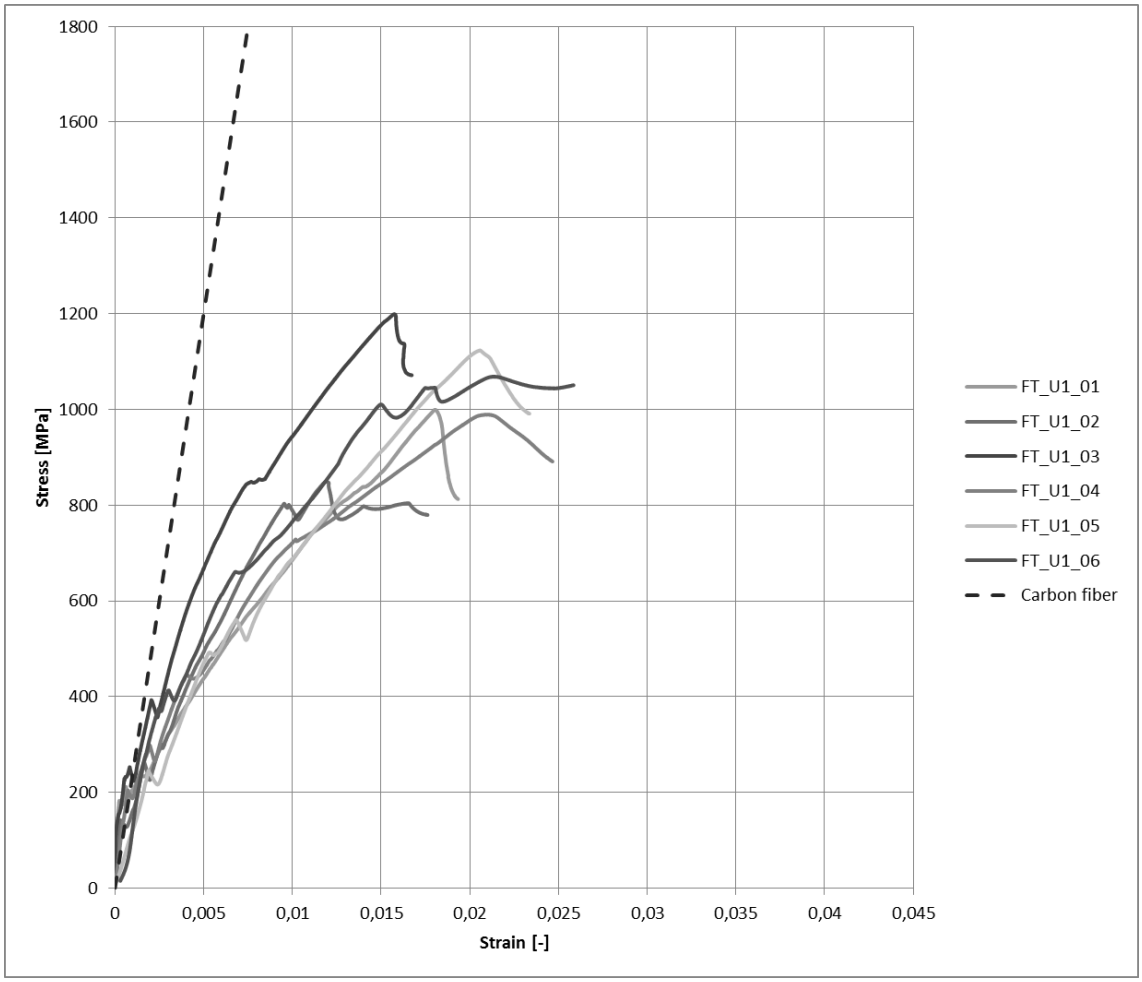

Figure 5. 4 - Freezing and thawing resistance

Table 5. 4- Parameters for Freezing and thawing tests

	E_1 [MPa]	E_2 [MPa]	f_{ft} [MPa]	ε_{ft} [-]	f_{fu} [MPa]	ε_{fu} [-]
FT_01	1137374	39666	286	0,000252	1000	0,018230
FT_02	501579	69995	168	0,000336	849	0,010063
FT_03	-	50457	-	-	1199	0,015107
FT_04	-	31576	-	-	989	0,019863
FT_05	-	44287	-	-	1123	0,019807
FT_06	-	46664	-	-	1069	0,015920
Average	819476	47108	227	0,000294	1038	0,016498
Stand. Dev.	449575	12960	83	0,000059	121,3833	0,003713
C.o.V.	54,86%	27,51%	36,71%	20,18%	11,69%	22,51%

The variability on the outcomes is quite low except the ultimate strain and the deformation at the transition point, and the reason was explained in the Section 3.9. For some specimens was not possible to compute the modulus E_1, and consequently the coordinates of the transition point, because of an accuracy issue of the extensometer For all the specimens the failure mode was slippage of the fabric from the mortar within the tabs after the formation of three or four macro cracks. The behavior of the specimens after freezing and thawing cycles was the same observed with the control specimens. The average ultimate strength is significantly lower than the one of the control specimens, but a statistical analysis is needed to prove it.

5.4 Analysis of the results

In this section the results of the tensile test after the exposure to different environment are discussed. Section 5.4.1 shows how the results were evaluated by using a statistical analysis and conclusions are offered in section 5.4.2.

5.4.1 Comparison of the results

In order to understand how the studied environments affect the tensile characteristics of the FRCM, the results of the exposed specimens and those of the control specimens were compared. The goal is to find which environment is detrimental to the tensile strength performance. The most important parameters to characterize the durability behavior of the FRCM system are the ultimate strength and the elastic modulus of the cracked specimen E_2. In Table 5.5 all the parameters computed from the tensile tests are shown.

Having the averages of these parameters is not enough to compare the results, in particular for the case of a material which is characterized by a high variability like the FRCM composite. For this reason a statistical evidence of the effect of the exposure to the environments is needed. There is the necessity to understand if the difference between the averages is significant, so it is possible to conclude that the environment affected the tensile behavior of the specimens, or the difference is random. In particular, for the intrinsic high variability of the FRCM material it is crucial to run a statistical analysis.

Table 5. 5 - Parameters comparison

		E_1 [MPa]	E_2 [MPa]	f_{ft} [MPa]	ε_{ft} [-]	f_{fu} [MPa]	ε_{fu} [-]
CC	**Average**	1327580	56529	362	0,000322	1297	0,016397
	Stand.Dev.	596480	8010	104	0,00015	162	0,002252
	C.o.V.	44,93%	14,17%	28,82%	46,62%	12,46%	13,74%
AR	**Average**	-	48918	-	-	1185	0,018372
	Stand.Dev.	-	10258	-	-	208	0,003048
	C.o.V.	-	20,97%	-	-	17,56%	16,59%
WR	**Average**	861704	60061	312	0,000372	1253	0,01599
	Stand.Dev.	150394	14473	64	0,000101	175	0,005209
	C.o.V.	17,45%	24,10%	20,64%	27,21%	14,00%	32,58%
SW	**Average**	415310	56183	408	0,001073	1219	0,015924
	Stand.Dev.	151519	11787	46	0,000358	194	0,00308
	C.o.V.	36,48%	20,98%	11,17%	33,39%	15,89%	19,34%
F/T	**Average**	819476	47108	227	0,000294	1038	0,016498
	Stand.Dev.	449575	12960	83	0,000059	121,3833	0,003713
	C.o.V.	54,86%	27,51%	36,71%	20,18%	11,69%	22,51%

In order to determine if two sets of data are significantly different from each other, the first thing to do is to choose the most suitable statistic test. The analysis of variance (ANOVA) allows to verify whether or not the means of several groups are equal, but one of the hypothesis to apply this statistical test is that the different groups must have the same number of element, that is not the case of this study. For the control condition the results from nine specimens are available, six for the alkaline resistance and seven for sea water and freeze/thaw. A t-test was chosen in order to compare separately every environment to the control condition. The significance level for the analysis is α=5%, indicating the probability of a false rejection of the null hypothesis in the statistical test. The null hypothesis is that the means of the two population considered are equal and if the p-value is below the threshold chosen of 0,05, then the null hypothesis is rejected in favor of the alternative hypothesis of having two populations with different means.

The t-test analysis was performed using the software Minitab with which was possible to obtain the p-value for all the groups, as can be seen in Table 5.6 in which are present the results of the t-test done for the ultimate stress.

Table 5. 6- Result from t-test analysis: ultimate stress

Environment	T-value	p-value
AR_01	1,11	0,299
WR_01	0,48	0,640
SW_01	0,85	0,413
FT	3,53	0,040

With the t-value is possible to find the p-value using a table of values from Student's t-distribution, but the software already give us the p-value. The p-value is the lowest level of significance at which the observed value of the test statistic is significant. From the Table 5.6 it is possible to see that the p-value is significantly higher than 0,05 for alkaline, water vapor and sea water environment, so the null hypothesis cannot be rejected. This mean that the 1000 hours exposure to these environments did not affect the tensile strength of the FRCM material.

Different is the case of the freezing and thawing, for which the p-value is equal to 0,04 and the null hypothesis can be rejected. Thus, there is a probability of 96% that the two populations have different means. For this reason it is possible to state that the freezing and thawing cycles were detrimental for the tensile strength of the specimens.

The same analysis can be performed on the elastic modulus E_2, that is the other important parameter for the design. In Table 5.7 the results of the t-test analysis for the elastic modulus E_2 are shown.

Table 5. 7 - Result from t-test analysis: cracked elastic modulus

Environment	T-value	p-value
AR_01	1,53	0,164
WR_01	-0,54	0,603
SW_01	0,07	0,948
FT	1,59	0,156

In the case of the cracked elastic modulus E_2 the statistical analysis establishes that, being the p-value significantly higher than the chosen threshold of 0,05, there is no differences in the cracked elastic modulus between the control condition and the other environment exposure.

5.5 Conclusion

Figure 5.5 and Figure 5.6 show the average values of ultimate strength and cracked elastic modulus, together with their standard deviations. Two values can be considered different if the mean of one of them does not fall inside the error interval of the other one. This is the case only of the ultimate strength of the freezing and thawing with respect to the ultimate strength of the control condition, as suggested by the statistical analysis performed.

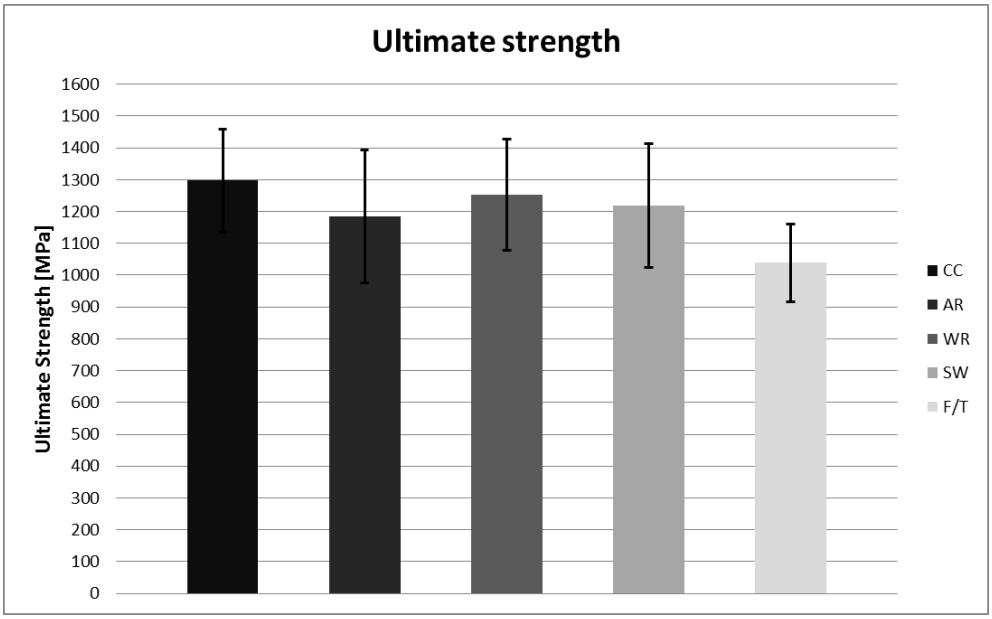

Figure 5. 5 - Ultimate strength after exposure to different environments

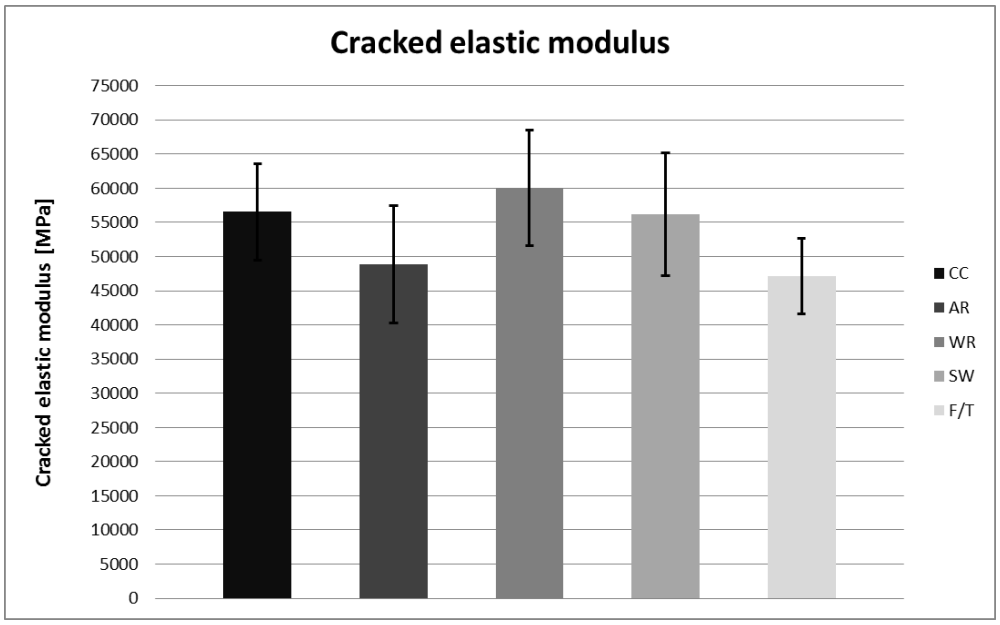

Figure 5. 6 - Cracked elastic modulus after exposure to different environments

From the durability study it is possible to obtain important conclusions. Except for the freezing and thawing exposure, the selected environments do not affect the tensile strength of the FRCM specimen after an exposure of 1000 hours. On one side, this result is very important because the FRCM material is proposed as an alternative solution to the FRP material for repairing purpose and it was obtained that FRCM composite is resistant to the environments which are detrimental for FRP.

On the other side there is the need to test the FRCM composite with different environments which can be detrimental for the cementitious matrix. In fact, it is the mortar that constitutes the innovation with respect to the FRP material and gives to the composite a high resistance to the environments studied. It is known that water vapor and sea water cannot affect the properties of the mortar, and the alkali-aggregate reaction that can be inducted by the exposure to alkaline environment, can be avoided simply with a low percentage of additives. The only environmental exposure that has been established to be dangerous for the specimens is the freezing and thawing. The water contained in the matrix pores, freezing and increasing the volume, damages the cementitious mortar affecting the adhesion between the fabric and the matrix. Testing the material with the clevis-type grip, the load is carried by the adhesion between the mortar and the fabric, thus the ultimate strength after the exposure is lower.

6.

FINAL CONCLUSIONS

The aim of this work was to extend the knowledge on the FRCM composite material, an innovative material that will be very useful and widely used in future strengthening applications. The big innovation brought by FRCM with respect to FRP is the cementitious matrix that, even if it has some drawbacks because it is a brittle material and it is not able to fully impregnate the fibers, has a lot of positive aspects. The good bond that the cementitious matrix is able to form with the concrete substrate, the good fire resistance, the ease of installation and reversibility of this new repairing system make the FRCM a very good alternative to the FRP composite material. After the durability study performed in this work, the author believes that also the durability is improved with respect to FRP material thanks to the different matrix.

After an intense experimental campaign, it was recognized that the variability of the results is significant and it is important to be very careful during the casting and testing of the specimens. For this reason, a section about all the problems related to data analysis was written, in order to be helpful for future researches in this field.

It would have been very interesting to test also specimens with three and four plies, in order to better understand the behavior of multiple ply systems. Some tests have been performed on three ply specimens but the ultimate strength of these specimens was not reached because the adhesion between the mortar and the tabs was not strong enough to carry higher load, and the failure was debonding of the tabs from the specimen.

As far as the influence of the tab length on the ultimate strength is concerned, it was found that a higher anchorage length of the fabric leads to an increase of the

ultimate strength using the clevis-type grip, but at the same time that the increase has a decreasing rate. This fact suggests the existence of an ideal tab length for which no further increasing in the ultimate strength would be observed for higher tab length. The author believes that this optimal length should be close to 250 mm, and for this reason would be interesting to test specimens with this tab length. For tensile testing the test frame used in this work limits the specimen length and so there was the idea of doing a second study for comparison, using a double shear test with equivalent contact length of 150 and 200 mm. If a correlation had been found in the contact length of the two tests, further experiments would have been performed with 250 mm to establish the limit of contact length for testing. Even if the boundary conditions of the tensile and double shear tests are different, performing the tensile test with the clevis-type grip that leads to a slippage failure, some similarities between the two tests can be found. Unfortunately problems with the machine frame arose the during the stay at the University of Miami, and it was not possible to perform the double shear tests on specimens that had already been cast.

Further investigations are also needed to understand the difference in the value of the cracked elastic modulus for varying tab length, which was found to be higher for shorter tab length.

In conclusion, the author believes that a good tab length to perform tensile test on FRCM composite material is 250 mm, because the coefficients of variances on the parameters computed for this length are the lowest.

REFERENCES

- Arboleda, D., (2014), "Fabric reinforced cementitious matrix (FRCM) composites for infrastructure strengthening and rehabilitation: characterization methods." *Ph.D. thesis, University of Miami, Miami, Florida*.

- Badanoiu, A., Holmgren, J. (2003), "Cementitious composites reinforced with continuous carbon fibres for strengthening of concrete structures." *Cement and Concrete Composites* 25, 387–394

- Banholzer, B., Brockmann, T., Brameshuber, W. (2006). "Material and bonding characteristics for dimensioning and modeling of textile reinforced concrete (TRC) elements." *Materials and Structures*, 39 (8), 749–763

- Berardi, F., Focacci, F., Mantegazza, G., Miceli, G., (2011) "Rinforzo di un viadotto ferroviario con PBO-FRCM," 22. *Proceedings, 1°Convegno Nazionale Assocompositi,* Milano, Italy, May 2011

- Bianchi, G., Arboleda, D., Carozzi, F. G., Nanni, A., & Poggi, C. (2013). "Fabric Reinforced Cementitious Matrix (FRCM) materials for structural rehabilitation". *Proceedings of the 39th IAHS World Congress*.

- Bianchi, G., Carozzi, F. G., Poggi, C., & Nanni, A. (2013). "Fabric-Reinforced- Cementitious-Matrix (FRCM) per la riabilitazione strutturale: aderenza al supporto". *Proceedings of the Congreso Mundial REHABEND*.

- Bianchi, G., (2013). "Mechanical characterization of fabric reinforced cementitious matrix (FRCM) materials for structural strengthening." *Master thesis, Politecnico di Milano, Milano, Italia*.

- Brückner, A., Ortlepp, R., Curbach, M. (2006). “Textile reinforced concrete for strengthening in bending and shear”. *Materials and structures, 39(8), 741-748*.

- Carozzi, F. G. & Poggi, C. (2015). “Mechanical properties and debonding strength of Fabric Reinforced Cementitious Matrix (FRCM) systems for masonry strengthening”. *Composite Part B*

- Curbach, M., Ortlepp, R., Triantafillou, T. C. (2006). “TRC for rehabilitation.” *Rep. TC 201-TRC, RILEM, Aachen, Germany.*

- D’Ambrisi, A., Focacci, F. (2011). “Flexural strengthening of RC beams with cement-based composites.” *Journal of Composites for Construction, 15(5), 707- 720.*

- D’Ambrisi, A., Feo, L., & Focacci, F. (2012). “Bond-slip relations for PBO-FRCM materials externally bonded to concrete”. *Composites Part B: Engineering, 43*(8), 2938-2949.

- De Santis, S., de Felice, G. (2014). “Tensile behavior of mortar-based composites for externally bonded reinforcement systems”. *Composites Part B: Engineering*, 401-413.

- Hartig, J., Häußler-Combe, U., Schicktanz, K. (2008). “Influence of bond properties on the tensile behaviour of textile reinforced concrete.” *Cem. Concr. Compos.*, 30, 898–906.

- Hegger, J., Will, N., Bruckermann, O., Voss, S. (2006). “Load-bearing behavior and simulation of textile reinforced concrete.” *Mater. Struct.*,39, 765–776.

- Leardini, L., Loreto, G., Poggi, C., & Nanni, A. (2013). "Shear Experimental Analysis of RC Beams Strengthened with FRCM". *Proceedings of the 39th IAHS World Congress*.

- Leardini, L., Loreto, G., Poggi, C., & Nanni, A. (2013). "Studio sperimentale del comportamento a taglio di travi in calcestruzzo armato rinforzate con FRCM (Fabric-Reinforced-Cementitious-Matrix)". *Proceedings of the Congreso Mundial REHABEND*.

- Loreto, G., Leardini, L., Arboleda, D., & Nanni, A. (2013). "Performance of RC Slab-Type Elements Strengthened with Fabric-Reinforced Cementitious-Matrix Composites". *Journal of Composites for Construction, 18*(3).

- Leardini, L., (2013). "Performance of RC beam elements reinforced with fabric-reinforced cementitious matrix (FRCM) for bending and shear." *Master thesis, Politecnico di Milano, Milano, Italia*.

- Loreto, G., Babaeidarabad, S., Leardini, L., & Nanni, A. (2014). "RC beams shearstrengthened with Fabric-Reinforced-Cementitious-Matrix (FRCM)". *Materials and Structures*.

- Mela, D., (2013). "Shear bond strength of carbon FRP laminates to concrete". *Master thesis, Politecnico di Milano, Milano, Italia*.

- Ombres, L. (2009). "Failure modes in reinforced concrete beams strengthened with PBO fiber reinforced mortars." *Proc., 9th Int. Symposium on Fiber Reinforced Polymer Reinforcement for Concrete Structures (FRPRCS-9), American Concrete Institute (ACI), Detroit.*

- Ombres, L. (2011). "Flexural analysis of reinforced concrete beams strengthened with a cement based high strength composite material." *Composite Structure*, 94(1), 143- 155.

- Ombres, L. (2012), "Debonding analysis of reinforced concrete beams strengthened with fibre reinforced cementitious mortar*." Engineering Fracture Mechanics 81 (2012) 94–109*.

- Ortlepp, R., Hampel, U., Curbach, M. (2006) "A new approach for evaluating bond capacity of TRC strengthening." *Cement & Concrete Composites* 28, 589–597.

- Nanni, A. (2012). "A new tool in the concrete and masonry repair*". Concr. Int. Des. Constr, 34, 43-49.*

- Pascucci, G., (2012). *"."Master thesis, Politecnico di Milano, Milano, Italia*.

- Scorcella, M., (2014). "Studio di sistemi innovativi per il rinforzo delle murature." *Master thesis, Università politecnica delle Marche,Ancona, Italia*.

- Sneed, L., D'Antino, T., Carloni, C., (2014). "Investigation of bond behavior of PBO fiber-reinforced cementitious matrix composite-concrete interface." *ACI Materials Journal (Vol. 3, No.1-6)*

- Soranakom, C., Mobasher, B. (2010) "Geometrical and mechanical aspects of fabric bonding and pullout in cement composites" *Materials and Structures, DOI 10.1617/s11527-008-9422-6*

- Wiberg, A. (2003). "Strengthening of concrete beams using cementitious carbon fibre composites." *Ph.D. thesis, Royal Institute of Technology, Stockholm, Sweden*.

- Zastrau, B., Lepenies, I., Richter, M. (2008). "On the multi scale modeling of textile reinforced concrete." *Technische Mechanik, 28(1), 53–63.*